The Thesis Committee for Jacob Robert Kondo
Certifies that this is the approved version of the following thesis:

Pullout Evaluation of Uniaxial Geogrids Embedded in Dredged Material

APPROVED BY
SUPERVISING COMMITTEE:

Supervisor:

Jorge G. Zornberg

Robert B. Gilbert

Pullout Evaluation of Uniaxial Geogrids Embedded in Dredged Material

by

Jacob Robert Kondo, B.S.C.E

Thesis

Presented to the Faculty of the Graduate School of

The University of Texas at Austin

in Partial Fulfillment

of the Requirements

for the Degree of

Master of Science in Engineering

The University of Texas at Austin

May 2013

Acknowledgements

I would like to thank Dr. Jorge Zornberg for his mentorship during my time at the University of Texas. His guidance and expert knowledge has helped me to fulfill a major step in my engineering career. I greatly appreciate the opportunity to be a part of his research team and I wish nothing but the best in their future endeavors. I would also like to thank Dr. Grubb for his support on this project. His contributions helped shape the background for this thesis.

Abstract

Pullout Evaluation of Uniaxial Geogrids Embedded in Dredged Material

Jacob Robert Kondo, MSE

The University of Texas at Austin, 2013

Supervisor: Jorge Zornberg

With the ever increasing need for MSE walls, the study of the interaction between soil and geosynthetics has become increasingly relevant. New concepts are constantly being researched, including the use of industrial byproducts as alternative backfill materials. The idea that byproduct material could somehow be a suitable fill for these MSE walls may spark new opportunities. One such byproduct being researched is dredged material. The suitability of dredged material as a backfill would not only contribute to lower construction costs, but would also benefit local confined disposal facilities looking to reduce their already overflowing dredged material accumulation.

This thesis further considers the use of dredged material by evaluating its interface shear strength with uniaxial geogrids. A series of laboratory pullout tests were conducted using two types of uniaxial geogrids (UX1400 and UX1700) embedded in three different soil types (Monterey Sand and two different dredged materials). The laboratory results are used to examine the effect on the coefficient of interaction of the various parameters governing the pullout resistance.

The results of this study show that: (1) the presence of adhesion to characterize the soil-reinforcement interface shear strength causes a decrease in the coefficient of interaction with increasing normal stress, (2) the reinforcement length of the geogrid was found not to affect the coefficient of interaction; provided that boundary effects are minimized, (3) the dredged material, tested wet of optimum, showed a response consistent with an undrained behavior, which produced pullout resistances significantly lower than that of the Monterey Sand, (4) the coefficient of interaction for the UX1700 was comparatively higher than that for the UX1400; however the differences obtained when testing Monterey Sand were similar to those obtained when testing the dredged materials.

Table of Contents

List of Tables ix

List of Figures x

Chapter 1: Introduction 1

1.1 Research Motivation 1

1.2 Background on Geogrids 2

1.3 Purpose of Reusing Dredged Material 4

1.4 Methodology 5

1.5 Research Objectives 5

1.6 Overview of Thesis 6

Chapter 2: Background on Pullout Testing 7

2.1 Transfer Mechanisms of Geogrid Interface 7

2.2 Boundary Conditions 8

2.2.1 Top Boundary 9

2.2.2 Frictional Characteristics of Front Wall 11

2.3 Coefficient of Interaction 13

2.4 Test Result Trends From Previous Studies 17

2.4.1 Normal Stress 17

2.4.2 Reinforcement Length 22

2.4.3 Influence of Spacing Between Transverse Members 24

2.4.4 Tests with Single Isolated Members 27

2.4.5 Reduction in Bearing Efficiency 29

Chapter 3: Pullout Testing Equipment and Materials 35

3.1 Overview 35

3.2 Characteristics of Geogrids 36

3.3 Monterey Sand Properties 37

3.4 MPA Dredged Material Properties 39

3.5 Philadelphia Dredged Material Properties 43

3.6 Pullout Testing Procedures 47

Chapter 4: Pullout Test Results and Analysis 54

4.1 Scope of Testing Program 54

4.2 Pullout Tests Conducted with Monterey Sand 55

4.2.1 Pullout Test Results Using Monterey Sand 55

4.2.2 Analysis of the Results 61

4.3 Pullout Tests Conducted with MPA Dredged Material 66

4.3.1 Pullout Test Results Using Dredged Materials 66

4.3.2 Analysis of the Pullout Parameters of MPA Dredged Material 70

4.4 Pullout Tests With Philadelphia Dredged Material 76

4.4.1 Analysis of the Pullout Parameters of Philadelphia Dredged Material 80

4.5 Comparison of Pullout Results of MPA and Philadelphia Dredged Materials 83

Chapter 5: Conclusions and Recommendations 86

5.1 Conclusion 86

5.2 Recommendations 88

Appendix A: Monterey Sand Pullout Test Results 89

Appendix B: Dredged Material Pullout Test Results 120

References 155

List of Tables

Table 1.1: Polymers used in geosynthetics. 2

Table 3.1: Geogrid characteristics. 37

Table 3.2: Small fluctuations in dry density with each Monterey Sand test.....39

Table 3.3: Soil properties of the MPA dredged material. 40

Table 3.4: Dry density for each MPA dredged material test. 42

Table 3.5: Undrained Shear Strength of the MPA dredged material. 42

Table 3.6: Soil properties of the Philadelphia dredged material. 44

Table 3.7: Dry density for each Philadelphia dredged material test. 45

Table 3.8: Undrained Shear Strength of the dredged material. 46

Table 4.1: Dry density for each Philadelphia dredged material test. 54

List of Figures

Figure 1.1: Interaction mechanisms in a reinforced wall, (Palmeira, 2009).....1

Figure 1.2: Uniaxial geogrid.....3

Figure 1.3: Biaxial geogrid.....3

Figure 1.4: Triaxial geogrid.....4

Figure 2.1: Transverse and longitudinal rib contributions to the pullout resistance. (Palmeira, 2004).....7

Figure 2.2: The development of skin friction as a result of the pullout force and the normal pressure bearing down on longitudinal and transverse ribs. (FHWA NHI-05-046). 8

Figure 2.3: Pullout force versus displacement for rigid and top boundaries. (Palmeira and Milligan, 1989). 9

Figure 2.4: Pullout load versus displacement for varying pullout box heights. (Dias, 2003). 11

Figure 2.5: Normalized bond stress versus displacement for different front wall textures, (Palmeira and Milligan, 1989). 12

Figure 2.6: The tangent of delta is the interface shear strength over the normal stress.....14

Figure 2.7: Interface shear components at interface of geogrid. (Wilson-Fahmy and Koerner, 1993). 15

Figure 2.8: Different hypothetical relationships between Pullout Force vs. Normal Stress. 17

Figure 2.9: Different hypothetical relationships between Ci vs. Normal Stress. 18

Figure 2.10: Linear relationship with intercept. (Palmeira, 2004). 19

Figure 2.11: Relationship between Ci and Normal Stress. (Palmeira, 2004).....19
Figure 2.12: Linear relationship of max pullout versus normal stress showing an intercept, (Abu-Farsakh et. al., 2006) 21
Figure 2.13: relationship between Ci and Normal Stress, (Abu-Farsakh et. al., 2006) 21
Figure 2.14: Normalized bond stress versus reinforcement length, (Palmeira and Milligan, 1989). 22
Figure 2.15: Constant Ci with varying reinforcement lengths, (Teixeira, 2007) ..23
Figure 2.16: Linear relationship between pullout load and reinforcement length, (Teixeira, 2007).....24
Figure 2.17: Friction coefficient versus displacement for different S/B ratios, (Palmeira and Milligan, 1989). 25
Figure 2.18: Optimum transverse rib spacing, (Teixeira, 2007). 26
Figure 2.19: Pullout test results on isolated transverse members with different cross-sections, (Palmeira 2008).....27
Figure 2.20: Normalized bond stress versus displacement for single and isolated bearing members, (Palmeira and Milligan, 1989). 28
Figure 2.21: Bearing stress ratio versus soil friction angle, (Palmeira and Milligan, 1989). 29
Figure 2.22: Pullout force versus displacement. Set up #1 is with first transverse rib separated by a distance “d” from front wall, (Palmeira and Milligan, 1989). 30
Figure 2.23: Pullout force versus displacement results for geogrids tested with and without transverse members, (Palmeira 2008).....31
Figure 2.24: Interference between grid transverse members, (Palmeira 2008).....32

Figure 2.25: Weakened state of stress behind grid transverse members, (Palmeira 2008). 32
Figure 2.26: Pullout force versus displacement for bearing members with different spacing, (Palmeira and Milligan, 1989).....33
Figure 2.27: Degree of interference versus S/B, (Palmeira and Milligan, 1989). .34
Figure 3.1: Large scale pullout box testing equipment. 35
Figure 3.2: Grain Size Distribution Curve for Monterey Sand. 38
Figure 3.3: Grain size distribution curve for dredged material from MPA. 40
Figure 3.4: Modified compaction curve for dredged material from MPA 41
Figure 3.5: Direct shear results for MPA dredged material. 43
Figure 3.6: Grain size distribution curve for dredged material from Philadelphia.44
Figure 3.7: Modified compaction curve for dredged material from Philadelphia45
Figure 3.8: Direct shear results for MPA and Philadelphia dredged material.....46
Figure 3.9: Prepared geogrid specimen with tell-tales attached. 47
Figure 3.10: Geogrid clamped to the roller grip. 49
Figure 3.11: Geogrid turned 270 degrees to minimize stress concentrations.....50
Figure 3.12: Placement of plywood footings. 51
Figure 3.13: Placement of air cylinders. 52
Figure 3.14: Placement of reaction frames on top of cylinders. 52
Figure 4.1: Monterey Sand with UX1400 under a normal stress of .5psi. 56
Figure 4.2: Monterey Sand with UX1400 under a normal stress of 4psi. 56
Figure 4.3: Monterey Sand with UX1400 under a normal stress of 6psi. 57
Figure 4.4: Monterey Sand with UX1400 under a normal stress of 8psi. 58
Figure 4.5: Monterey Sand with UX1700 under a normal stress of .5psi. 58
Figure 4.6: Monterey Sand with UX1700 under a normal stress of 4psi. 59

Figure 4.7: Monterey Sand with UX1700 under a normal stress of 6psi. 60
Figure 4.8: Monterey Sand with UX1700 under a normal stress of 8psi. 60
Figure 4.9: Max pullout force versus normal stress for Monterey Sand. 61
Figure 4.10: Ci versus normal stress for Monterey Sand. 62
Figure 4.11: Lower friction angle for UX1400 results in bigger difference in shear strength. 63
Figure 4.12: Max pullout load versus reinforcement length for Monterey Sand. .64
Figure 4.13: Ci versus reinforcement length for Monterey Sand. 64
Figure 4.14: Ci versus S/B for geogrids tested in Monterey Sand. 65
Figure 4.15: Dredged material from MPA with a UX1400 under a normal stress of 4psi. 67
Figure 4.16: Dredged material from MPA with a UX1400 under a normal stress of 6psi. 67
Figure 4.17: Dredged material from MPA with a UX1400 under a normal stress of 8psi. 68
Figure 4.18: Dredged material from MPA with a UX1700 under a normal stress of 4psi. 68
Figure 4.19: Dredged material from MPA with a UX1700 under a normal stress of 6psi. 69
Figure 4.20: Dredged material from MPA with a UX1700 under a normal stress of 8psi. 69
Figure 4.21: Pullout load versus normal stress for MPA dredged material. 71
Figure 4.22: Ci versus normal stress for MPA dredged material. 71
Figure 4.23: Pullout load versus reinforcement length for MPA dredged material.73
Figure 4.24: Ci versus reinforcement length for MPA dredged material. 74

Figure 4.25: Ci versus transverse member spacing normalized by member thickness. 75
Figure 4.26: Dredged material from Philadelphia with a UX1400 under a normal stress of 4psi.....76
Figure 4.27: Dredged material from Philadelphia with a UX1400 under a normal stress of 6psi.....77
Figure 4.28: Dredged material from Philadelphia with a UX1400 under a normal stress of 8psi.....77
Figure 4.29: Dredged material from Philadelphia with a UX1700 under a normal stress of 4psi.....78
Figure 4.30: Dredged material from Philadelphia with a UX1700 under a normal stress of 6psi.....79
Figure 4.31: Dredged material from Philadelphia with a UX1700 under a normal stress of 8psi.....79
Figure 4.32: Pullout load versus normal stress for Philadelphia dredged material.80
Figure 4.33: Ci versus normal stress for Philadelphia dredged material.....81
Figure 4.34: Ci versus transverse member spacing normalized by member thickness. 83
Figure 4.35: Ci versus transverse member spacing normalized by member thickness. 84
Figure 4.36: Ci versus transverse member spacing normalized by member thickness. 85

Chapter 1: Introduction

1.1 RESEARCH MOTIVATION

Earth retaining structures are often key components in infrastructure design projects. While conventional retaining wall systems have been around for many years, new concepts continue to emerge with the objective of improving efficiency, performance, cost, or the ability to accommodate space constraints. Earth retaining structures are classified into four categories. The category with relevance to this thesis is internally stabilized fill walls. An example of these structures are the Mechanically Stabilized Earth (MSE) walls. These types of walls rely on geogrids or some other type of reinforcement to provide strength across failure planes that may develop through the reinforced fill. Figure 1.1 shows an example of an internally reinforced wall.

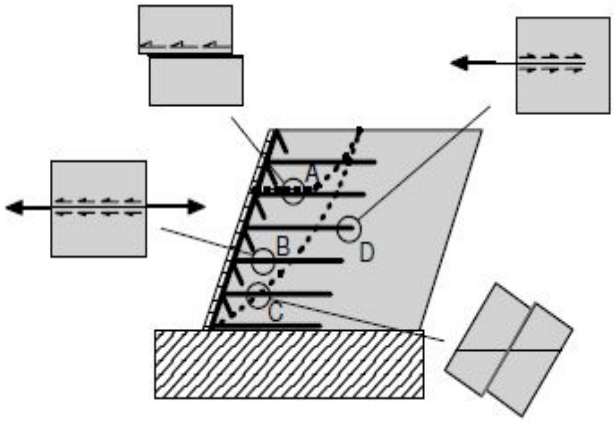

Figure 1.1: Interaction mechanisms in a reinforced wall, (Palmeira, 2009)

As the figure suggests, there are several potential failure mechanisms associated with internally stabilized walls. The failure mechanism with relevance to this thesis is the pullout failure, which is illustrated as mode failure "D" in the figure. This type of failure mechanism is dependent on the interaction between the soil and reinforcement. In

order to properly select a type of reinforcement that will provide sufficient interaction strength, the soil reinforcement interaction should be characterized using pullout tests. This thesis looks into the evaluation of the interaction between non-conventional soils and geosynthetics by analyzing pullout test results.

1.2 BACKGROUND ON GEOGRIDS

Geogrids are most commonly used for reinforcement of earth retaining structures. There are two main characteristics used to define the types of geogrids. The first being the type of material used to manufacture the geogrid. Table 1.1 relates the typically used type of polymer for the different geosynthetic materials.

Geosynthetic material	Main polymers used
Geomembranes	Polyethylene (HDPE and LLDPE) Plasticized PVC Polypropylene
Geonets	Polyethylenes (HDPE)
Geogrids	Polyethylene (HDPE) Polyesters Polypropylene
Geopipes	Polyethylene (HDPE) PVC
Geotextiles	Polypropylene Polyester

Table 1.1: Polymers used in geosynthetics.

The polymer types commonly used to manufacture geogrids include: HDPE, PP, and PE. Geogrids also come in different rib arrangements. Manufacturers have produced three types of rib arrangements: uniaxial, biaxial, and triaxial. Examples of each are shown in Figures 1.2, 1.3, and 1.4.

Figure 1.2: Uniaxial geogrid.

Uniaxial geogrids provide load resistance in one single direction. They are mainly used for soil reinforcement applications, as they can provide comparatively high pullout resistance relative to the biaxial and triaxial geogrids.

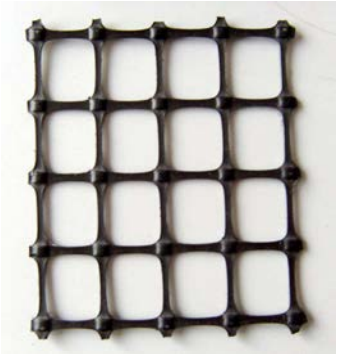

Figure 1.3: Biaxial geogrid.

Biaxial geogrids can provide load resistance in two directions. This partially depends on the thickness of the transverse members. They have been typically used for

reinforcing asphalt pavements. They have been used in the base course layer of pavement structures to reduce short term rutting effects, long term fatigue and low temperature cracking.

Figure 1.4: Triaxial geogrid.

The new development of geogrids is the triaxial arrangement. These geogrids were developed to provide uniform resistance in multiple directions.

1.3 PURPOSE OF REUSING DREDGED MATERIAL

Several hundred million cubic yards of sediment is dredged in the United States every year. This industry plays a vital role in providing safe passage in navigational ship channels for commercial, national defense, and recreational purposes. The growing demand for dredging has caused many of the dredged material containment facilities in the United States to be filled to capacity. New containment sites are difficult to establish due to a variety of economic and environmental issues. An alternative to the traditional "dredge and dispose" method is to simply reuse the dredged material found in the

containment facilities. The beneficial use of the dredged material would save resources that would otherwise be spent on finding and managing disposal sites, it would reduce capacity-related problems in existing disposal sites, and it would reduce the need for identifying future disposal sites. The problem facing the beneficial use of dredged material is mainly the lack of acceptability. Users are hesitant of the costs associated with reusing dredged material as well as with the suitability of the material properties. If the stigmas related to reusing byproduct materials could be overcome, then the market for dredged material would provide promising opportunities.

1.4 METHODOLOGY

The research for this thesis analyzed previous pullout test results and evaluated governing mechanisms based off these results. Then, a series of laboratory pullout tests were conducted with three different soil types and two different geogrids all under normal stresses of 4, 6, and 8 psi. Finally, the laboratory pullout test results were analyzed to verify the governing mechanisms found in the research and to evaluate the parameters of: soil type, reinforcement type, reinforcement length, and normal stress.

1.5 RESEARCH OBJECTIVES

The objectives for this thesis include the following:

- Identify the mechanisms that govern pullout resistance;
- Identify the parameters that affect the governing mechanisms;
- Develop a series of laboratory pullout tests based on the parameters of: soil type, reinforcement type, reinforcement length, and normal stress;

- Analyze the effectiveness of parameters on the pullout resistance and coefficient of interaction using the laboratory pullout test results.

1.6 OVERVIEW OF THESIS

This thesis is divided into five chapters. Chapter two provides background information regarding pullout testing. This chapter also presents test results from previous studies. These results are used for the comparative analysis to be presented in Chapter four. Chapter three describes the procedures for the pullout testing conducted for this research program. It specifically describes new experimental developments within the pullout testing procedures that were adopted to improve the quality of the experimental data. Chapter four presents all of the test results for the Monterey Sand and the two dredged materials. The test results are then analyzed considering the variation of the coefficient of interaction with the different parameters that govern the pullout behavior. Chapter five provides a summary of the findings and recommendations for further developments.

Chapter 2: Background on Pullout Testing

2.1 TRANSFER MECHANISMS OF GEOGRID INTERFACE

The design of reinforced soil structures require proper understanding of the stress transfer that occurs between the reinforcement and the soil. The stress transfer results in a redistribution of the stresses from the unstable portions of the soil mass into more stable soil zones, thereby increasing the internal stability of the reinforced structure. Geogrid reinforcements involve transverse and longitudinal ribs. These ribs use passive and interface shear resistance in order to induce the stress transfer mechanisms that results in pullout resistance.

Figure 2.1 illustrates the passive and interface shear contributions made by the transverse and longitudinal ribs.

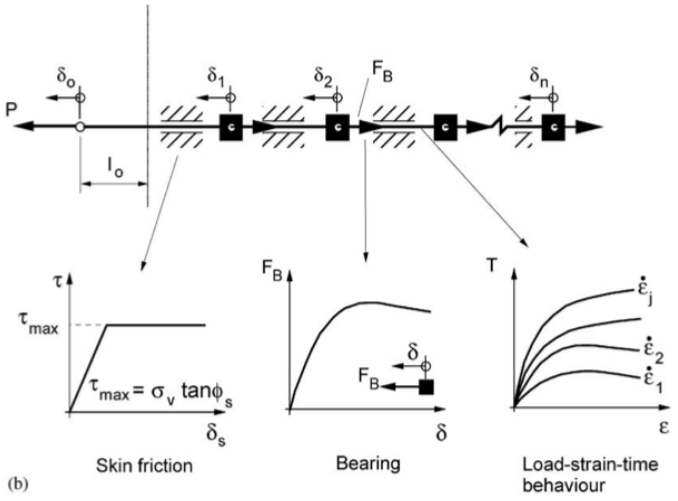

Figure 2.1: Transverse and longitudinal rib contributions to the pullout resistance. (Palmeira, 2004).

The longitudinal ribs, represented in Figure 2.1 by a thin black line in between the transverse ribs (squares), create skin friction along the geogrid interface. The soil normal

pressure and the pullout force create the skin friction. Figure 2.2, taken from FHWA NHI-05-046, illustrates the development of the skin friction.

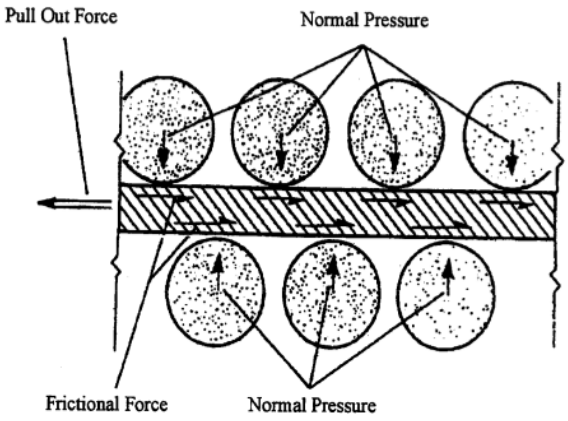

Figure 2.2: The development of skin friction as a result of the pullout force and the normal pressure bearing down on longitudinal and transverse ribs. (FHWA NHI-05-046).

The transverse ribs induces a bearing resistance, which decreases after a maximum force is reached. This decrease is due to the interference caused by the transverse ribs and is explained in more detail later in this chapter.

2.2 BOUNDARY CONDITIONS

Inconsistencies have been reported in pullout box results due to interference attributed to boundary conditions. Boundary conditions have been shown to have a significant effect on the pullout resistance.

2.2.1 Top Boundary

A vertical pressure is applied over the soil and geogrid during pullout testing. The rationale behind the top boundary influence is that if the top is a rigid plate, then the vertical pressure may not be evenly distributed within the soil. This may happen if the top of the soil specimen is not level and therefore does not have uniform contact with the rigid plate. This would cause the areas of the soil that are in direct contact with the rigid plate to experience higher vertical pressures than soil areas that are not in contact. An alternative to the rigid top plate is a flexible bag that is able to conform to varying levels in the soil surface. This approach is expected to provide a more uniform distribution of vertical pressures and lead to fewer inconsistencies in the pullout test results. Palmeira and Milligan (1989) tested the effect of the top boundary on a medium sized (0.25 x0.15x0.5 m.) pullout box. The results are shown in Figure 2.3.

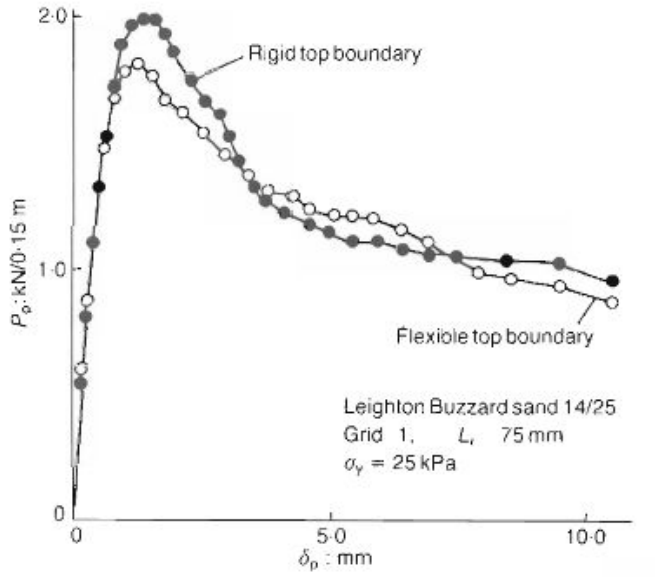

Figure 2.3: Pullout force versus displacement for rigid and top boundaries. (Palmeira and Milligan, 1989).

The results in Figure 2.3 show that the rigid top boundary results in a slightly higher pullout force compared to the flexible top boundary. Since the pullout force is higher for the rigid plate, the friction coefficient is also higher. The friction coefficient is defined by Palmeira and Milligan (1989) as:

$$\mu_{po} = \frac{\tau_b}{\sigma_v} \tag{2.1}$$

$$\tau_b = \frac{P_p}{2*Lr*Wr} \tag{2.2}$$

where:

$\mu_{po} = Friction\ coefficient\ in\ pullout\ test$

$\tau_b = mean\ shear\ stress\ between\ soil\ and\ reinforcement$

$\sigma_v = vertical\ pressure$

$P_p = pullout\ force\ for\ a\ grid\ with\ n\ bearing\ members$

$L_r = reinforcement\ length$

$W_r = reinforcement\ width$

Despite the different friction coefficient between the rigid and flexible boundaries, the value of both friction coefficients exceed the tangent of the soil friction angle (friction angle for Leighton Buzzard Sand 14/25 is 35°). This means that the strength at the interface between the geogrid and soil is stronger than the strength of the soil itself, so the pullout failure will not occur at the geogrid interface in an actual structure.

Dias (2003) conducted pullout test simulations on a reinforcement buried in sand using the finite element method. The simulations focused on the interference caused by

the proximity of the specimen to the top boundary. Figure 2.4 shows the results of the simulations.

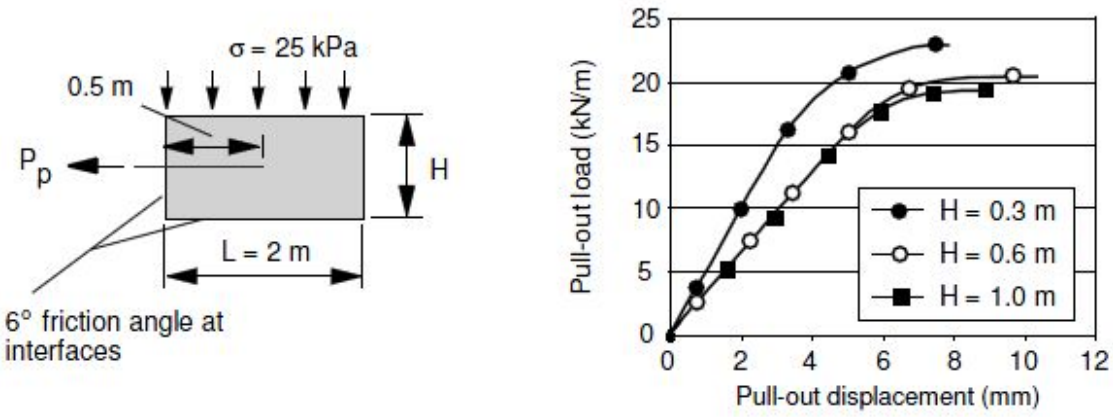

Figure 2.4: Pullout load versus displacement for varying pullout box heights. (Dias, 2003).

The results suggest that the interference from the top boundary increases the pullout load for specimens buried in a smaller pullout box height. As the height of the box increases the influence from the interference becomes less relevant. This suggests that the height of the pullout box should be taken into consideration when determining the maximum reinforcement length needed for testing in order to minimize the interference from the top boundary.

2.2.2 Frictional Characteristics of Front Wall

When a geogrid is tested under the confinement of dense sand, the soil tends to dilate. Dilation of the soil causes local stresses in the geogrid and general heave. General heave causes the soil above the geogrid to produce down drag on the sides of the

geogrid which increases the average vertical stresses. This increase in average vertical stress is governed by the frictional characteristics of the front wall. The reason being that the front wall takes on the majority of the lateral stresses in the pullout box compared to the side and rear walls. Palmeira and Milligan (1989) evaluated the influence of the frictional characteristics of the front wall using the medium sized (0.25 x0.15x0.5 m.) pullout box. The results are shown in Figure 2.5.

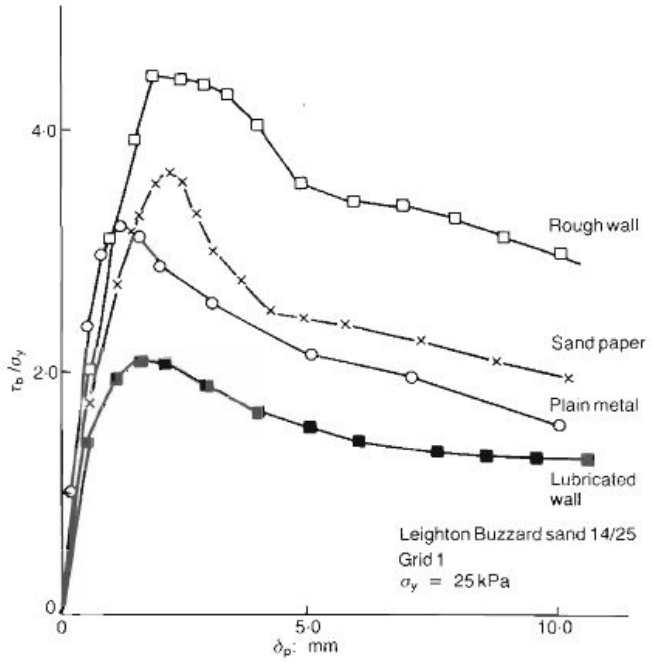

Figure 2.5: Normalized bond stress versus displacement for different front wall textures, (Palmeira and Milligan, 1989).

The significant variation in the normalized bond stress between the rough and lubricated wall suggests a significant influence by the frictional characteristics of the front wall.

One way to minimize the influence of the front wall interference is by using a sleeve. The use of a sleeve on the front wall has experimentally shown to decrease the amount of interference, but this benefit often depends on the other boundary conditions.

Palmeira suggests that for a large scale pullout box setup, a sleeve length of no less than 30 cm. should be used.

2.3 COEFFICIENT OF INTERACTION

The coefficient of interaction, Ci, is typically used to quantify the results of pullout tests. Although Ci is not a parameter measured directly from a pullout test, it is still a helpful variable in comparing the interface strength with the soil strength. Ci is a ratio of the interface and soil shear strength. The coefficient, Ci is defined as:

$$Ci = \frac{\tau_{f,interface}}{\tau_{f,soil}} \tag{2.3}$$

The interface shear strength has a normal stress component and an interface friction angle, delta. The parameter delta is often used to characterize the slope of the interface shear strength vs. normal stress line. An example is shown in Figure 2.6.

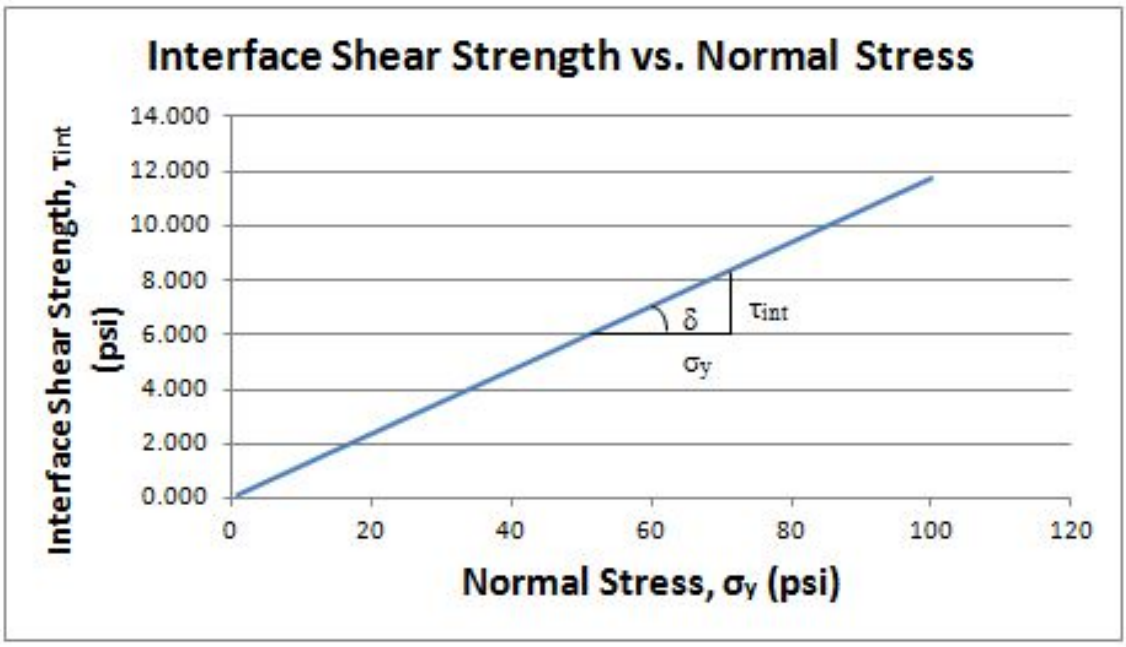

Figure 2.6: The tangent of delta is the interface shear strength over the normal stress.

Figure 2.6 shows the parameter delta as the slope of the interface shear strength and normal stress. The interface shear strength can be defined as:

$$\tau_{f,interface} = \sigma_y * \tan(\delta) \qquad (2.4).$$

where

$\sigma_y = normal\ stress$

$\tan(\delta) = interface\ friction\ angle$

If the interface shear strength between the geogrid and soil has an adhesion component, then this would be represented by a y-axis intercept. If the soil shear strength has a cohesion value, the interface is expected to have an adhesion value. Although this adhesion is an important part of the interface shear strength equation, most articles and

papers on pullout testing do not consider it. This may be due to the fact that the majority of pullout testing has been done with granular materials with little to no cohesion.

Another way to look at the interface shear strength is as the sum of the multiple forces that contribute to the pullout resistance. Figure 2.7 shows the free body diagram of a geogrid in a pullout test.

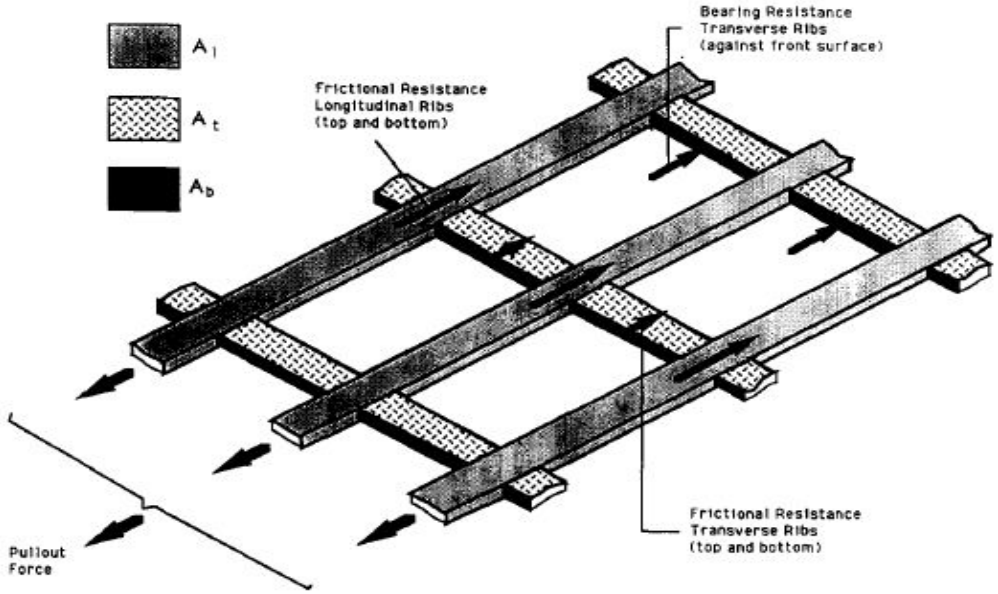

Figure 2.7: Interface shear components at interface of geogrid. (Wilson-Fahmy and Koerner, 1993).

The forces that resist the overall pullout force include the frictional forces from the longitudinal ribs and the bearing forces from the transverse members. Both of these force define the interface shear resistance, τ_{int}.

$$\tau_{int} = \frac{Pullout\ force, P_p}{2 * L_r * W} \qquad (2.5)$$

Combining this equation with the definition of interface shear strength yields:

$$\tan(\delta) = \frac{P_p}{2 * L_r * W * \sigma_y} \quad (2.6)$$

Taking the ratio of the interface shear strength, tan(δ), to the soil shear strength, tan(φ), yields:

$$Ci = \frac{\tan(\delta)}{\tan(\varphi)} \; or \; Ci = \frac{P_p}{2 * L_r * W * \sigma_y * \tan(\varphi)} \quad (2.7)$$

This simplified representation of the interface shear strength relies on important assumptions. To begin with, there is no cohesion (or adhesion in this case) that would cause the τ_{int} vs. σ_y graph to develop an intercept. This assumption can be true depending on the characteristics of the soil and geogrid being tested. A way assessing the validity of this assumption is by plotting the pullout results on a τ_{int} vs. σ_y graph.

Another assumption is that there is a linear relationship between τ_{int} and σ_y. Again, this assumption could be valid depending on the soil and geogrid type.

Another assumption is that τ_{int} remains constant throughout the embedment length. This is probably appropriate for inextensible geogrids, but for extensible geogrids the interface shear strength may vary significantly throughout the geogrid. Typical pullout tests results with extensible geogrids will show a lag in displacement between the front and last portion of the geogrid. The front portion of the geogrid will contribute the most towards the τ_{int}. This is due to the fact that displacement is needed in order to mobilize interface shear resistance. When the front and back portion of the geogrid displaces at the same rate, then the τ_{int} remains constant throughout the geogrid.

2.4 TEST RESULT TRENDS FROM PREVIOUS STUDIES

This section summarizes the trends from previous pullout test studies. The studies include different types of geosynthetics and different soils. The trends identified from the previous studies will be useful in evaluating the results obtained in this research.

2.4.1 Normal Stress

If the pullout force is directly proportional to the normal stress, then the Ci value for that interface would be a constant independent of the normal stress. If the pullout force versus normal stress shows an intercept or a non-linear relationship, then Ci will decrease with increasing normal stress. Figure 2.8 illustrates the different typical trends in these relationships.

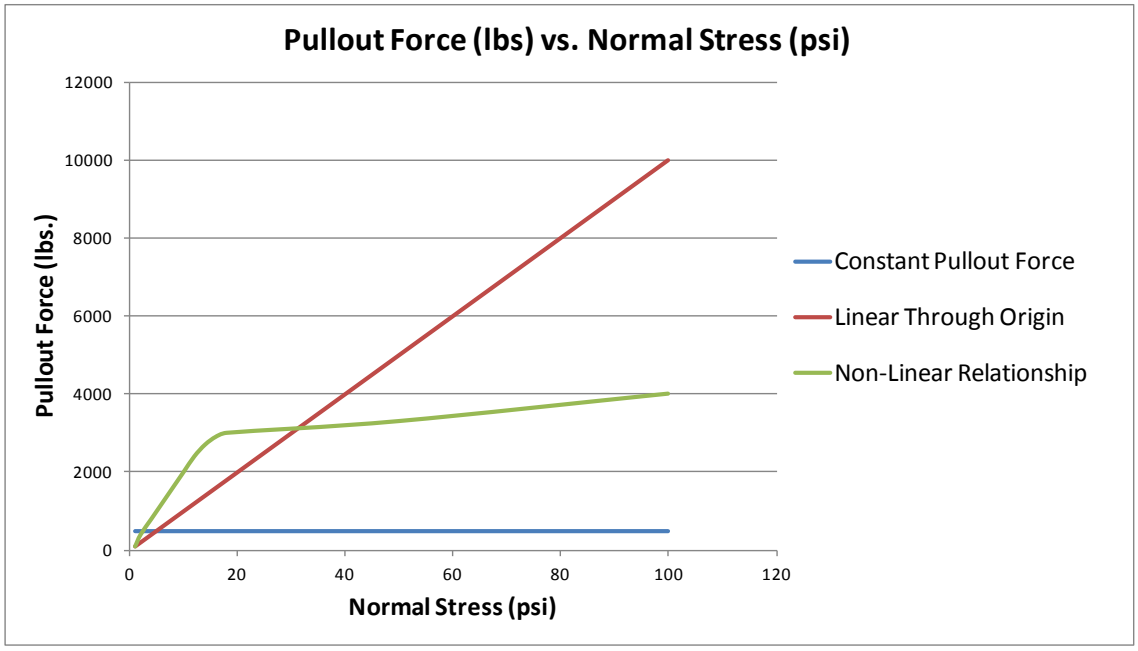

Figure 2.8: Different hypothetical relationships between Pullout Force vs. Normal Stress.

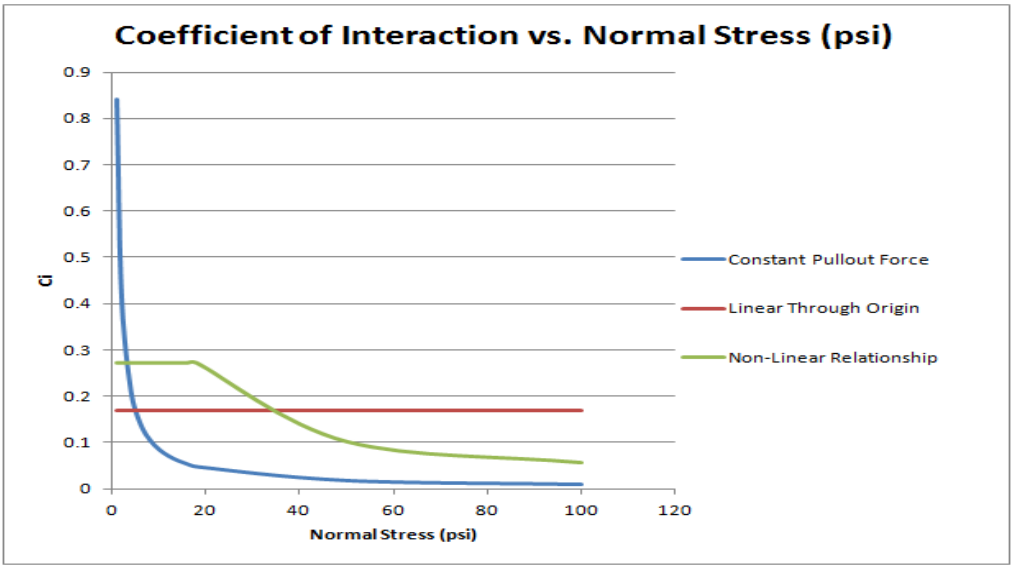

Figure 2.9: Different hypothetical relationships between Ci vs. Normal Stress.

In Figure 2.8, the line that passes through the origin represents a pullout force in a purely frictional material. The line showing an intercept represents an adhesion component in addition to the frictional one.

Palmeira (2004) reported the results of pullout tests with varying normal stresses. The tests used a polymeric geogrid against Leighton Buzzard Sand 14/25 which is characterized by a friction angle of 51°. The results are shown in Figures 2.10 and 2.11.

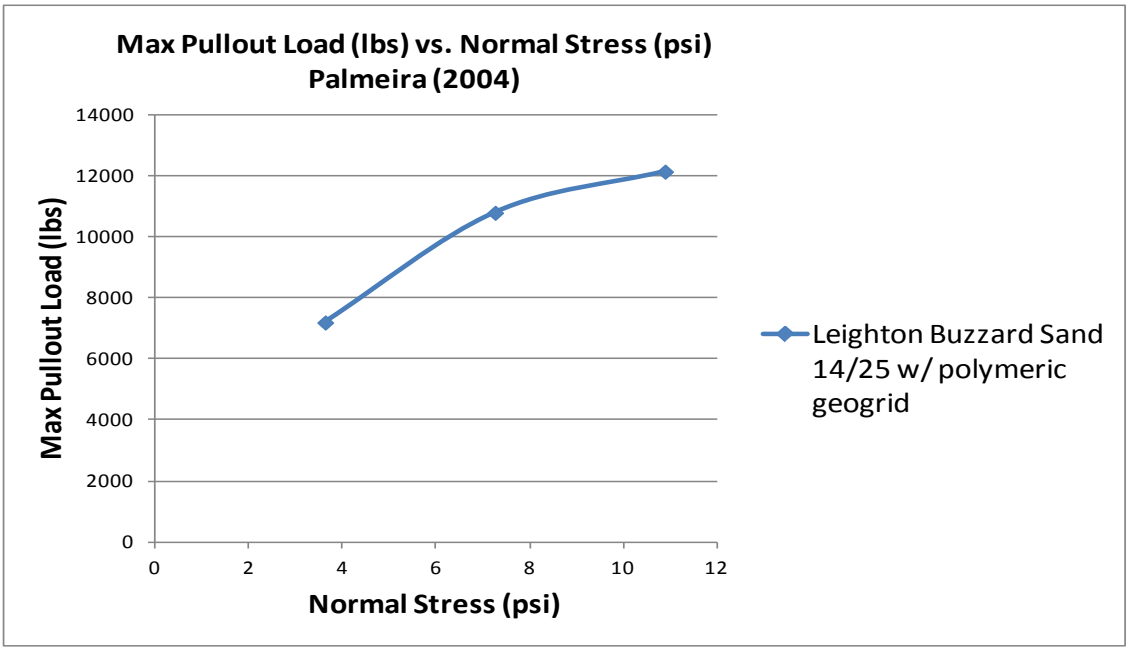

Figure 2.10: Linear relationship with intercept. (Palmeira, 2004).

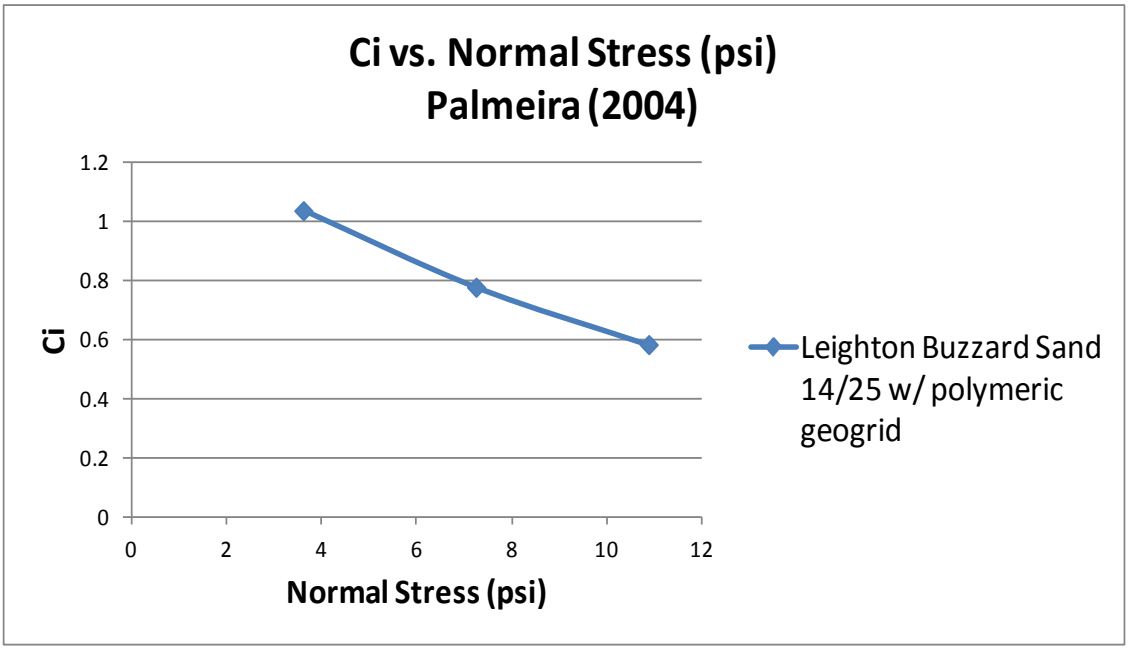

Figure 2.11: Relationship between Ci and Normal Stress. (Palmeira, 2004).

The pullout load shows a non-linear trend, as the Leighton Buzzard Sand does not have a cohesion intercept. As shown in Figures 2.10 and 2.11, this non-linear trend causes the Ci to decrease with increasing normal stresses ranging from 4 to 12 psi. At a normal stress range of 4 to 12 psi the pullout loads seem to have an intercept of 3,000 lbs. assuming a linear relationship. Since Ci corresponds to the ratio of two linear equations (i.e. interface shear strength and soil shear strength), the intercept is accounted for in the Ci equation. Because of this intercept, the Ci value decreases with increasing normal stress. The reason for the decrease is due to the normal stress in the denominator of the Ci equation:

$$Ci = \frac{\sigma * \tan(\delta) + a}{\sigma * \tan(\varphi) + c} \qquad (2.8)$$

Without the cohesion and adhesion values the normal stresses would cancel out, but with the adhesion and cohesion the increasing normal stress causes the Ci value to decrease. Physically, this means that the soil shear strength increases with increasing normal stress at a faster rate than the interface shear strength.

This is also shown by Abu-Farsakh et. al. (2006). This case study involves the testing of three different polymeric geogrids (UX750, UX1500, UX1700) on a silty clay soil. The clay soil tested had a medium plasticity index equal of 15; a maximum dry unit weight of 104 pcf; an optimum moisture content of 18.5%; an angle of internal friction of 24°; and a cohesion intercept of 300 psf.

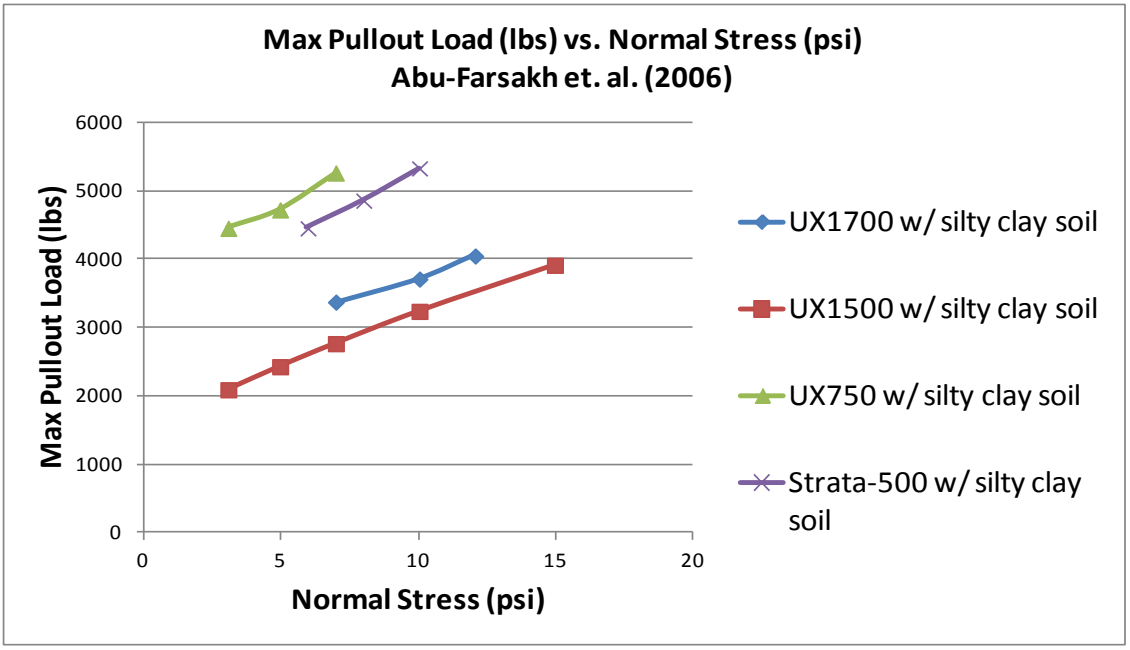

Figure 2.12: Linear relationship of max pullout versus normal stress showing an intercept, (Abu-Farsakh et. al., 2006)

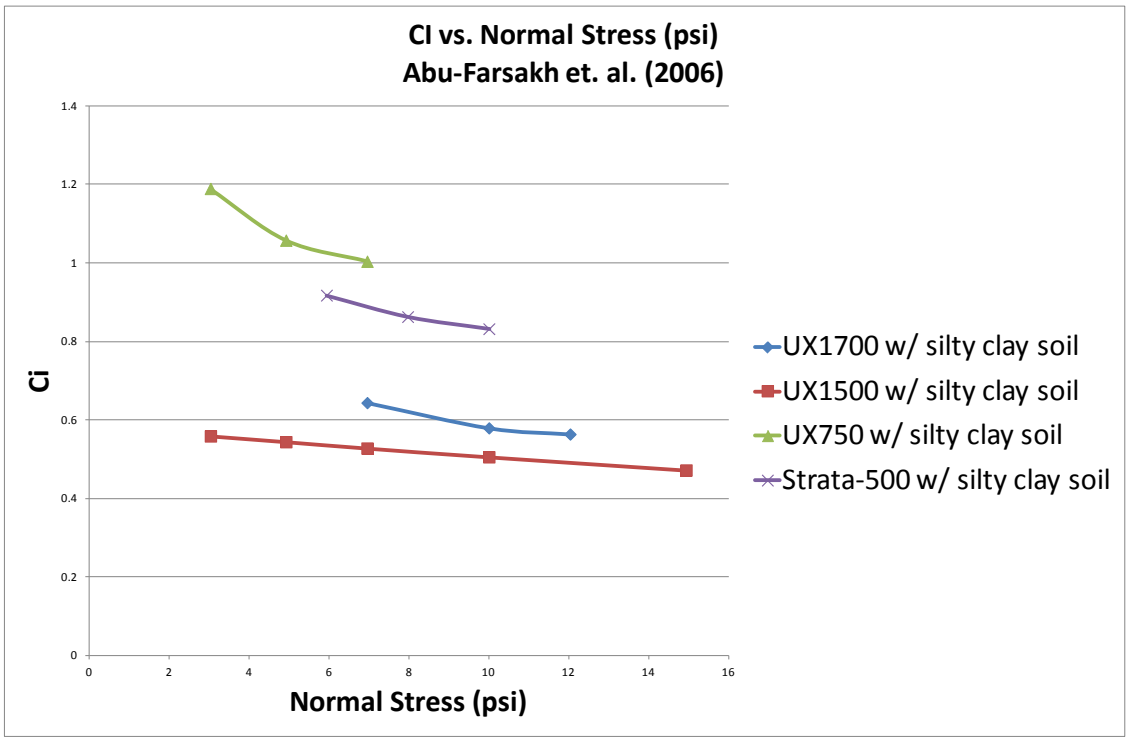

Figure 2.13: relationship between Ci and Normal Stress, (Abu-Farsakh et. al., 2006)

Figure 2.13 shows the coefficient of interaction results obtained using data reported by Abu-Faskah et. al. (2006). The results show a similar decreasing trend with Ci due to the adhesion in the interface shear strength.

2.4.2 Reinforcement Length

Palmeira and Milligan (1989) tested the effects of reinforcement length using a small pullout box. The results are shown in Figure 2.14.

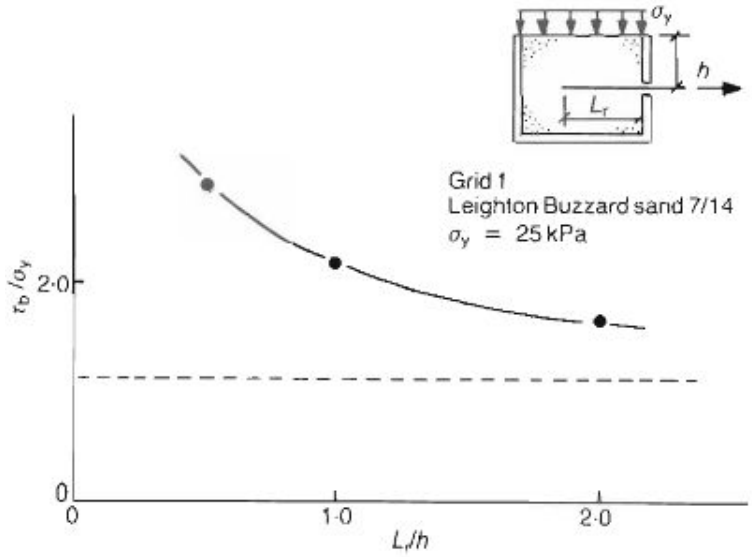

Figure 2.14: Normalized bond stress versus reinforcement length, (Palmeira and Milligan, 1989).

Figure 2.14 shows a graph of mean shear stress between soil and reinforcement normalized by the vertical pressure versus reinforcement length normalized by the half height of the box. The normalized mean shear stress at the interface decreases with increasing normalized reinforcement length. Increasing the reinforcement length causes an increase in the influence of the top and bottom boundaries. This is due to the reinforcement length increasing while the box dimensions stay the same. Since the large

pullout box has bigger dimensions, it can take on a bigger reinforcement length without experiencing interference from boundary conditions.

Teixeira (2007) conducted tests with varying reinforcement lengths using a large pullout box. The results agree with Palmeira and Milligan (1989) in that the coefficient of interaction results have smaller interference from top and bottom boundaries (i.e. Ci shows only a minor decreasing trend with increasing reinforcement length). The results are shown in Figure 2.15.

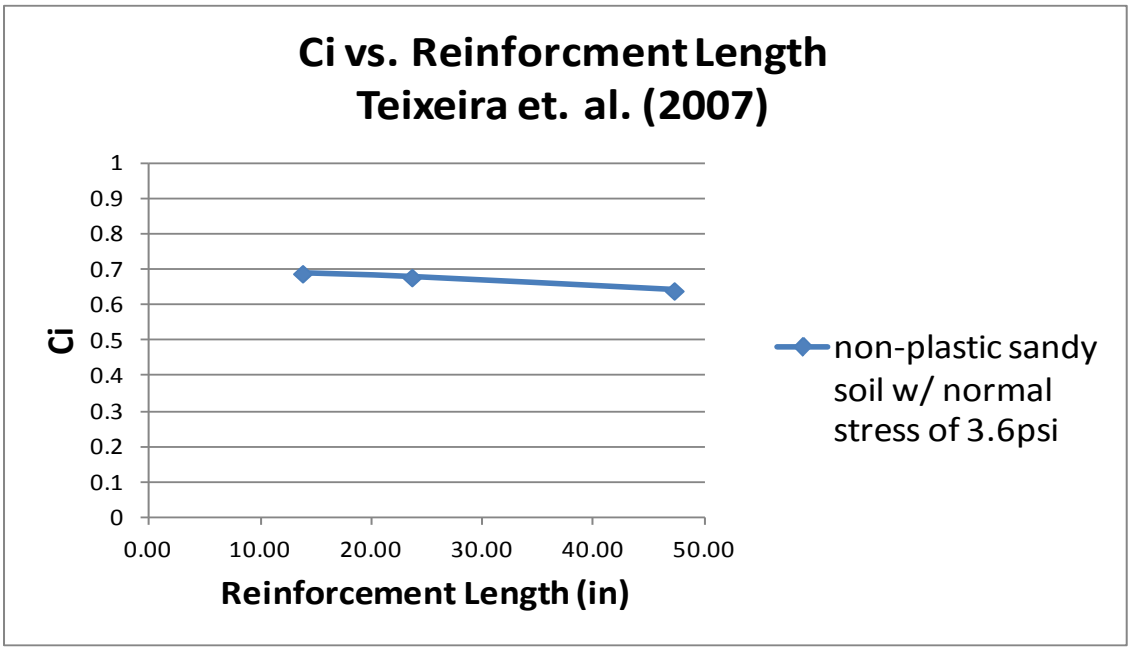

Figure 2.15: Constant Ci with varying reinforcement lengths, (Teixeira, 2007)

The figure shows that as the reinforcement length increases, the Ci value remains reasonably constant. If the ratio of pullout load to reinforcement length is linear with no intercept (i.e. constant), then Ci will also be constant. The pullout load vs. reinforcement length is in fact linear and is shown in Figure 2.16.

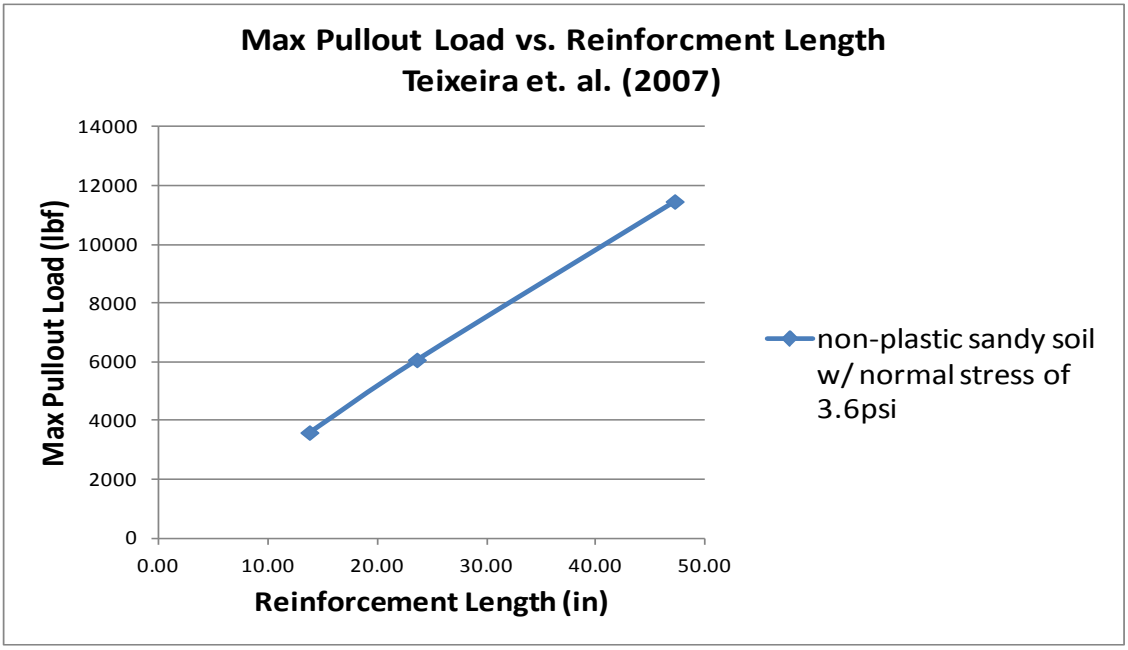

Figure 2.16: Linear relationship between pullout load and reinforcement length, (Teixeira, 2007).

The line in Figure 2.16 appears to have a small intercept, which explains the slight decrease in Ci. The intercept represents the influence caused by the top and bottom boundaries. This makes sense because at a reinforcement length of zero, the max pullout load should also be zero.

2.4.3 Influence of Spacing Between Transverse Members

The ratio between the spacing of geogrid transverse members and transverse member diameter (S/B ratio) is shown to have a significant effect on the pullout resistance. Palmeira and Milligan (1989) tested specimens with different S/B ratios and the results are shown in Figure 2.17.

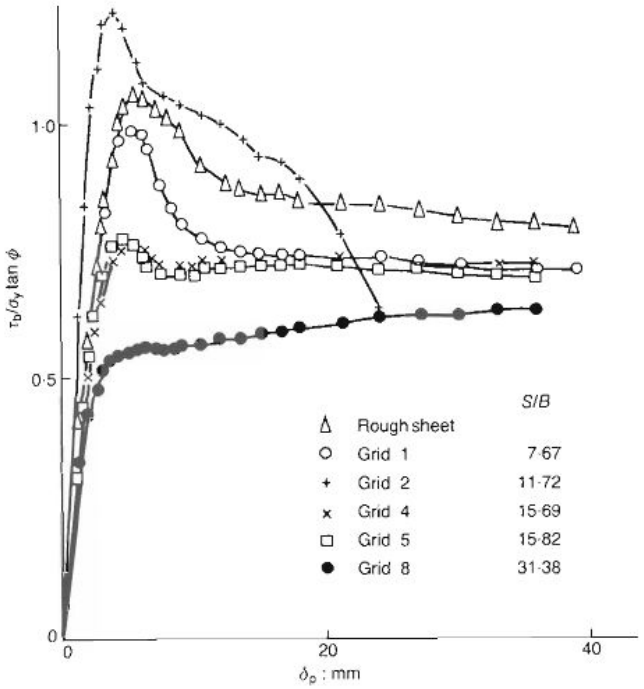

Figure 2.17: Friction coefficient versus displacement for different S/B ratios, (Palmeira and Milligan, 1989).

The y-axis is the friction coefficient and the x-axis is the pullout displacement. The graph shows that the larger S/B ratio not only results in a lower friction coefficient, but also results in no peak. The majority of the different S/B tests are below unity (i.e. $\tau b/\sigma y=\tan(\varphi)$). This means that the interface between the geogrid and soil has less friction resistance than the internal soil particles. The only exception is grid 2, which Palmeira and Milligan (1989) cannot explain as to why the peak is above unity. The reason for the decreasing friction coefficient is due to the larger S/B ratios having fewer transverse members inside the pullout box. Fewer transverse members decrease the amount of passive resistance and therefore decrease the pullout resistance. Teixeira (2007) found that an optimum spacing between transverse members exists such that the pullout resistance is maximized. Figure 2.18 shows this optimum spacing graph.

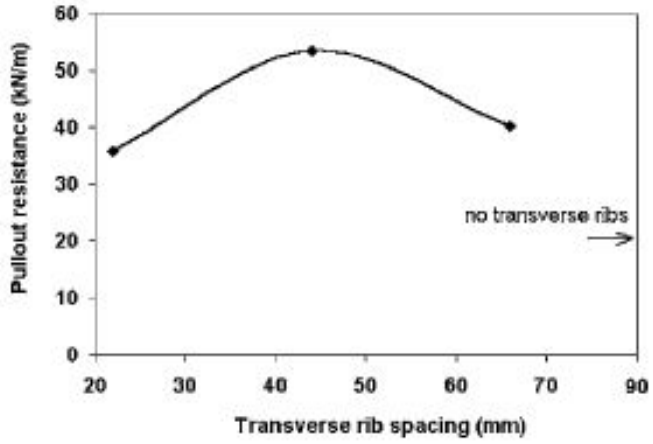

Figure 2.18: Optimum transverse rib spacing, (Teixeira, 2007).

The theory behind the optimum value relies on the interference between bearing members. This interference is caused by the leading bearing member leaving behind a trail of disturbed soil. This disturbed soil reduces the bearing resistance of the trailing bearing member. If the spacing is less of optimum, then more transverse members will be inside the pullout box causing more interference between not only the transverse members, but also the longitudinal members which create the frictional resistance. However, if the spacing is greater than optimum then there would be a lack of passive resistance due to fewer transverse members inside the pullout box.

Another influence of the transverse member is the ratio of transverse member thickness to soil particle size (B/D_{50}). Palmeira (2008) conducted tests on single isolated transverse members to evaluate the bearing stress of varying B/D_{50} ratios.

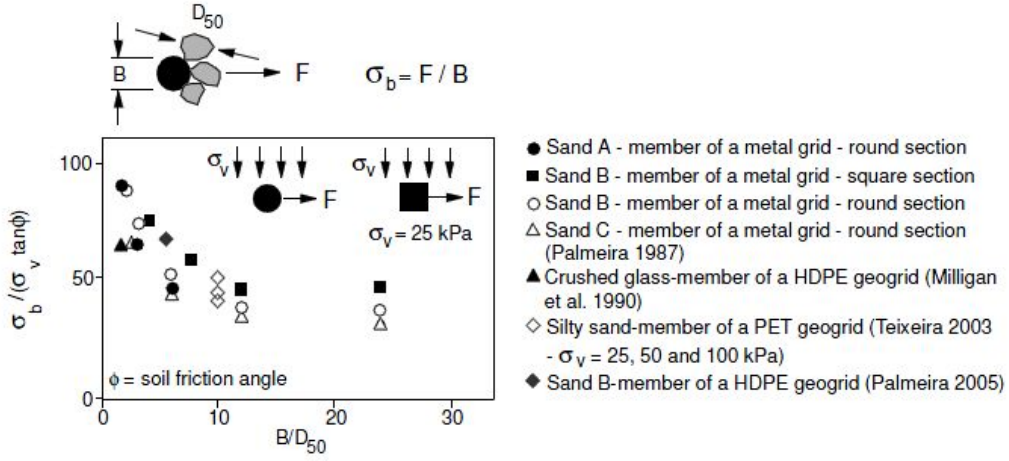

Figure 2.19: Pullout test results on isolated transverse members with different cross-sections, (Palmeira 2008).

The results from Figure 2.19 show that the bearing stress is greater for smaller B/D_{50} ratios. Also, the influence of the B/D_{50} ratio is insignificant beyond a ratio of 12. This large particle sizes have a larger contact area with the transverse members which contributes to more bearing and an increase in pullout resistance.

Another factor in the influence of the transverse member's contribution to the bearing stress is the shape of the transverse member. Transverse members with square shapes seem to produce slightly more bearing resistance than those with a circular shape. This is probably due to the fact that the square shape has more surface contact with the soil in front of it and so will have higher bearing stresses needed to overcome the larger surface area.

2.4.4 Tests with Single Isolated Members

Palmeira and Milligan (1989) performed various tests to see how transverse members affect each other. The results shown in Figure 2.20 show that as the bearing

member diameter to particle size ratio decreases the pullout displacement increases. This is significant because it shows the contribution of the bearing members to the pullout results.

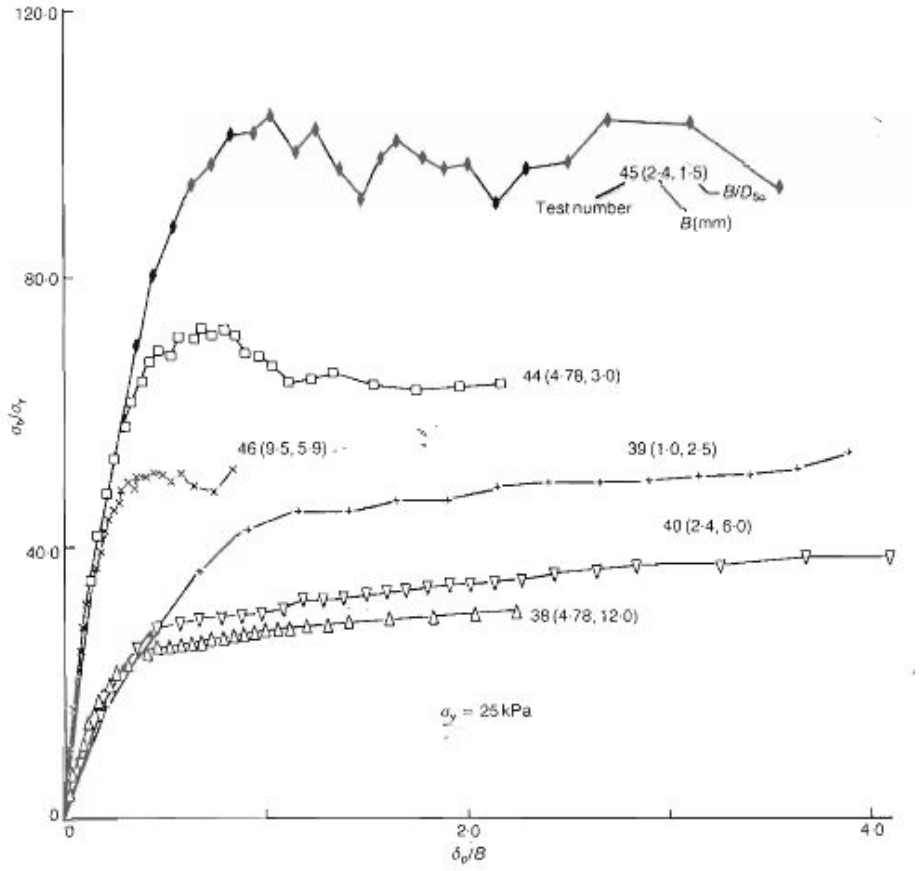

Figure 2.20: Normalized bond stress versus displacement for single and isolated bearing members, (Palmeira and Milligan, 1989).

Another important finding from these experiments was the positive correlation between the soil friction angle and the transverse member bearing stress, shown in Figure 2.21.

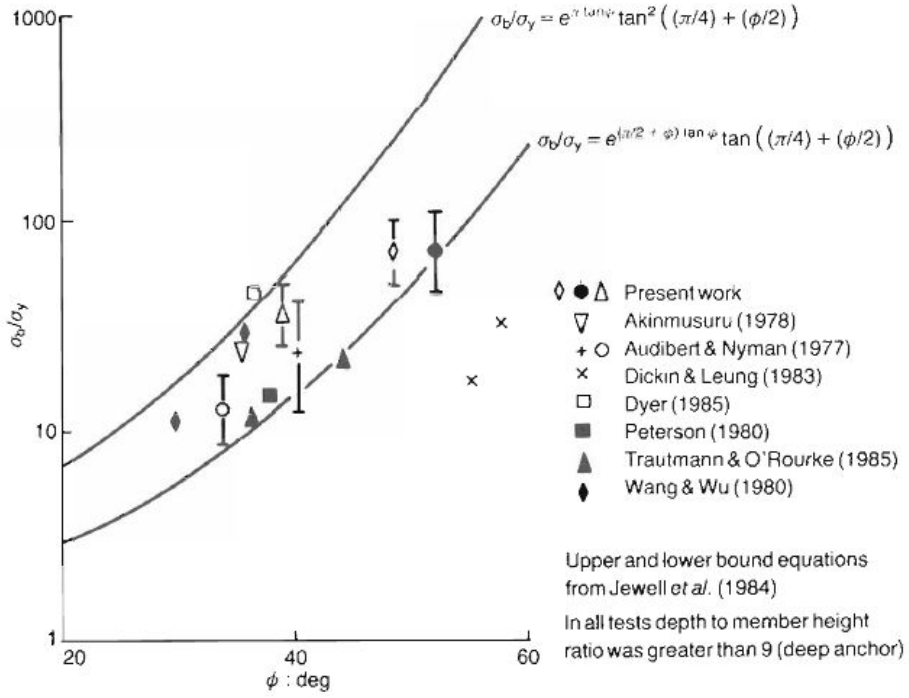

Figure 2.21: Bearing stress ratio versus soil friction angle, (Palmeira and Milligan, 1989).

The data is a collection of recent and past experiments put together to establish a upper and lower bounds. Such bounds can be used for future evaluations in order to predict a conservative estimate on the contribution of bearing stress.

2.4.5 Reduction in Bearing Efficiency

The large pullout box is not significantly affected by varying the location of the first transverse member to the front wall.

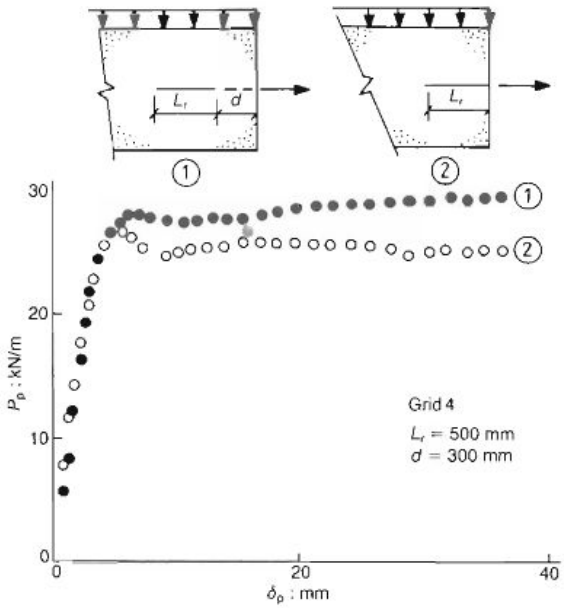

Figure 2.22: Pullout force versus displacement. Set up #1 is with first transverse rib separated by a distance "d" from front wall, (Palmeira and Milligan, 1989).

Figure 2.22 shows that there is no significant change in pullout load when the location of the first transverse rib varies. One important observation from this graph is the continuous increase in pullout load for the first setup where the reinforcement is at a distance "d" from the front wall. This is due to the first bearing member being able to find undisturbed soil ahead and the reinforcement length of the geogrid staying the same. The second setup shows that the first transverse rib does not have any undisturbed soil ahead and the reinforcement length will decrease as the specimen is being pulled out of the box.

The continuous increase in pullout load is an important result because it shows how the significant contribution the transverse members make towards the overall pullout load. Figure 2.23 shows results from tests where the longitudinal and transverse members are tested separately.

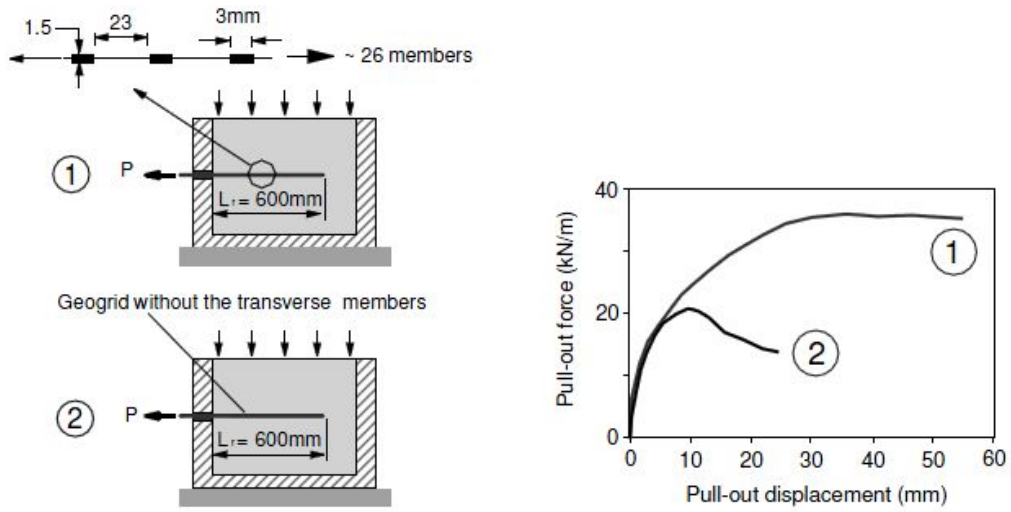

(a) Types of tests carried out. (b) Test results.

Figure 2.23: Pullout force versus displacement results for geogrids tested with and without transverse members, (Palmeira 2008).

Without the contribution of the transverse members the pullout force was found to experience a strain softening behavior with a discernible peak. Also, the longitudinal members only geogrid is less compliant and has half of the pullout force compared to the transverse and longitudinal member geogrid. The results show that the transverse members provide a significant portion of the total pullout force. They also show that a more compliant transverse member will allow the geogrid to take on higher pullout forces at higher displacements.

The majority of the forces generated in pulling out of a geogrid are from the bearing resistance of the soil acting against the transverse ribs. The load distribution between transverse members is uniform if there is a sufficient amount of spacing in-between each member. The photos shown in Figures 2.24 and 2.25 show examples of the reduction in bearing efficiency caused by close spacing of the transverse members.

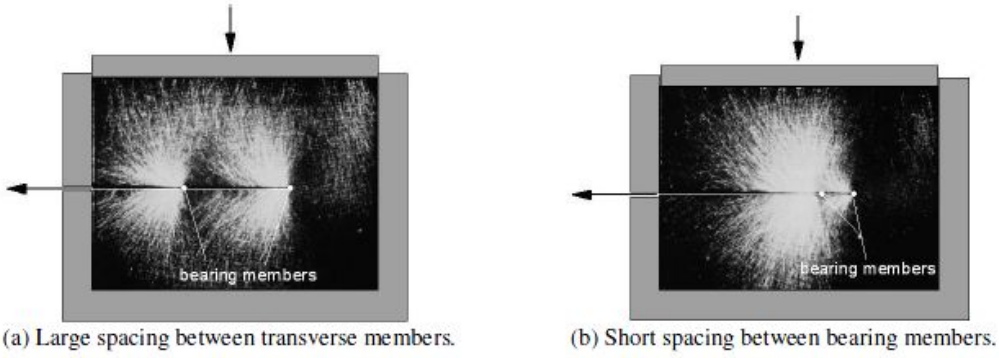

(a) Large spacing between transverse members. (b) Short spacing between bearing members.

Figure 2.24: Interference between grid transverse members, (Palmeira 2008).

If the spacing between members is short, as shown in Figure 2.24(b), then there is a significant difference in distribution loads among the transverse members. Figure 2.24(a) shows the pattern of stress distribution with sufficient spacing.

As the transverse members move through the soil they leave behind disturbed soil. This disturbed soil is shown to affect the trailing transverse members. Figure 2.25 shows an example of how the disturbed soil leads to a decrease in bearing efficiency for the bearing members.

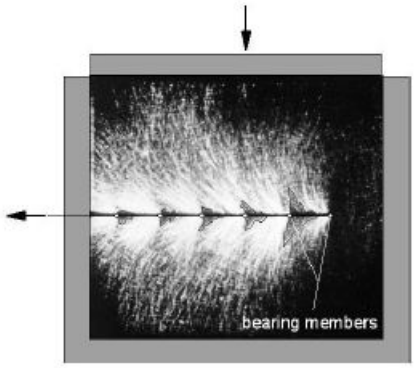

Figure 2.25: Weakened state of stress behind grid transverse members, (Palmeira 2008).

The darkened regions behind the transverse members are the disturbed soil regions created by the movement of the grid through the soil.

The reduction in bearing efficiency caused by insufficient spacing leads to a decrease in pullout resistance, but a larger spacing allows each transverse member to reach maximum bearing resistance. This can be seen from the results in Figure 2.26, which show an increasing trend of pullout force versus displacement.

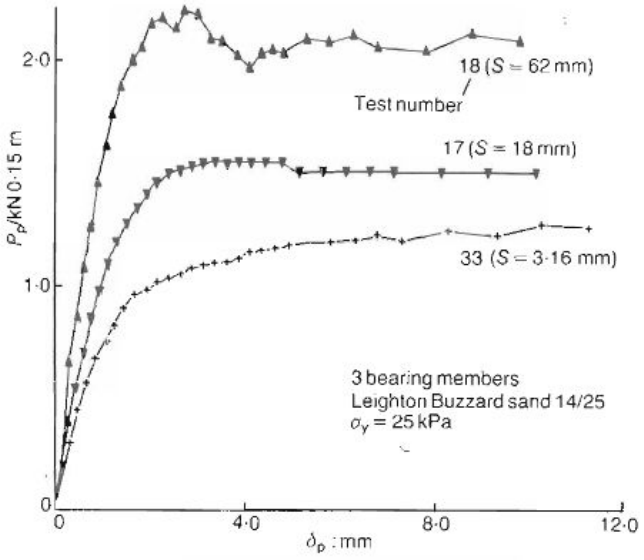

Figure 2.26: Pullout force versus displacement for bearing members with different spacing, (Palmeira and Milligan, 1989)

The reduction in bearing efficiency is defined by Palmeira and Milligan (1989) as the degree of interference between transverse ribs. This degree of interference can be found using the equation from Palmeira and Milligan (1989).

$$DI = 1 - \frac{P_p}{nP_o} \tag{2.9}$$

where P_P is the maximum pullout load for a geogrid with n bearing members; n is the number of bearing members; and P_o is the maximum pullout load for an isolated bearing member of the same geogrid.

Equation (2.9) compares the pullout load for a given geogrid with a pullout load for a geogrid that has no interference between bearing members (i.e. all bearing members are single isolated members). Figure 2.27 shows how the degree of interference varies with the spacing between bearing members.

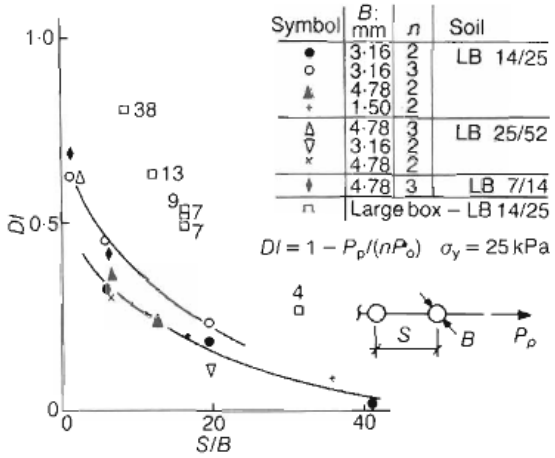

Figure 2.27: Degree of interference versus S/B, (Palmeira and Milligan, 1989).

The figure shows that for a spacing to transverse rib thickness ratio of 50 or higher the degree of interference becomes negligible.

Chapter 3: Pullout Testing Equipment and Materials

3.1 Overview

The purpose of pullout tests is to characterize the interface strength between the geogrid and soil. Pullout is one of the main modes of failure considered in the design of retaining walls.

The pullout box used for this study is shown in Figure 3.1. The pullout box is considered a large scale pullout box and has dimensions 24 in. wide by 60 in. long by 11 in. deep.

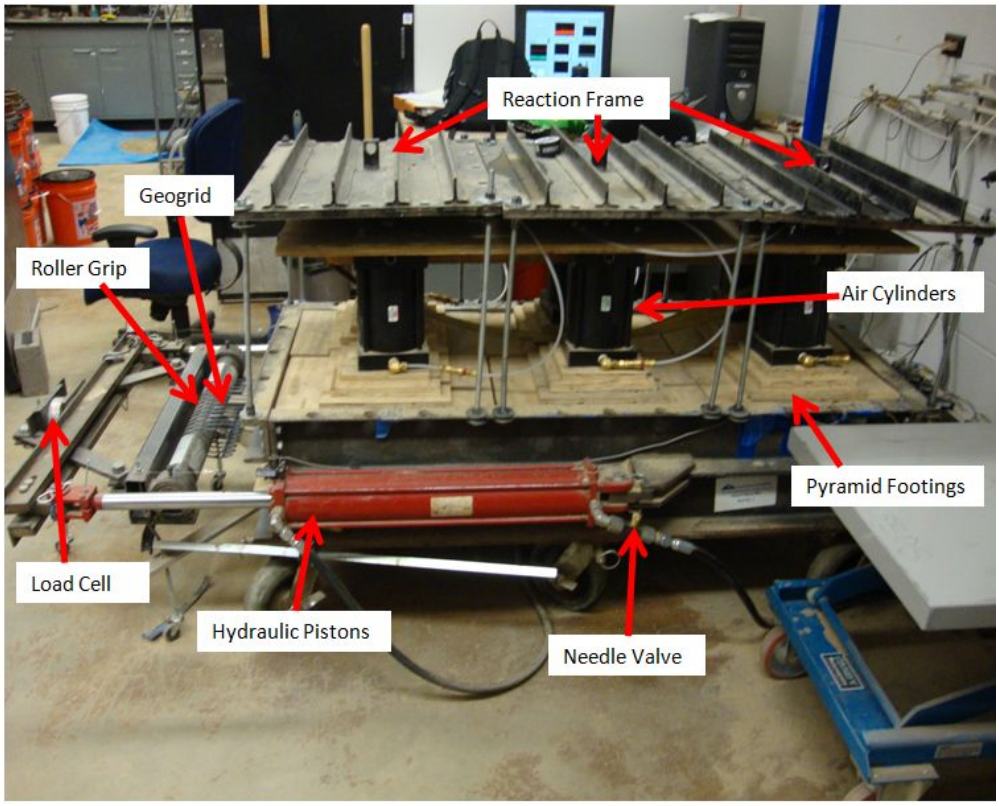

Figure 3.1: Large scale pullout box testing equipment.

Attached to the box are two hydraulic pistons, shown in Figure 3.1. The pistons uses hydraulic oil to generate pressure and extend the piston rods. The piston rods extend to 25 in. and their rate of displacement is controlled by two needle valves; one on each piston. There is a potential for error when using two hydraulic pistons due to the possibility that if not properly monitored the two piston rods can have different displacement rates. This will cause different pullout forces at different locations along the width of the specimen. An operator is needed to constantly monitor the displacement rate to ensure similar displacement rates.

As explained in the literature review, the sides and bottom of the pullout box need to have a frictionless surface. All sides of the box were aligned with non-textured HDPE geomembrane material. The geomembrane material was replaced if protrusions were found.

3.2 CHARACTERISTICS OF GEOGRIDS

The UX1400 and UX1700 were the two types of uniaxial geogrids used for the evaluation of both the Monterey Sand and dredged material. Both geogrids were provided by Tensar and consist of a high-density polyethylene polymer. The specifications for the geogrids are found in Table 3.1.

measured geogrid section	UX1400MSE	UX1700MSE
junction thickness (in)	0.146	0.322
cross machine direction rib width (in)	0.796	0.83
cross machine direction aperture size (in)	0.71	0.65
cross machine spacing (in)	17.6	17.9
machine direction rib width (in)	0.202	0.221
machine direction spacing (in)	0.91	0.87
machine direction aperture size (in)	16.8	17.1
machine direction thickness (in)	0.059	0.12

Table 3.1: Geogrid characteristics.

The UX1400 has a smaller transverse and longitudinal rib thickness compared to the UX1700. Since the transverse rib spacing is approximately the same for both geogrids, the UX1700 has a lower spacing to thickness ratio, S/B. This ratio is used often in the analysis of the literature review as well as the interpretation of the data in the following sections.

3.3 MONTEREY SAND PROPERTIES

The Monterey Sand used in the pullout testing is a SP sand described as rounded to sub-rounded, consisting of mainly of quartz with a small amount of feldspars and other minerals. The medium particle size distribution, D_{50}, is 0.7 mm. The particle size distribution curve is shown in Figure 3.2.

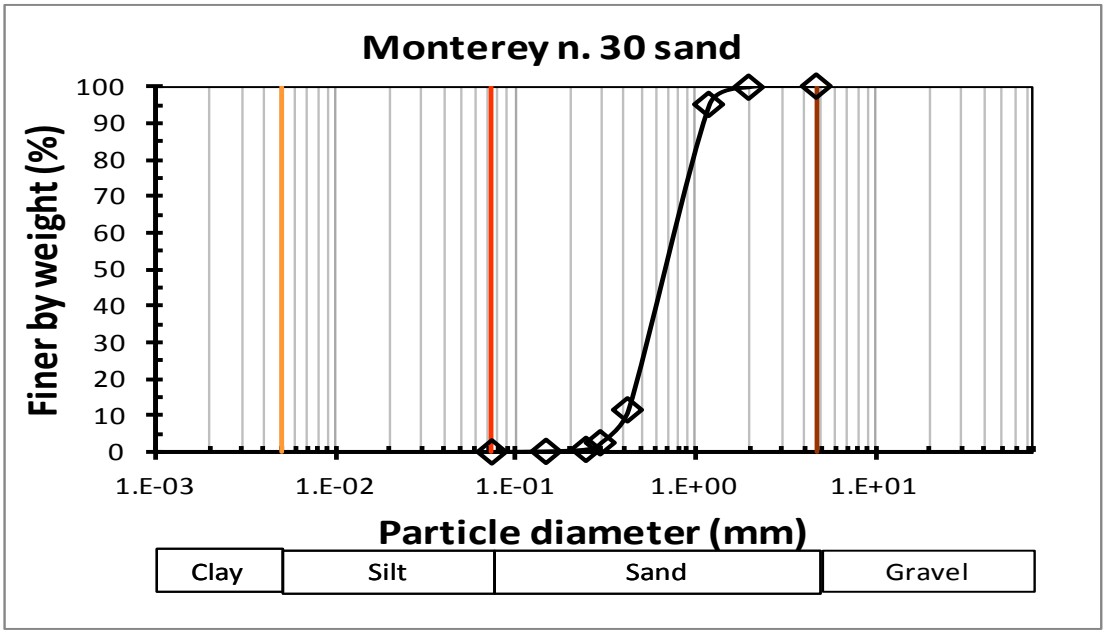

Figure 3.2: Grain Size Distribution Curve for Monterey Sand.

The sand was tested using a relative density of 65%, with a corresponding effective friction angle of 35°. For control purposes, the moisture content was kept a constant 1.5% for all testing with the sand.

A dry density of 99.3 pcf was used in the calculations for determining the correct weight of each lift for each of the Monterey Sand tests. Small fluctuations in the density were found despite the precautions used to ensure constant compaction energy.

Type	Test #	Normal Stress (psi)	Dry Density (pcf)
UX1400	103	0.5	99.467
UX1400	37	4	99.410
UX1400	90	4	100.300
UX1400	107	4	99.545
UX1400	108	4	99.545
UX1400	33	6	99.350
UX1400	91	6	101.300
UX1400	32	8	99.290
UX1400	89	8	99.220
UX1700	104	0.5	100.198
UX1700	34	4	99.440
UX1700	85	4	99.140
UX1700	87	6	99.300
UX1700	92	8	101.300
UX1700	35	8	99.390

Table 3.2: Small fluctuations in dry density with each Monterey Sand test.

Table 3.2 shows all of the Monterey Sand tests and the dry densities that were measured prior to starting each test. There are some small changes in the dry density with each test, but not enough to cause significant distortion of the pullout test results.

3.4 MPA DREDGED MATERIAL PROPERTIES

The laboratory component of this research involved two types of dredged materials; one of them was obtained from Baltimore, Maryland and the other from Fort Mifflin, Philadelphia, Pennsylvania. A series of laboratory tests were performed in Drexel University to evaluate the basic physical properties of the dredged materials including as-received moisture content, specific gravity (Gs), loss on ignition (LOI), grain-size distribution, and Atterberg limits. The soils were then classified as an OH soil according to the USCS and the American Association of State Highway Transportation Officials (AASHTO) systems. Table 3.3 summarizes the physical properties of the MPA dredged material.

			Particle Size			
Soil Tested	Specific Gravity	Loss on ignition	Gravel (%)	Sand (%)	Fines (%)	USCS
DM-MPA	2.58	11.76	0	1.2	98.8	OH

Table 3.3: Soil properties of the MPA dredged material.

LOI was used to determine the organic matter content of the DM. As shown in Table 3.3 the MPA DM had an LOI of 11.76. The grain size curves for the DM from Maryland Port Authority (MPA) is presented in Figures 3.3. The DM curve in Figure 3.3 is the top line that is almost horizontal. This DM curve shows that the majority of the particle sizes are fines.

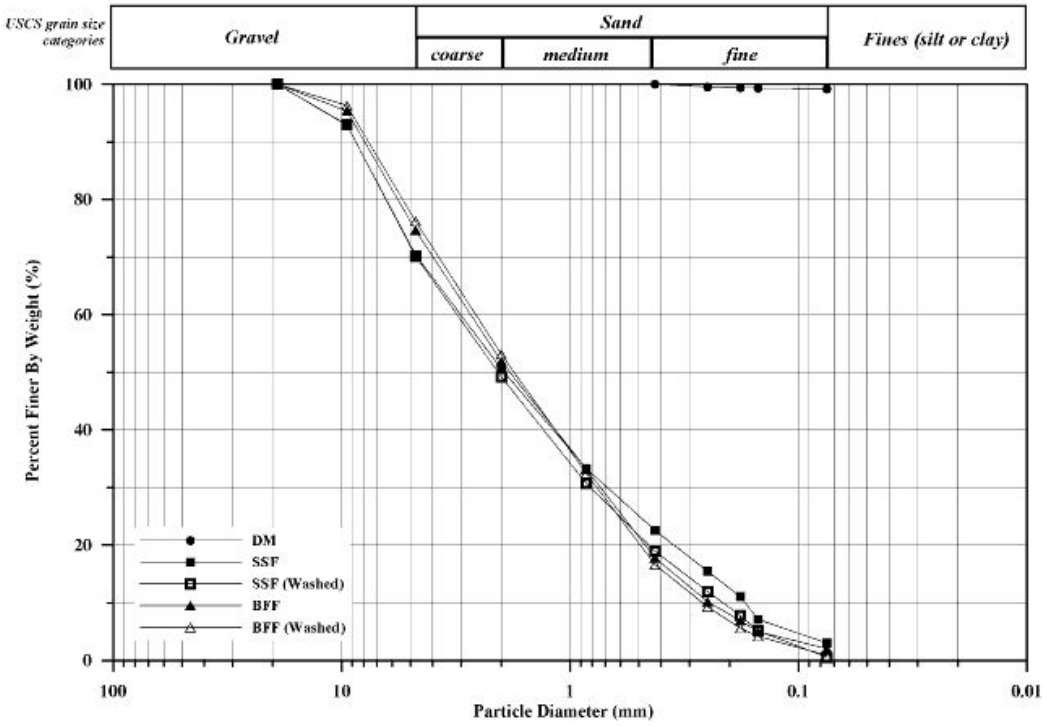

Figure 3.3: Grain size distribution curve for dredged material from MPA.

Laboratory moisture–density relationships were developed following the modified (ASTM D1557, ASTM 2000a) Proctor method using five or six moisture–density points. The laboratory test results for the Modified Proctor tests are shown for the dredged material from Maryland in Figure 3.4. The DM moisture curve is the bottom curve shown in Figure 3.4. These moisture–density curves exhibit the characteristic convex shape typical of OH soils. The maximum dry density observed were 86 pcf for the Maryland DM samples, while the optimum water contents were 28%.

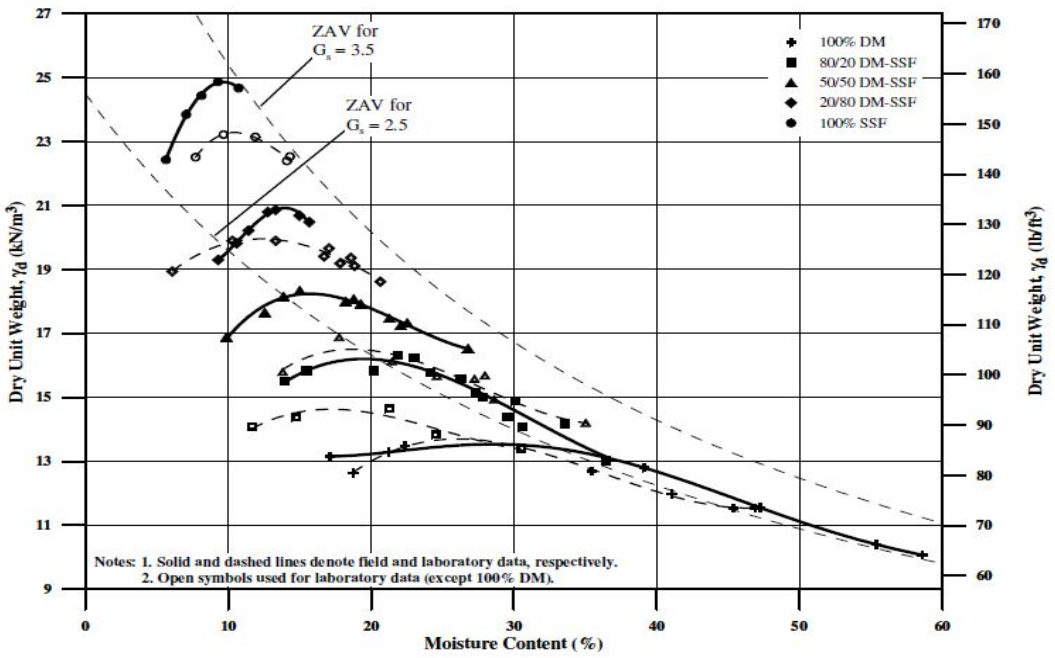

Figure 3.4: Modified compaction curve for dredged material from MPA

The target dry density used for determining the weight of each lift was 68pcf for the MPA dredged material. Table 3.4 shows the actual dry densities ultimately used for

each test. The actual dry densities were reasonable similar throughout the testing and within reasonable variations to the target dry densities. The moisture content for the MPA DM was well over the optimum moisture content. The MPA was tested at moisture contents ranging from 37 to 44% whereas the optimum moisture content for the MPA DM was 28%.

Soil Type	Test #	Geogrid Type	Normal Stress (psi)	Dry Density (pcf)	Moisture Content (%)
DM-(MPA)	97	UX1400	4	67.88	38
DM-(MPA)	49	UX1400	6	70.66	44
DM-(MPA)	48	UX1400	8	66.13	40
DM-(MPA)	50	UX1700	4	67.27	38
DM-(MPA)	95	UX1700	6	68.64	37
DM-(MPA)	96	UX1700	8	67.83	40

Table 3.4: Dry density for each MPA dredged material test.

Direct shear tests were performed on the DM in order to determine the shear strengths of the materials for the moisture and density conditions used in the pullout testing program. All direct shear tests for this pullout testing program were tested at the University of Texas at Austin. The direct shear tests were conducted to define the shear strengths of the DM at a normal stress range of 4 to 8 psi. These test results are shown in Table 3.5.

	normal stress (psi)	shear stress (psi)	cohesion (psi)	friction angle
DM-MPA	4	7.5	5.35	27.7
	6	8.4		
	8	9.6		

Table 3.5: Undrained Shear Strength of the MPA dredged material.

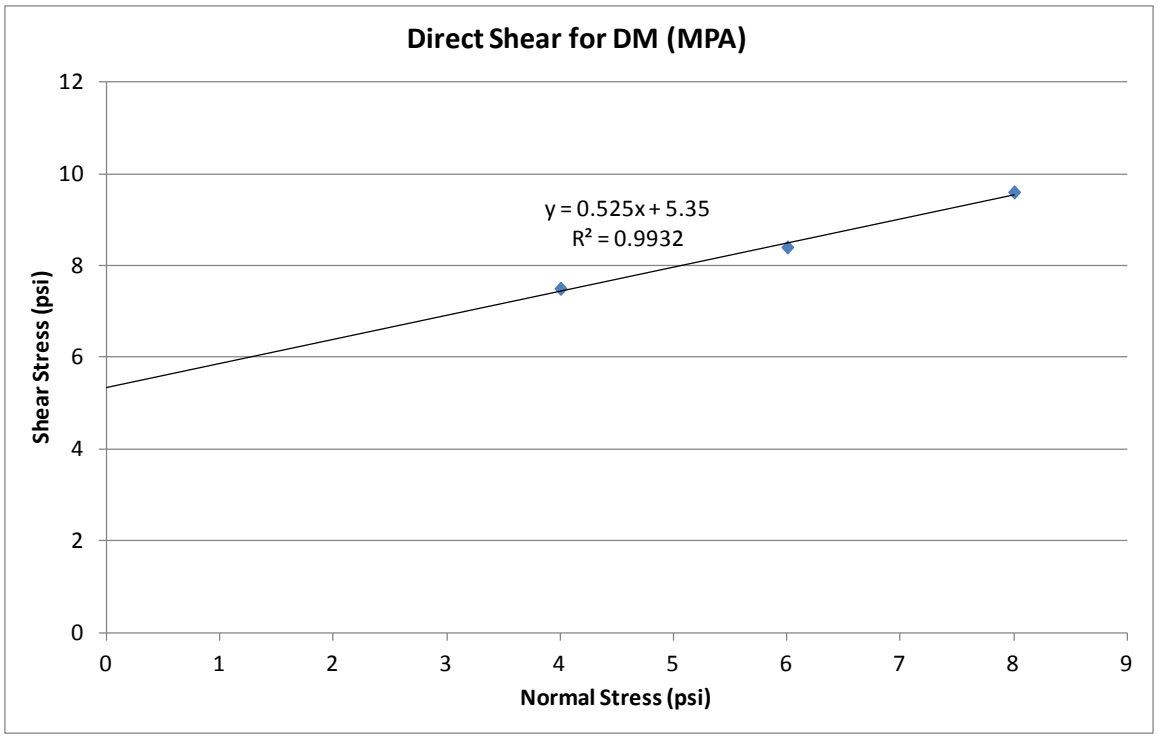

Figure 3.5: Direct shear results for MPA dredged material.

The direct shear results show a typical undrained shear strength for a cohesive soil. The friction angle is less than the friction angle for the Monterey Sand, but there is a cohesive component to the MPA DM shear strength.

3.5 PHILADELPHIA DREDGED MATERIAL PROPERTIES

The second dredged material that was used in this study was the Philadelphia dredged material. The laboratory tests used to evaluate the basic physical properties of the Philadelphia dredged material were conducted at Drexel University. The Philadelphia dredged material showed physical properties similar to the MPA DM. Table 3.6 summarizes the physical properties of the Philadelphia dredged material.

			Particle Size			
Soil Tested	Specific Gravity	Loss on ignition	Gravel (%)	Sand (%)	Fines (%)	USCS
DM-Philadelphia	2.4	11	0	3.4	96.6	OH

Table 3.6: Soil properties of the Philadelphia dredged material.

The grain size curves for the DM from Philadelphia is presented in Figure 3.6. Form the grain size curve and the particle size results shown in Table 3.6, the Philadelphia DM has a similar particle size as the MPA DM and both are classified as organics clays, OH.

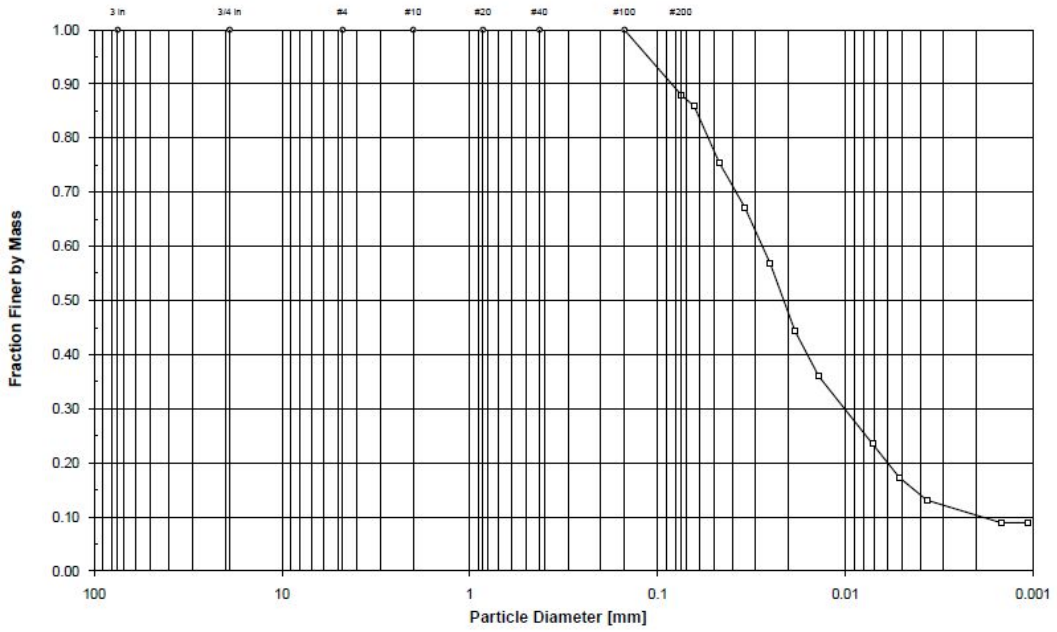

Figure 3.6: Grain size distribution curve for dredged material from Philadelphia.

Figure 3.7 shows the Modified Proctor tests results for the dredged material from Philadelphia. The figure shows a maximum dry density of 90 pcf with a optimum water content of 23%. The Philadelphia has a slightly larger maximum dry density compared to the MPA DM, but a lower optimum water content.

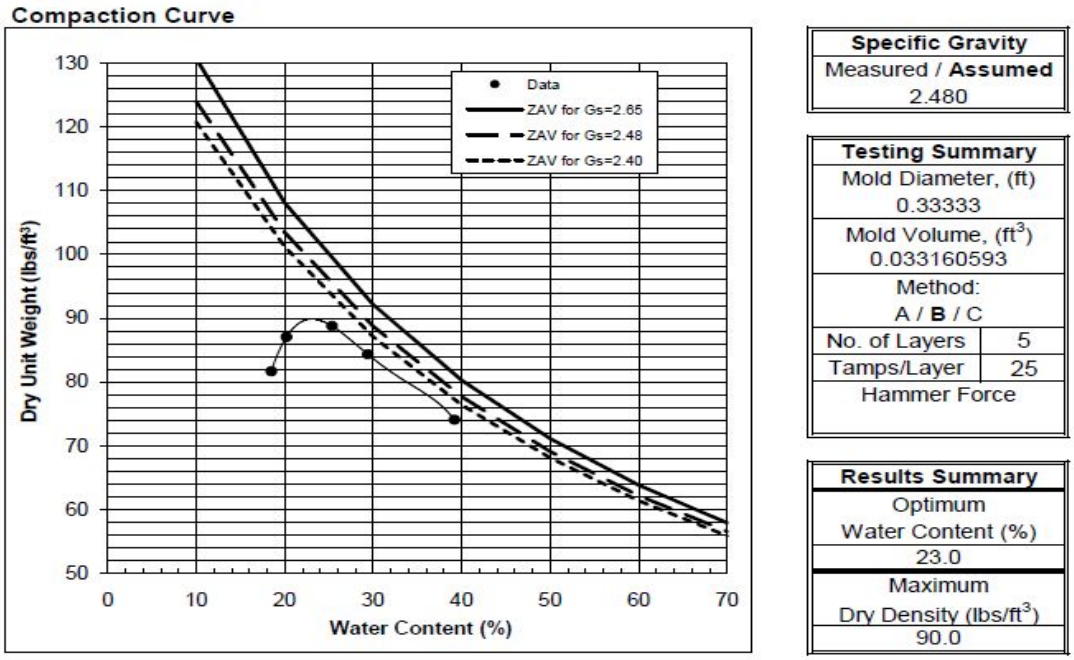

Figure 3.7: Modified compaction curve for dredged material from Philadelphia

The target dry density used for determining the weight of each lift was 60 pcf for the Philadelphia dredged material. Table 3.7 shows the actual dry densities for each test. The actual dry densities look to have been held constant throughout the testing and within reasonable variations to the target dry densities.

Soil Type	Test #	Geogrid Type	Normal Stress (psi)	Dry Density (pcf)	Moisture Content (%)
DM-(Philadelphia)	56	UX1400	4	60.25	51
DM-(Philadelphia)	57	UX1400	6	60	50
DM-(Philadelphia)	58	UX1400	8	60	50
DM-(Philadelphia)	59	UX1700	4	60	50
DM-(Philadelphia)	60	UX1700	6	60	50
DM-(Philadelphia)	61	UX1700	8	60	50

Table 3.7: Dry density for each Philadelphia dredged material test.

Direct shear tests were performed on the Philadelphia DM at the University of Texas at Austin. The purpose of the direct shear tests was to determine the undrained shear strengths of the soils. The direct shear tests evaluates the shear strengths of the DM at a normal stress range of 4 to 8 psi. These test results are shown in Table 3.8 and Figure 3.8.

	normal stress (psi)	shear stress (psi)	cohesion (psi)	friction angle
DM-Philadelphia	4	4.9	3.12	25.5
	6	6.25		
	8	6.81		

Table 3.8: Undrained Shear Strength of the dredged material.

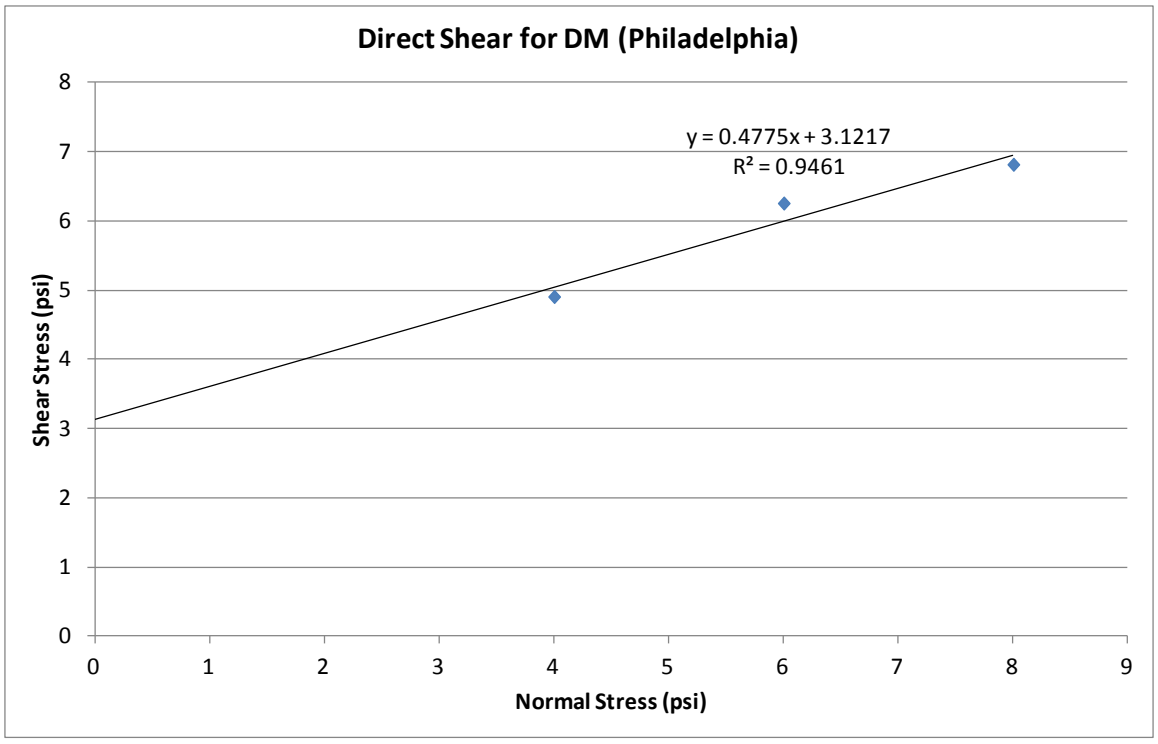

Figure 3.8: Direct shear results for MPA and Philadelphia dredged material.

3.6 PULLOUT TESTING PROCEDURES

Prior to running the tests, the geogrid specimen needs to be prepared in accordance with ASTM D6706-01. In addition to trimming the specimen to its proper dimensions, tell-tales are tied around three transverse members. Figure 3.9 shows the placement of the tell-tales in relation to the geogrid.

Figure 3.9: Prepared geogrid specimen with tell-tales attached.

The tell-tales are made of inextensible string, usually piano wire or fishing line. The tell-tales are then encased inside a polyethylene tube. The tube is to minimize friction between the tell-tales and soil. In addition to prepping the geogrid, the control of the moisture content of the soil is critical in determining the optimum conditions for the interaction between geogrid and soil. Optimum moisture content would obviously maximize density in our soil, but a few of the materials that were tested were wet of

optimum and could not reach optimum moisture content. Instead constant moisture content was used for the entire testing of that soil sample (i.e. all of the 100% dredged material tests).

Once the soil weight per lift was determined, the first lift was then placed into the box. The soil for each lift was stored in a sealed container in order to maintain the moisture content of the soil sample. Once the correct amount of soil is placed for the first lift, the lift is leveled and compacted to the proper dimensions, as determined based on the target density for the test. Typically each lift is compacted at a volume of two cubic feet. The compaction method adopted to prepare the dredged material involved using a combination of a hand tamper and a hammer drill. Once the layer has been compacted and checked for target density (by measuring the height) the top is scarified.

The geogrid was carefully placed on top of the second layer. The end of the geogrid is clamped to the roller grip that will be displaced as the pistons move forward. The geogrid is clamped so the places where the screws attach to the bar have an even distribution of clamping force spread throughout the geogrid width. Figure 3.10 shows an example of how the geogrid is clamped to the roller grip.

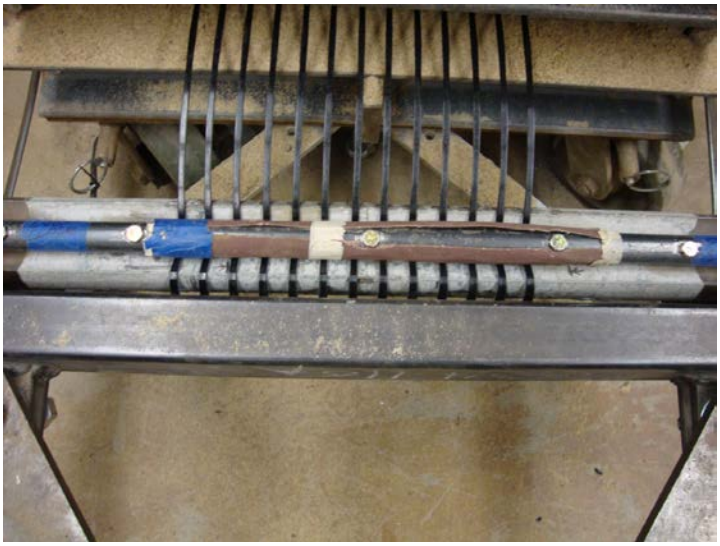

Figure 3.10: Geogrid clamped to the roller grip.

The geogrid inside the box must have an even distance from the end of the geogrid's transverse length to the side walls. The minimum distance should be 15cm. This is to ensure that the pullout test represents as closely to field conditions as possible. Once the geogrid is in place the roller grip is turned 270˚ so the geogrid wraps around the roller grip. Figure 3.11 shows an example of the geogrid wrapped around the roller grip.

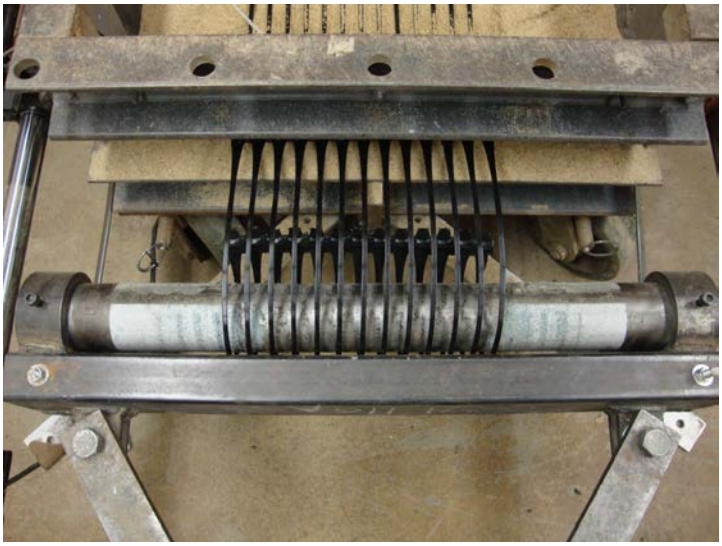

Figure 3.11: Geogrid turned 270 degrees to minimize stress concentrations.

An earth pressure cell was placed flat and around fine soil (previously sieved) to prevent large aggregates to press down on the earth pressure cell causing the results to become skewed. The purpose of the earth pressure cell is to verify the magnitude of the normal pressure. The location of the earth pressure cell varied in different tests all along the geogrid specimen to ensure all parts of the specimen were subjected to the correct amount of normal stress.

An additional layer of neoprene was placed in between the top layer of soil and the footings for the air cylinders. The neoprene acts as a flexible mat to help distribute the overburden stress evenly to the top layer of soil.

Use of plywood footings were another modification made to the equipment to transfer the load from the air cylinders evenly throughout the pullout box.

Figure 3.12: Placement of plywood footings.

Figure 3.12 shows the arrangement of the footings. Initial tests with the earth pressure cell showed that the normal stress from the air cylinders did not distribute the load evenly when flat plywood sheets were used instead of the pyramid footings. The footings replaced the plywood sheets in order to better distribute the load throughout the pullout box.

The air cylinders were arranged as shown in Figure 3.13 and used to induce the target normal stress acting on the soil and geogrid interface.

Figure 3.13: Placement of air cylinders.

Air cylinders were used instead of the air bladder system. Previous earth pressure cell readings showed that the air bladder system induced normal stresses that were below the required minimum threshold.

Reaction frames, shown in Figure 3.14, covered the top of the air cylinders.

Figure 3.14: Placement of reaction frames on top of cylinders.

When the air pressure entered the cylinders the piston arms elevated until contact was made with the reaction frames. Normal stress was verified with the earth pressure cell inside the pullout box as well as a pressure gage attached to the end of the tubing system that supplied the air pressure to the cylinders.

The displacement of the geogrid was controlled by two horizontal pistons attached on the outside of the pullout box. The displacement rate adopted in all tests was one millimeter per minute.

Chapter 4: Pullout Test Results and Analysis

4.1 Scope of Testing Program

For this thesis a total of 36 pullout tests were conducted. Within these tests certain parameters were changed in order to evaluate their effectiveness. Table 4.1 shows the schedule of the pullout tests and the different parameters that were assigned to a specific test.

Test #	Date	Geogrid Type	Soil Type	Normal Stress (psi)	Embedment Length (in)	Width (in)
97	2-Nov-12	UX1400	MPA DM	4	35.64	12
98	11-Nov-12	UX1400	MPA DM	4	53.52	12
47	25-Apr-12	UX1400	MPA DM	4	35.64	12
49	29-Apr-12	UX1400	MPA DM	6	35.64	18
48	28-Apr-12	UX1400	MPA DM	8	35.64	12
50	30-Apr-12	UX1700	MPA DM	4	35.64	12
95	19-Oct-12	UX1700	MPA DM	6	35.64	12
96	30-Oct-12	UX1700	MPA DM	8	35.64	12
51	1-May-12	UX1700	MPA DM	8	36	12
99	19-Nov-12	UX1700	MPA DM	12	35.64	12
56	4-Jul-12	UX1400	Philadelphia DM	4	34.44	12
57	5-Jul-12	UX1400	Philadelphia DM	6	34.08	12
58	6-Jul-12	UX1400	Philadelphia DM	8	34.44	12
59	6-Jul-12	UX1700	Philadelphia DM	4	34.08	12
60	7-Jul-12	UX1700	Philadelphia DM	6	34.44	12
61	9-Jul-12	UX1700	Philadelphia DM	8	34.08	12
103	9-Jan-13	UX1400	Monterey Sand	0.5	35.64	12
37	2-Apr-12	UX1400	Monterey Sand	4	35.64	18
90	19-Jul-12	UX1400	Monterey Sand	4	34.44	12
107	8-Feb-13	UX1400	Monterey Sand	4	20.592	12
108	13-Feb-13	UX1400	Monterey Sand	4	55.44	12
33	27-Mar-12	UX1400	Monterey Sand	6	37.68	18
91	19-Jul-12	UX1400	Monterey Sand	6	34.44	12
32	26-Mar-12	UX1400	Monterey Sand	8	35.64	18
89	18-Jul-12	UX1400	Monterey Sand	8	36	12
104	9-Jan-13	UX1700	Monterey Sand	0.5	34.8	12
34	28-Mar-12	UX1700	Monterey Sand	4	34.44	18
85	17-Jul-12	UX1700	Monterey Sand	4	34.44	12
87	17-Jul-12	UX1700	Monterey Sand	6	34.44	12
92	20-Jul-12	UX1700	Monterey Sand	8	34.44	12
35	29-Mar-12	UX1700	Monterey Sand	8	35.64	18

Table 4.1: Dry density for each Philadelphia dredged material test.

Each soil type was tested with the UX1400 and UX1700 geogrid with normal stresses ranging from 4 to 8 psi. Additional tests were conducted for the evaluation of the geogrid embedment length. These tests varied the embedment length from 20 to 55 in. using the UX1400 geogrid at a normal stress of 4 psi.

4.2 PULLOUT TESTS CONDUCTED WITH MONTEREY SAND

Granular soils are primarily used as the backfill of choice in reinforced soil walls and embankments. Their advantages in drainage and superior frictional resistance make for a better interaction with the geosynthetic reinforcements. For this research sand was used as a control material. Its purpose is to: 1). verify that the pullout system recreated conditions that produced results similar to results found in the literature review and 2). provide a baseline of results in which to compare the dredged material with.

4.2.1 Pullout Test Results Using Monterey Sand

The tests conducted on the Monterey Sand used two different types of geogrids (UX1400 and UX1500) at confining pressures ranging from .5psi to 8 psi. The results, in Figure 4.1 are for Test 103 in Table 4.1.

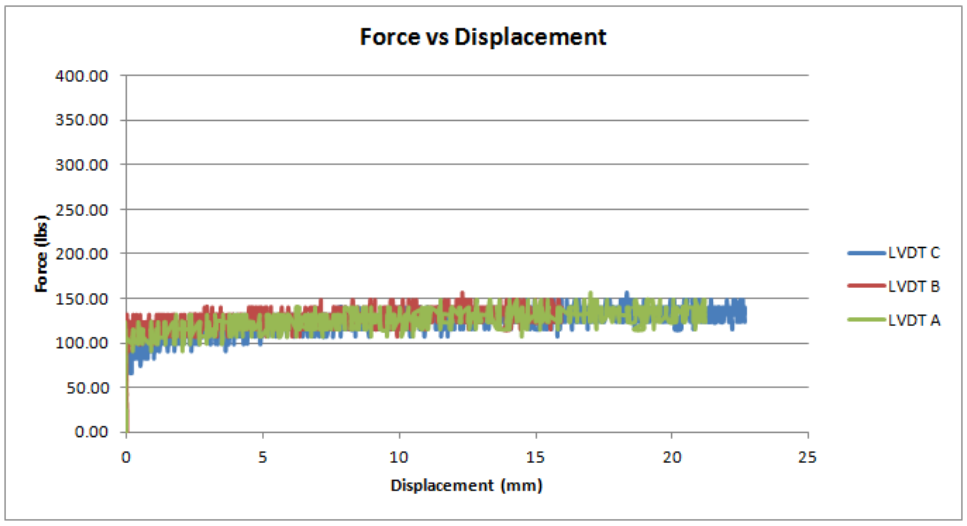

Figure 4.1: Monterey Sand with UX1400 under a normal stress of .5psi.

Figure 4.1 shows the displacement of the lvdts in relation to the pullout force. The lvdts are attached to the geogrid as shown in Figure 3.9. The results from Figure 4.1 show that the test reaches a plateau at around 150 lbs. of pullout load with a normal stress of .5 psi. The .5 psi is the dead load of all the components that help distribute the dead load (i.e. air cylinders, pyramid footings, neoprene sheet).

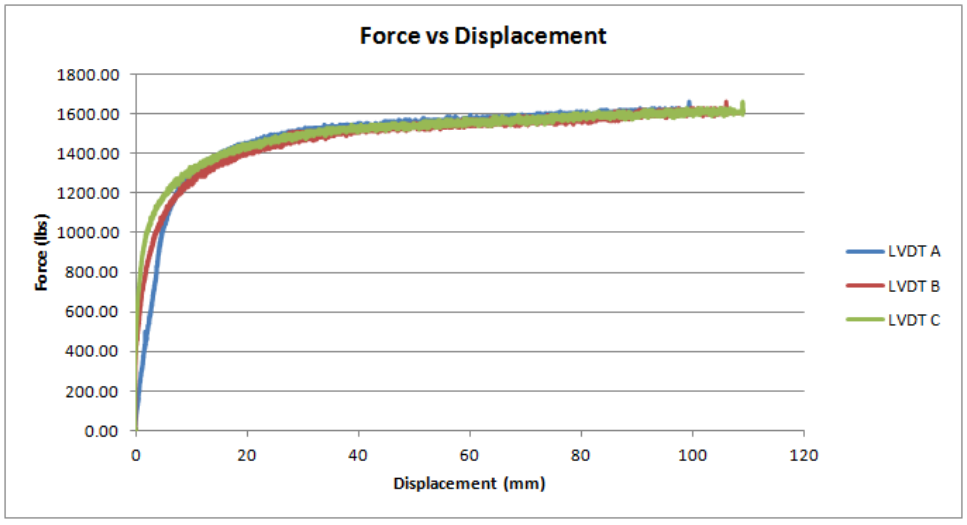

Figure 4.2: Monterey Sand with UX1400 under a normal stress of 4psi.

Figure 4.2 shows the results for Test 37. With an increase in normal stress to 4 psi, the pullout resistance increases an order of magnitude higher. In addition, the maximum lvdt displacements increase to 100 millimeters. Lvdt A displaces first since it is attached to the transverse rib nearest the load cell.

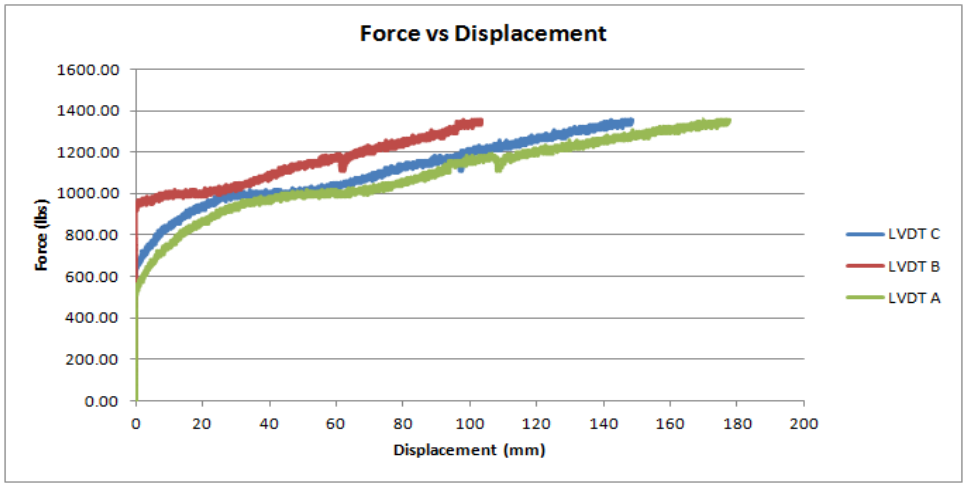

Figure 4.3: Monterey Sand with UX1400 under a normal stress of 6psi.

Figure 4.3 shows the results for Test 33. The test looks to not have reached a pullout failure. This is shown by the continuous increase in pullout resistance as the lvdts continue to displace. Instead, the test was stopped due to the hydraulic pistons reaching their maximum displacement capacity.

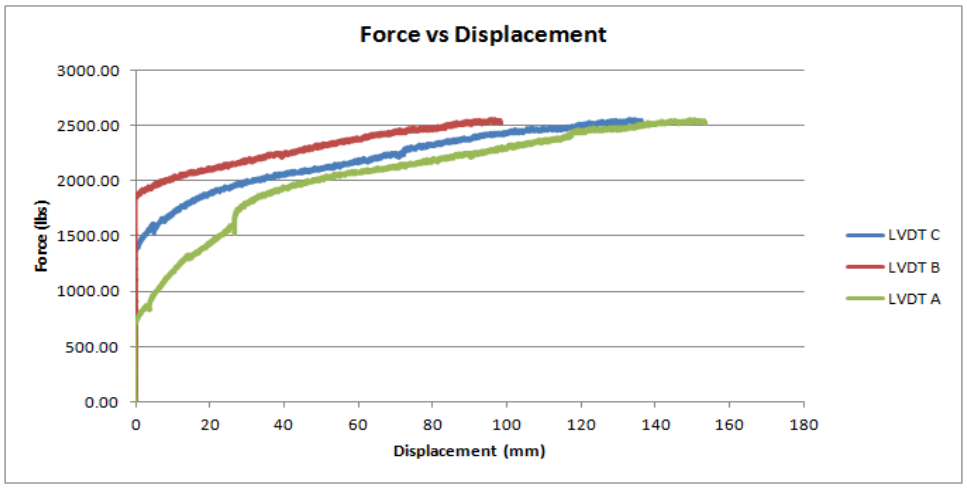

Figure 4.4: Monterey Sand with UX1400 under a normal stress of 8psi.

Figure 4.4 shows the results for Test 89. The results show a pullout failure which is characterized by the plateau from the lvdts. The pullout resistance is approximately 2,500 lbs., which is the highest pullout resistance out of all the UX1400 Monterey Sand tests. This was expected since Test 89 had a normal stress of 8 psi, which was the highest normal stress tested.

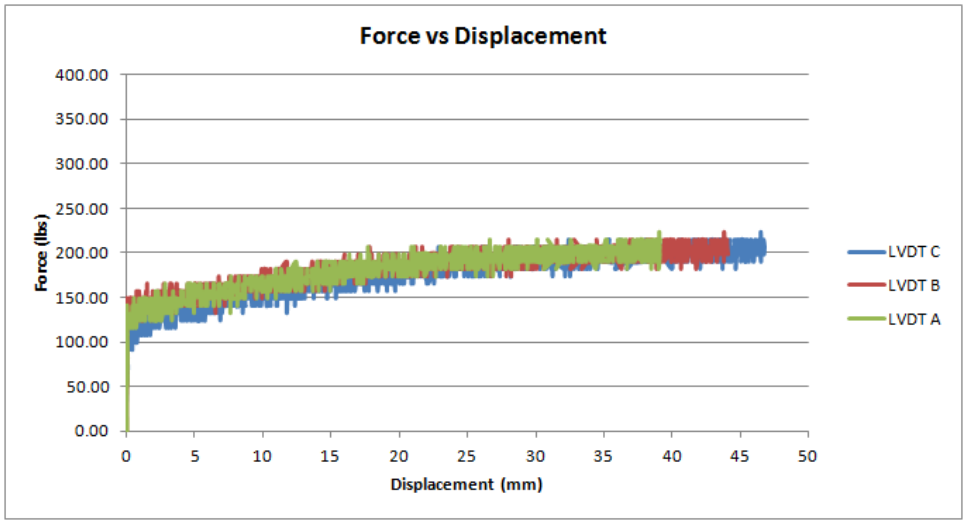

Figure 4.5: Monterey Sand with UX1700 under a normal stress of .5psi.

Figure 4.5 shows the results for Test 104. The dead load was used as the normal stress for this test. The UX1700 geogrid produced a pullout resistance of 200 lbs. which is 50 lbs. higher than the UX1400.

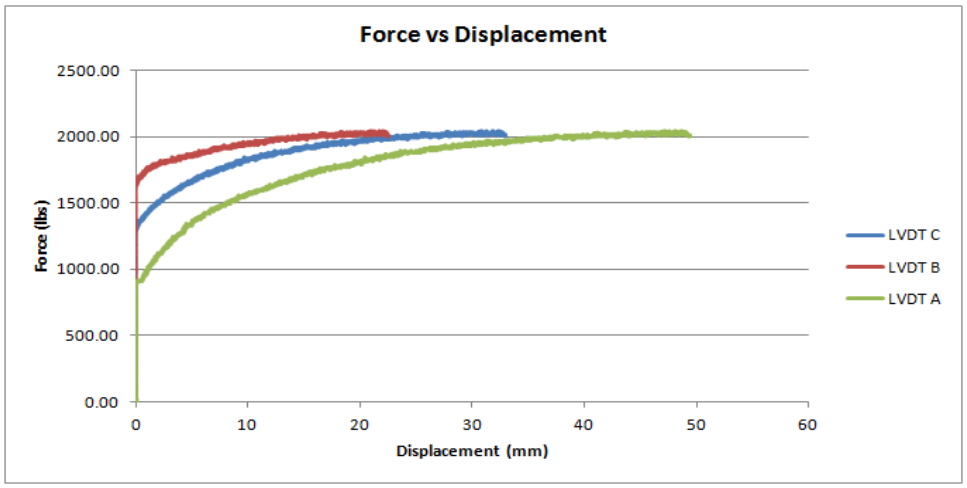

Figure 4.6: Monterey Sand with UX1700 under a normal stress of 4psi.

Figure 4.6 shows the results for Test 85. Similar to Test 37, the pullout resistance increases by an order of magnitude when the normal stress is increased to 4 psi.

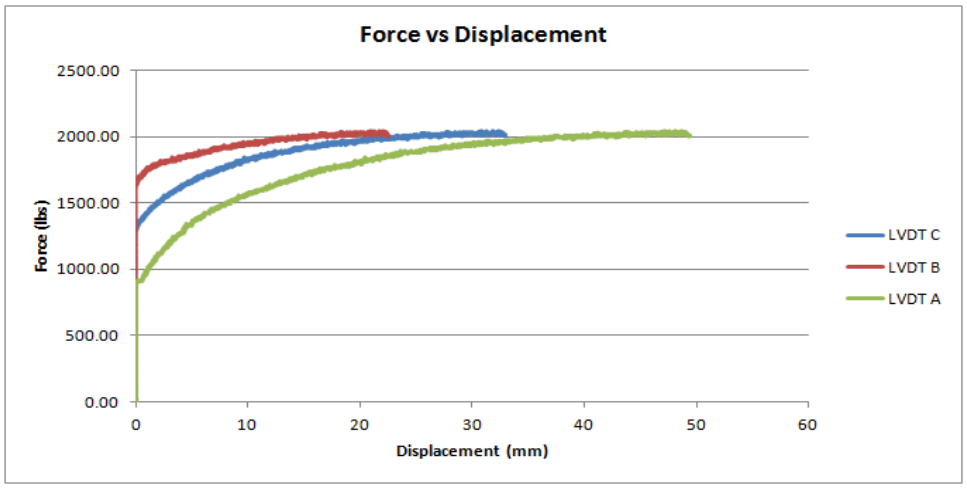

Figure 4.7: Monterey Sand with UX1700 under a normal stress of 6psi.

Figure 4.7 shows the results for Test 87. The pullout resistance for this test is similar to Test 85 even with an increase in normal stress.

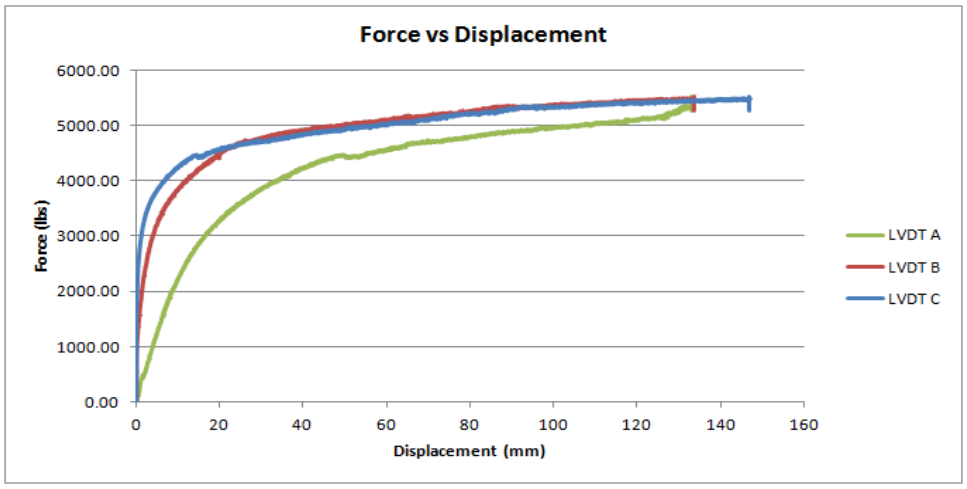

Figure 4.8: Monterey Sand with UX1700 under a normal stress of 8psi.

Figure 4.8 shows the results for Test 35. These results show an increase in pullout resistance of up to 3,500 lbs. when compared to Test 87.

The set of results, in Figures 4.1 to 4.8, for both the UX1400 and UX1700 show no well defined peak, but rather a continuous increase until a plateau is reached. Results showing an lvdt displacement greater than 140 mm. do not show a plateau in the pullout force versus displacement graph. This is due to the limitations of the hydraulic pistons reaching max displacement. However, since these tests were close to reaching a plateau there maximum pullout force and Ci results were used in the evaluation.

4.2.2 Analysis of the Results

The results from the previous section were used to analyze the different parameters and compare with the literature review trends. The first parameter that is analyzed is normal stress and its effect on the pullout resistance.

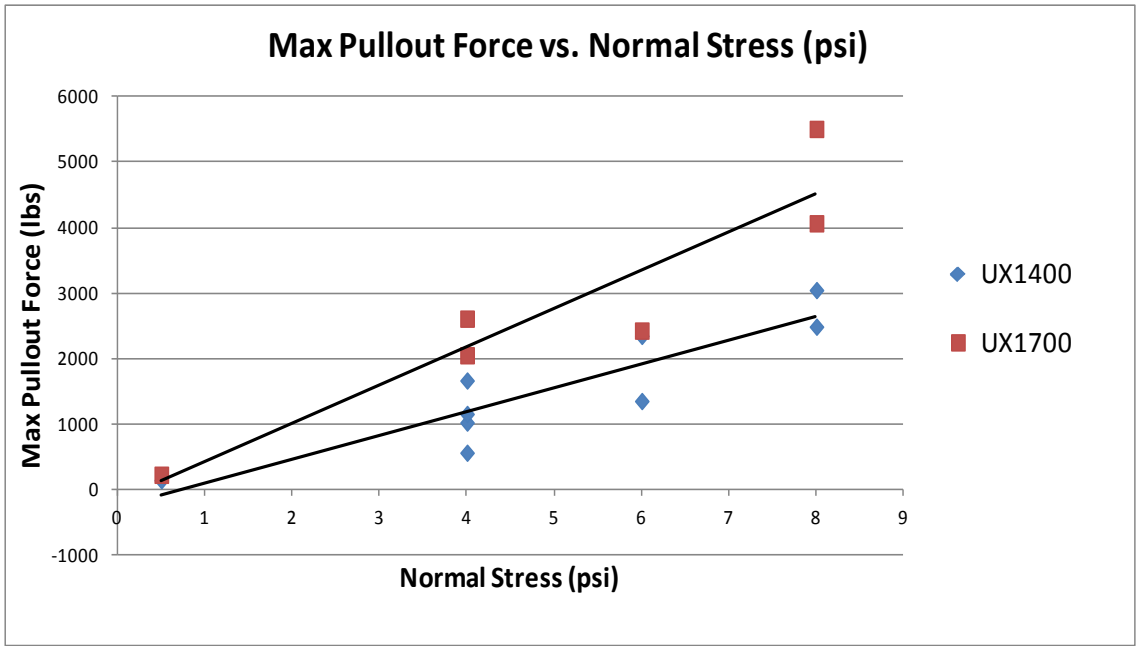

Figure 4.9: Max pullout force versus normal stress for Monterey Sand.

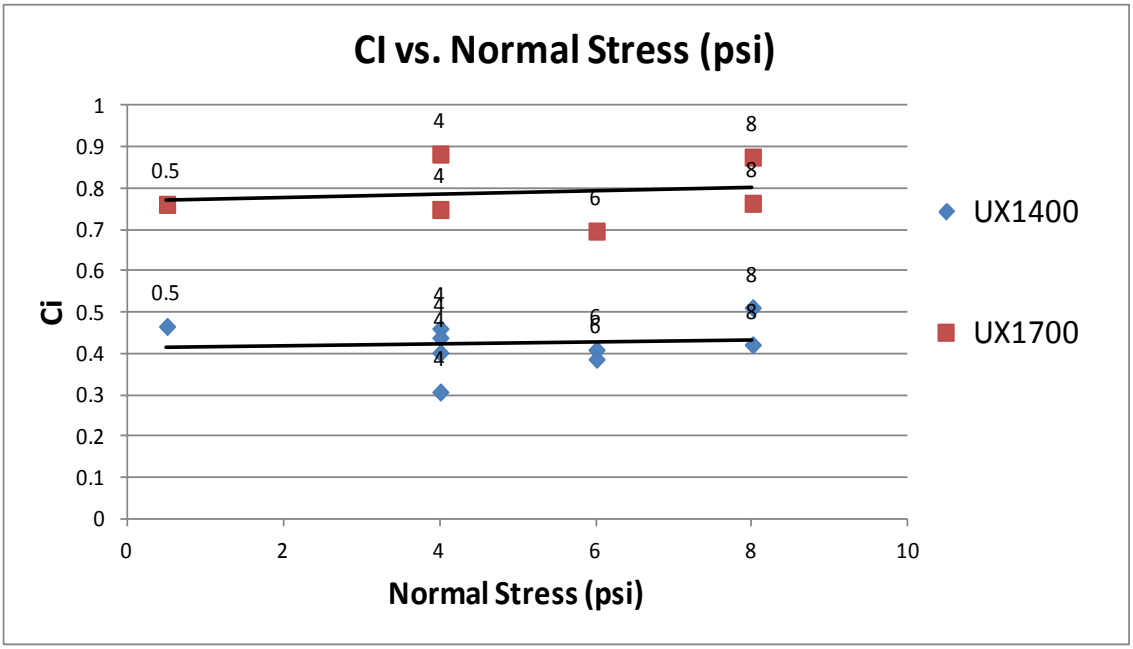

Figure 4.10: Ci versus normal stress for Monterey Sand.

Figure 4.9 shows that the max pullout force defines a linear relationship with normal stress, with no adhesion component. This translates into a constant Ci value for varying normal stresses shown in Figure 4.10. The constant Ci results from having no adhesive component in the pullout results. Figure 4.10 also shows that the UX1400 has lower Ci values compared to the UX1700.

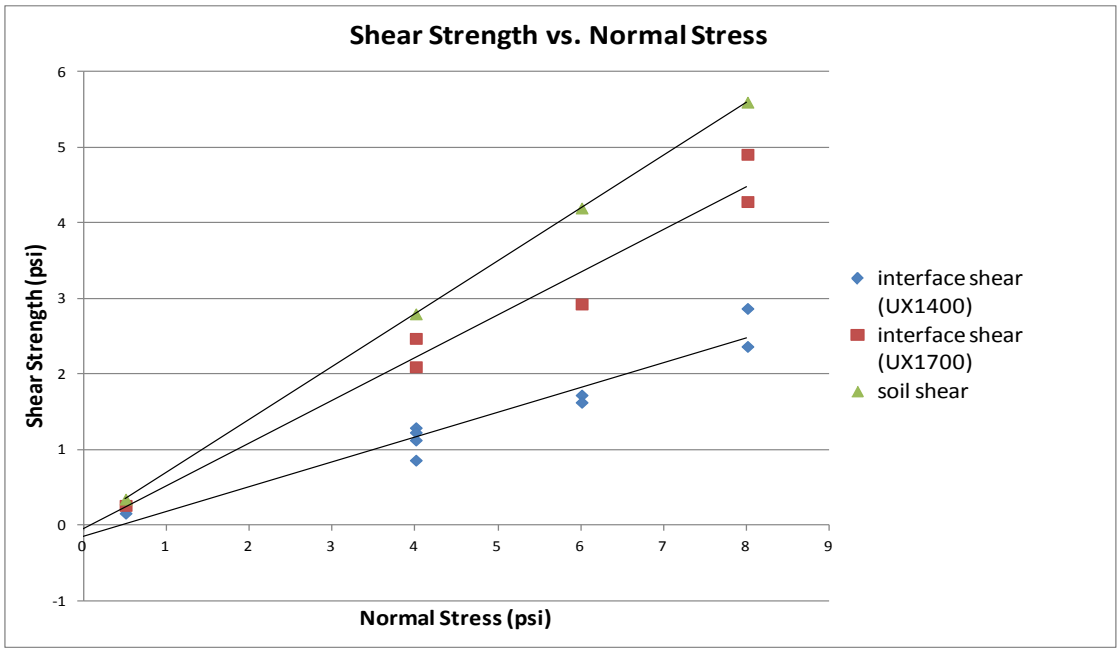

Figure 4.11: Lower friction angle for UX1400 results in bigger difference in shear strength.

Figure 4.11 compares the interface shear strength of both the UX1400 and UX1700 with the Monterey Sand shear strength. Since the UX1400 has a smaller interface friction angle, the ratio between the UX1400's interface shear strength and the soil shear strength decreases.

The reinforcement length is another parameter that was analyzed for the given set of results. Figure 2.15 from Teixeira et al (2007) shows that Ci is constant for varying reinforcement lengths.

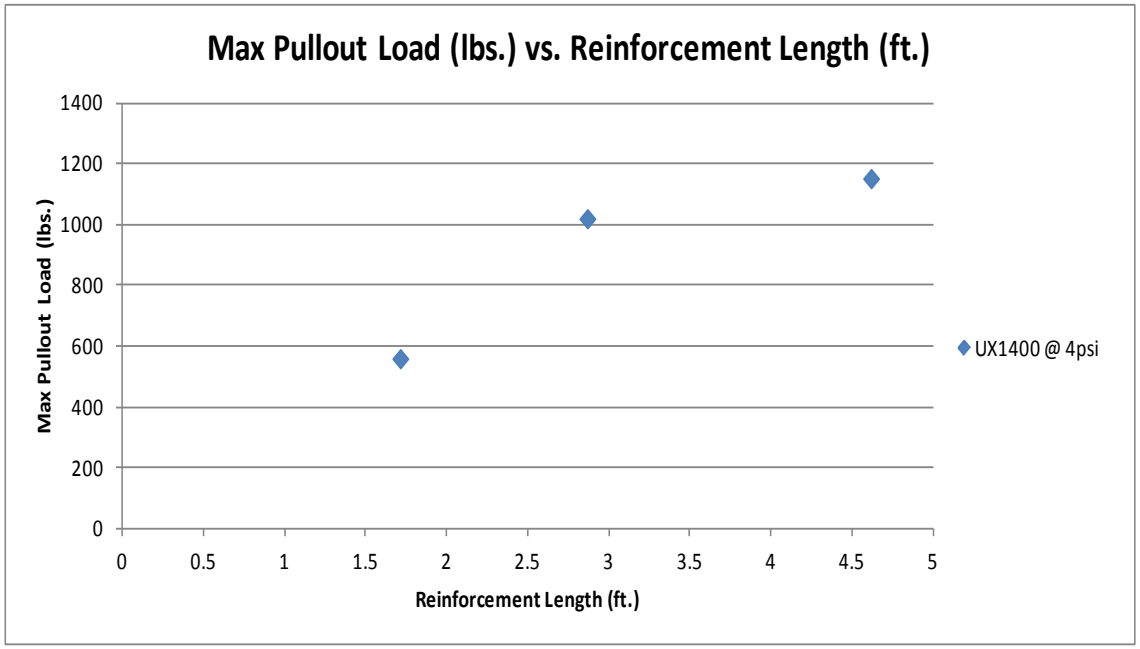

Figure 4.12: Max pullout load versus reinforcement length for Monterey Sand.

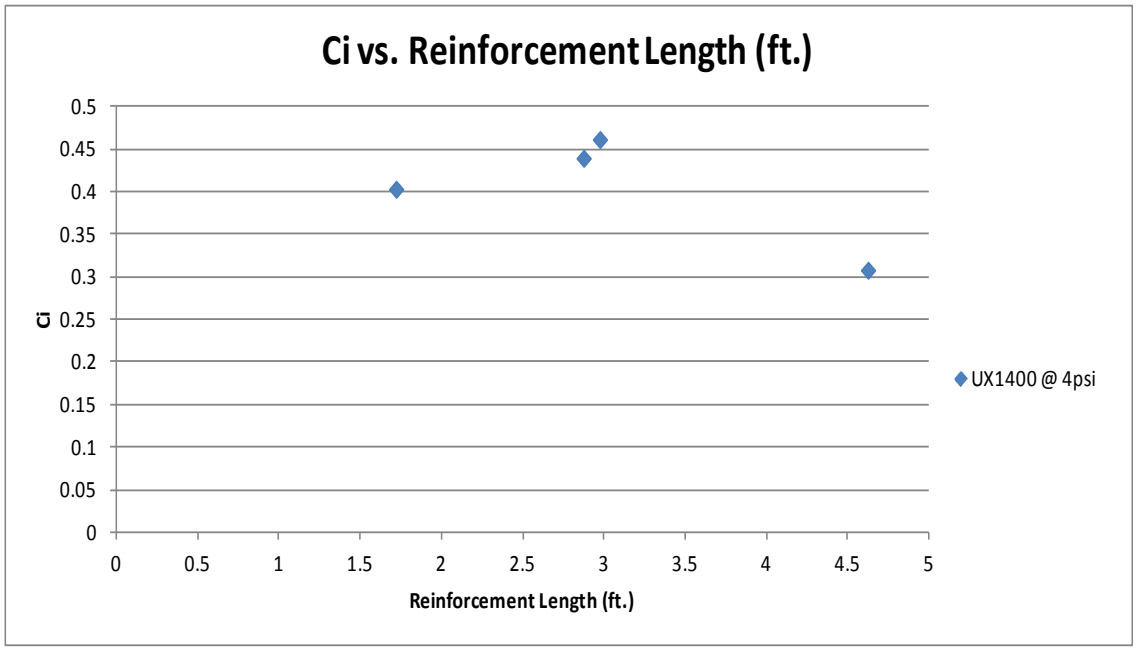

Figure 4.13: Ci versus reinforcement length for Monterey Sand.

The analysis of the effect of reinforcement length on the pullout resistance of the UX1400 geogrid is evaluated for tests conducted at a normal stress of 4 psi. The set of test results for UX1400 at 4 psi was used since this set produced the clearest trend results with little scatter. The reinforcements were tested at lengths of 1.7,3, and 4.6 feet. Figure 4.12 shows a non-linear relationship between the max pullout load and reinforcement length. The results in Figure 4.13 show a reasonably constant Ci up until a reinforcement length of 4.6 feet. The results suggest that boundary effects may become more significant at a reinforcement length of 4.6 ft. leading to a decrease in the Ci value.

The effect of spacing of the transverse members on pullout resistance was also analyzed. None of the figures from section 4.2.2 have well defined pullout load peaks which may be due to the large transverse member spacing of the geogrids that were tested. The large spacing prevents transverse member interference. This is why the pullout curves reach a plateau instead of a peak followed by a drop.

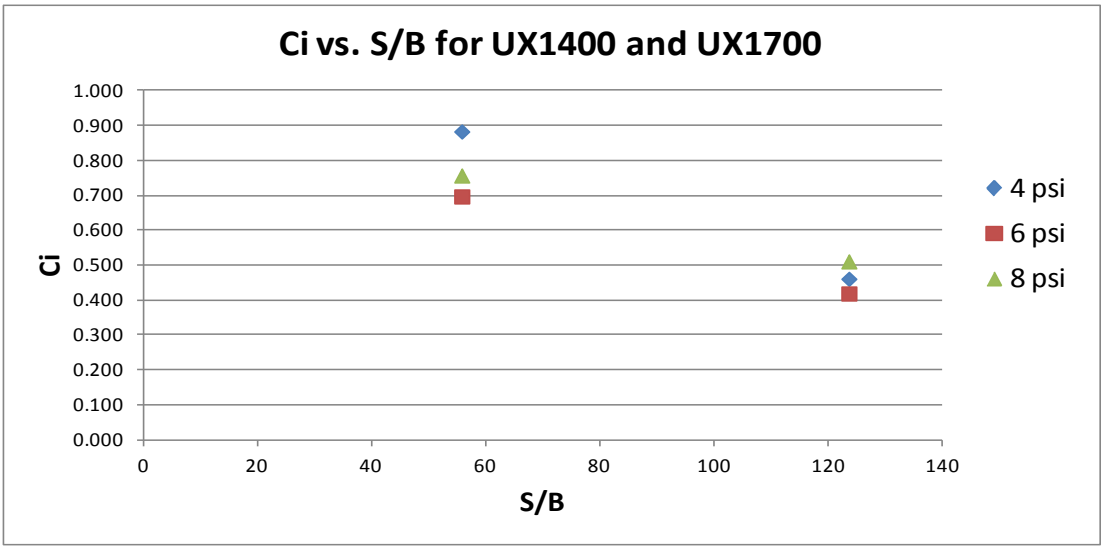

Figure 4.14: Ci versus S/B for geogrids tested in Monterey Sand.

Figure 4.14 shows the reduction in Ci due to the decrease in transverse rib thickness. These results show a similar trend compared to Palmeira's results from Palmeira and Milligan (1989). This trend lies on the right side of Teixeria's optimum spacing curve (Figure 2.18). According to Figure 2.18, in order for Ci to increase to its optimum value, the spacing for the UX1400 and UX1700 geogrids would need to decrease from 447mm. to around 45 millimeters.

4.3 PULLOUT TESTS CONDUCTED WITH MPA DREDGED MATERIAL

There are few case studies involving the testing of geogrids embedded in a cohesive soil backfill (Abu-Faraskh et. al., 2006). Most involve the use of a granular soil due to it being a highly recommended backfill for soil reinforcement embankments or walls. However, using marginal soils as a backfill can provide an advantage in cost and time. As more interests are venturing towards this relatively new concept more case studies and evaluations are emerging. The analysis of data presented in this section evaluates the pullout response between uniaxial geogrids and dredged material. The results are compared with the Monterey Sand analysis in order to compare the trends in the results with a baseline case.

4.3.1 Pullout Test Results Using Dredged Materials

The tests conducted on MPA dredged material are shown in Figures 4.15 to 4.20. The Tensar UX1400 and UX1700 geogrids were used with three different normal stresses: 4, 6, and 8 psi.

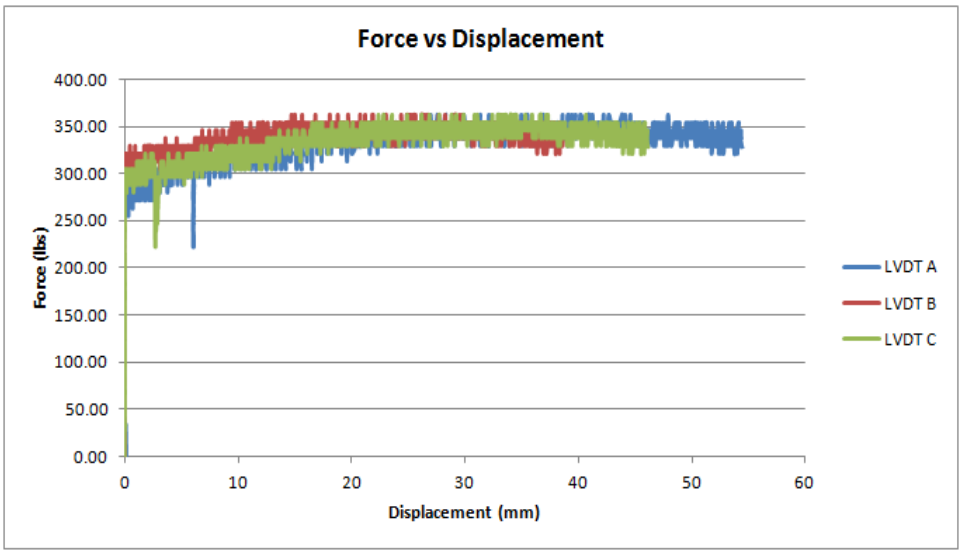

Figure 4.15: Dredged material from MPA with a UX1400 under a normal stress of 4psi.

Figure 4.15 shows the results for Test 97. The results show a pullout load plateau at around 350 pounds. The pullout load for this test is very low compared to the Monterey Sand.

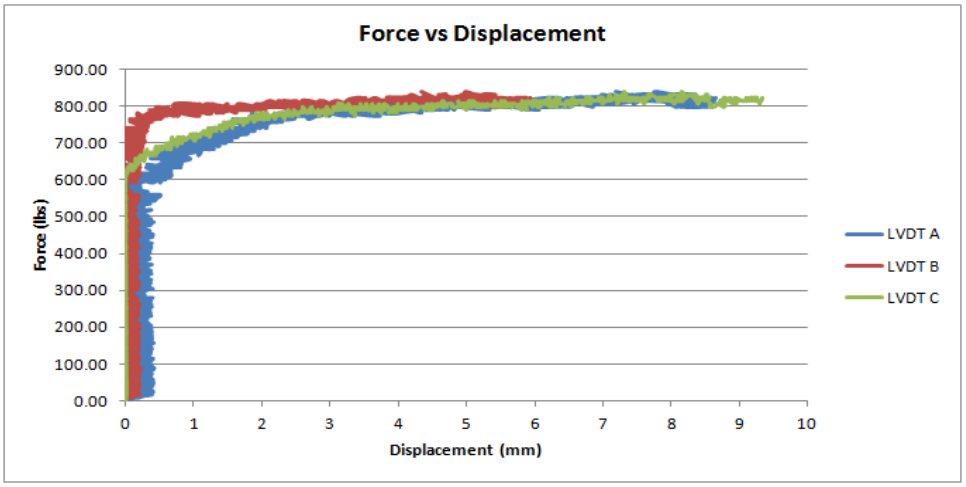

Figure 4.16: Dredged material from MPA with a UX1400 under a normal stress of 6psi.

Figure 4.16 shows the results for Test 49. The results show that the pullout load reaches a plateau at 800 pounds. It is also worth noting that the maximum displacement for the lvdts is only 9-10 millimeters. This is a very small displacement when compared to the Monterey Sand results.

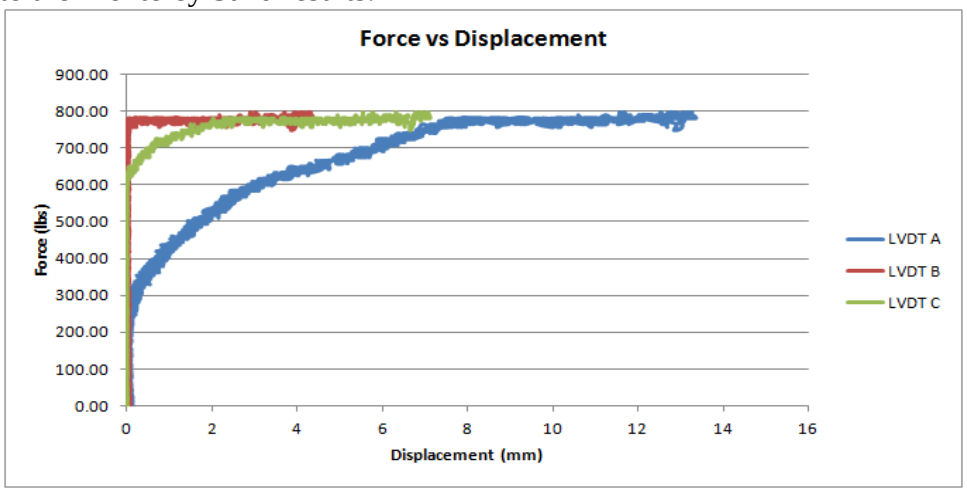

Figure 4.17: Dredged material from MPA with a UX1400 under a normal stress of 8psi.

Figure 4.17 shows the results for Test 48. The pullout load reaches a plateau at 800 pounds. Similar to Test 49 the maximum displacement for the lvdts are relatively small compared to the Monterey Sand results.

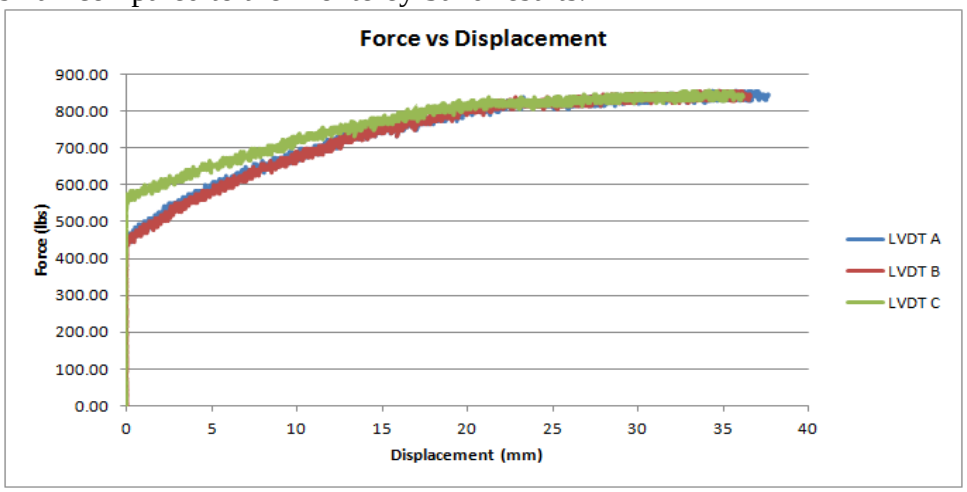

Figure 4.18: Dredged material from MPA with a UX1700 under a normal stress of 4psi.

Figure 4.18 shows the results for Test 50. The pullout load is around 800 pounds for this test. This is a 450 lb. difference when compared to the UX1400 at a normal stress of 4 psi.

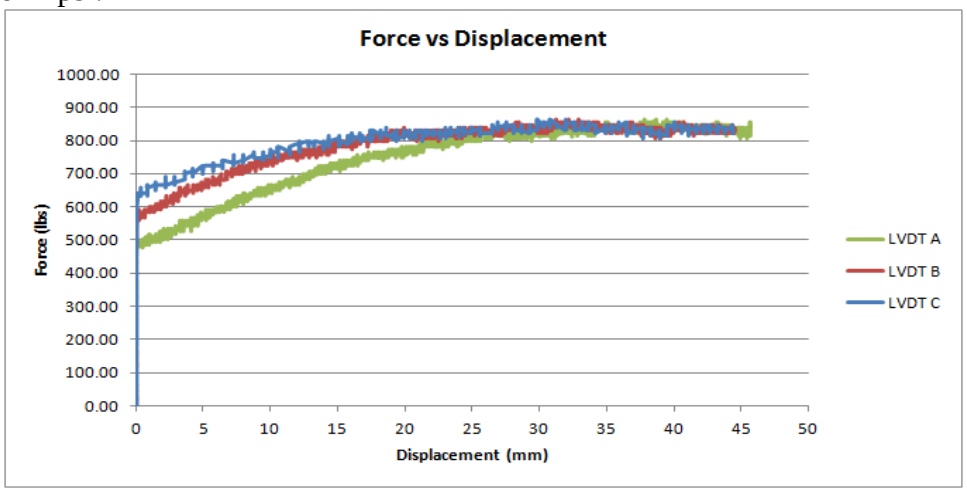

Figure 4.19: Dredged material from MPA with a UX1700 under a normal stress of 6psi.

Figure 4.19 shows the results for Test 95. The pullout load reaches approximately 850 lbs. for this test. This is only a 50 lb. difference in pullout load when compared to Test 50.

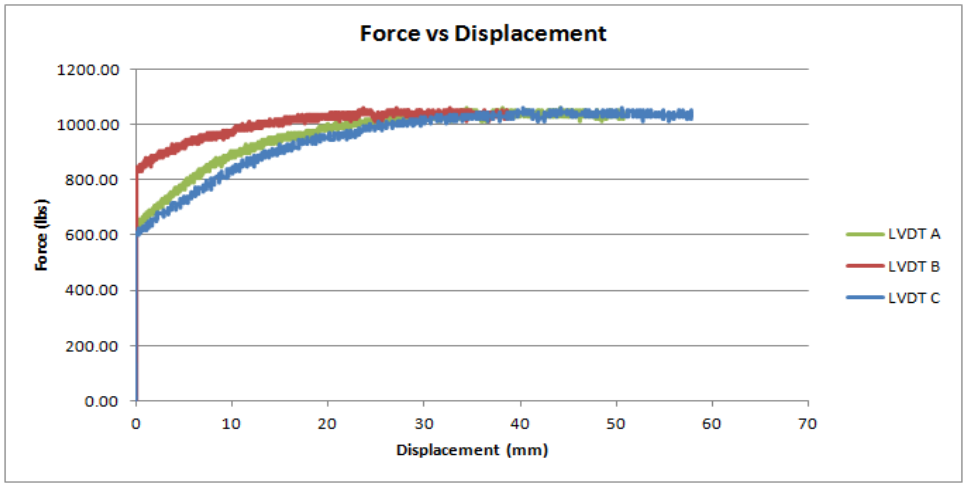

Figure 4.20: Dredged material from MPA with a UX1700 under a normal stress of 8psi.

Figure 4.20 shows the results for Test 96. The pullout load for this test is around 1,000 pounds. The pullout load increased by 200 lbs. when compared to Test 95. Also, it is worth noting that the Monterey Sand produced a pullout load five times higher than the MPA dredged material at a normal stress of 8 psi. This is the last of the tests for the MPA dredged material.

Similar to the pullout test results obtained with the Monterey Sand, the MPA dredged material results show a plateau in the force vs. displacement plots when pullout failure is reached. All results for the dredged material exhibited pullout failure within the displacement capabilities of the hydraulic pistons.

4.3.2 Analysis of the Pullout Parameters of MPA Dredged Material

The trends that were established in the literature review section are compared with those obtained for test results involving the MPA dredged material. It should be noted that most trends reported in the literature are for granular materials and not for fine-grained soils such as dredged materials. The Monterey Sand analysis is also used as a basis for the comparison in order to show the differences in the response.

The effect of normal stress on pullout resistance is examined first. Figures 4.21 and 4.22 show the pullout results and Ci values in relation to the varying normal stresses.

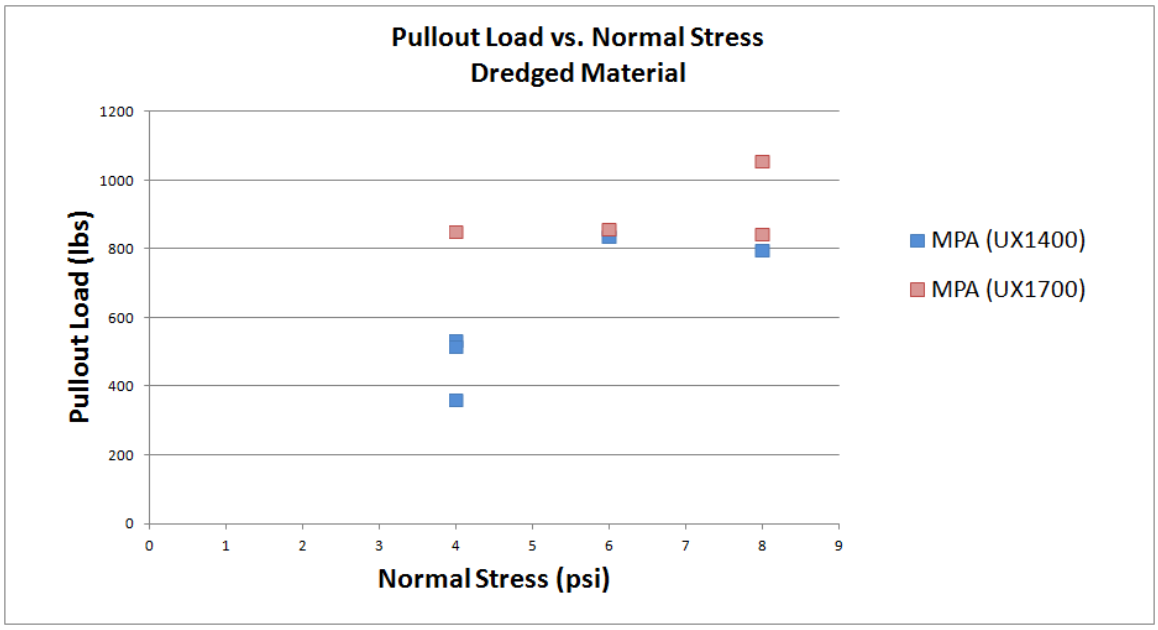

Figure 4.21: Pullout load versus normal stress for MPA dredged material.

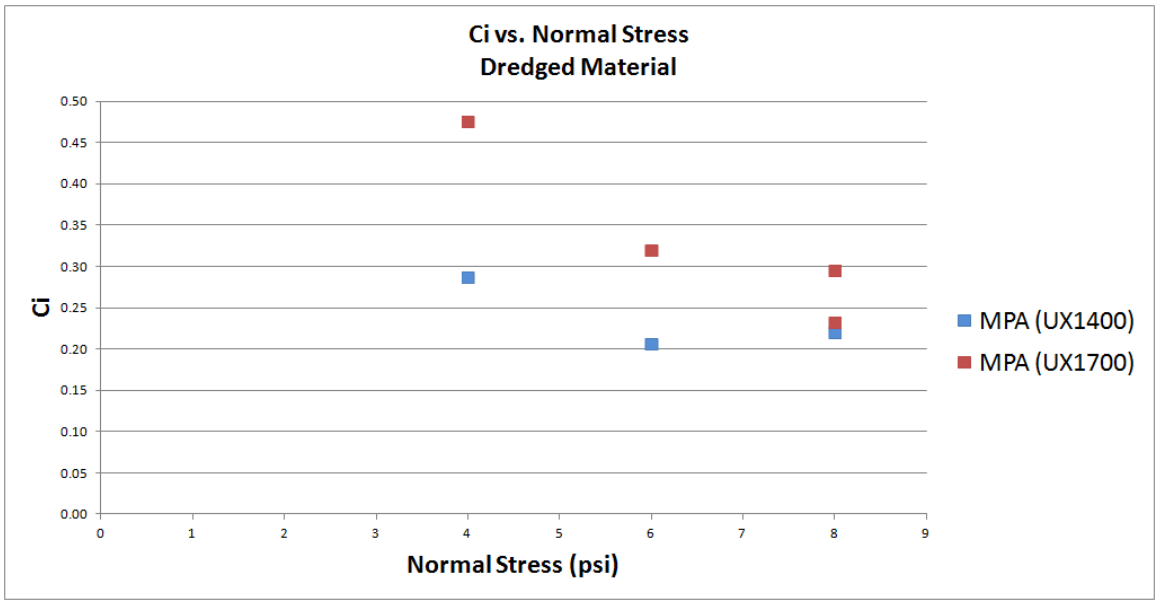

Figure 4.22: Ci versus normal stress for MPA dredged material.

Figure 4.21 shows that the linear relationship obtained using data generated within the 4 to 8 psi range leads to an adhesion intercept in the various sets of tests. Since no tests were conducted for normal stresses below 4 psi, the linear trend can only be assumed. Figure 4.22 shows a decreasing Ci with increasing normal stress. These results show a similar trend as the results in section 2.4.1 for cohesive soils. The adhesion intercept that is found from the linear trend of the 4 to 8 psi normal stress range in Figure 4.21 leads in turn to Ci values that decrease with increasing normal stress. The adhesion found in dredged materials was not present in the Monterey Sand. Accordingly, the Monterey Sand did show a pullout curve that is linear through the origin and a constant Ci with increasing normal stress.

The MPA dredged material results show a pullout load increase of approximately 400 lbs. for a normal stress window of 4 to 8 psi. This increase is approximately the same when using different geogrids (UX1400 and UX1700) and different dredged materials (MPA DM and Philadelphia DM). However, the Monterey Sand showed a pullout load increase that was an order of magnitude higher than the MPA dredged material. This increase in the pullout resistance of the Monterey Sand is consistent with a drained behavior. This is why the interface shear strength increases with increasing normal stresses. The dredged material seems to show a response that is more consistent with an undrained behavior in that the pullout resistance is relatively constant, at least when compared to the Monterey Sand. This undrained condition of the MPA DM caused pore pressures to develop.

Comparison of the MPA DM pullout resistance results, Figure 4.21, to those shown in Figure 2.12 (Abu-Faraskh et. al., 2006) reveal a significant difference. The pullout load for the MPA DM ranges from 400 to 1000 lbs. whereas the results from Abu-Faraskh are comparable to the Monterey Sand results, 2000 to 4000 lbs. The

dredged material has pullout resistance results consistent with what would be expected for an undrained behavior. The MPA DM was tested using samples prepared at moisture contents above optimum, which explains the reason for the undrained behavior. Abu-Faraskh et. al. (2006) tested at optimum moisture content with a pullout rate of 1.5 millimeters per minute. The pullout tests for Abu-Faraskh et. al. (2006) were still tested at undrained conditions, but at optimum moisture content the amount of pore pressures are significantly less than that of the MPA dredged material.

The effect of reinforcement length on pullout resistance was evaluated using lengths of 3 and 4.5 feet. Figure 4.23 and 4.24 shows the results of varying reinforcement lengths.

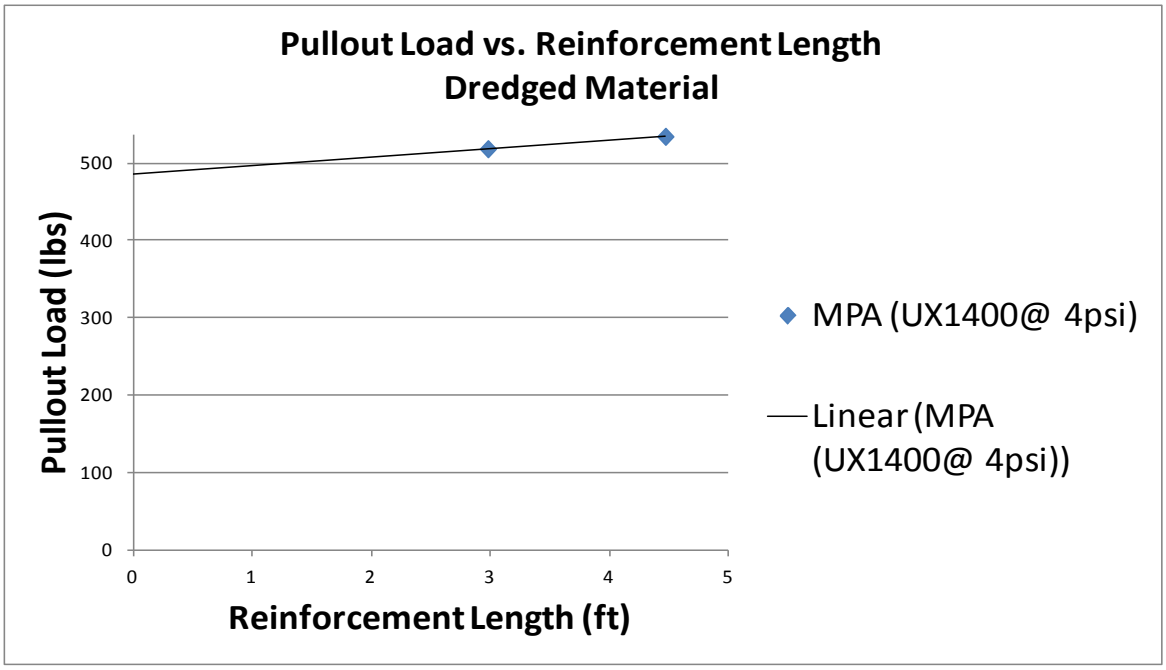

Figure 4.23: Pullout load versus reinforcement length for MPA dredged material.

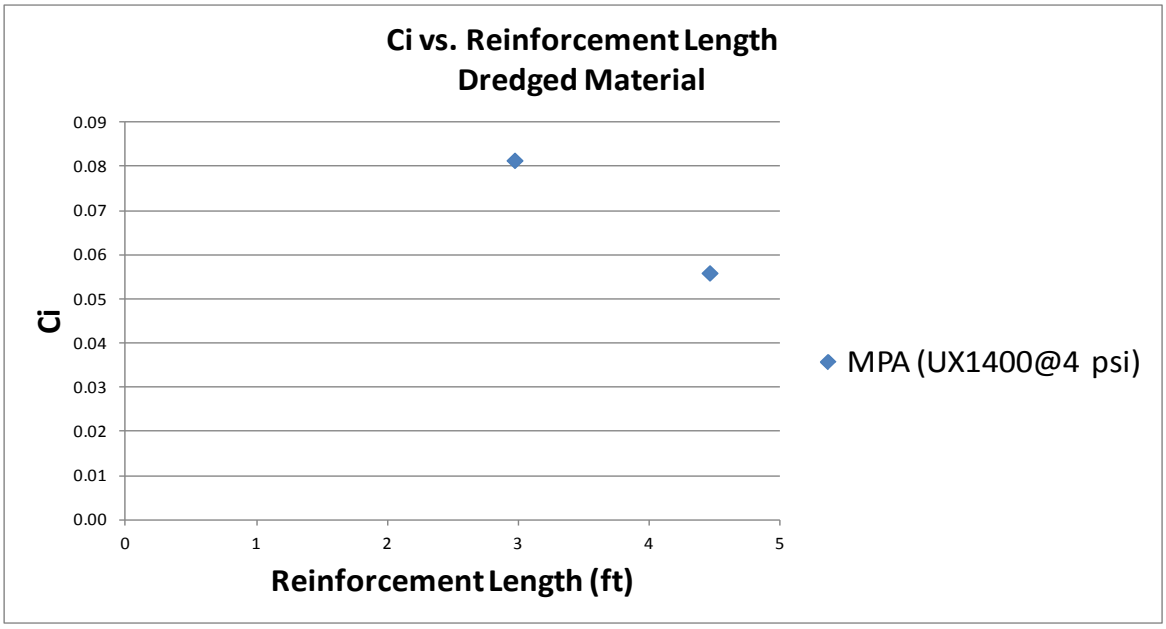

Figure 4.24: Ci versus reinforcement length for MPA dredged material.

The figures show an increasing pullout force, but decreasing Ci value with increasing reinforcement length. The decreasing Ci trend is due to the presence of an intercept component in the pullout resistance trend shown in Figure 4.23. The intercept is most likely caused by the influence of the rigid top and bottom boundaries. As the reinforcement length increases past a length of 4.5 ft., more influence from the top and bottom boundaries is created.

The results in Figure 4.25 shows that the UX1700 geogrid has a significantly higher Ci value when compared to the UX1400. The ratio between the two geogrid Ci results are similar in both the dredged material and Monterey Sand. One of the differences, in terms of dimensional characteristics, between the UX1400 and UX1700 is the thickness of the transverse and longitudinal members. The thicker members allow for a better interaction at the interface. Figure 4.25 shows a comparison between the

coefficient of interaction and the ratio between the geogrids transverse member spacing to thickness.

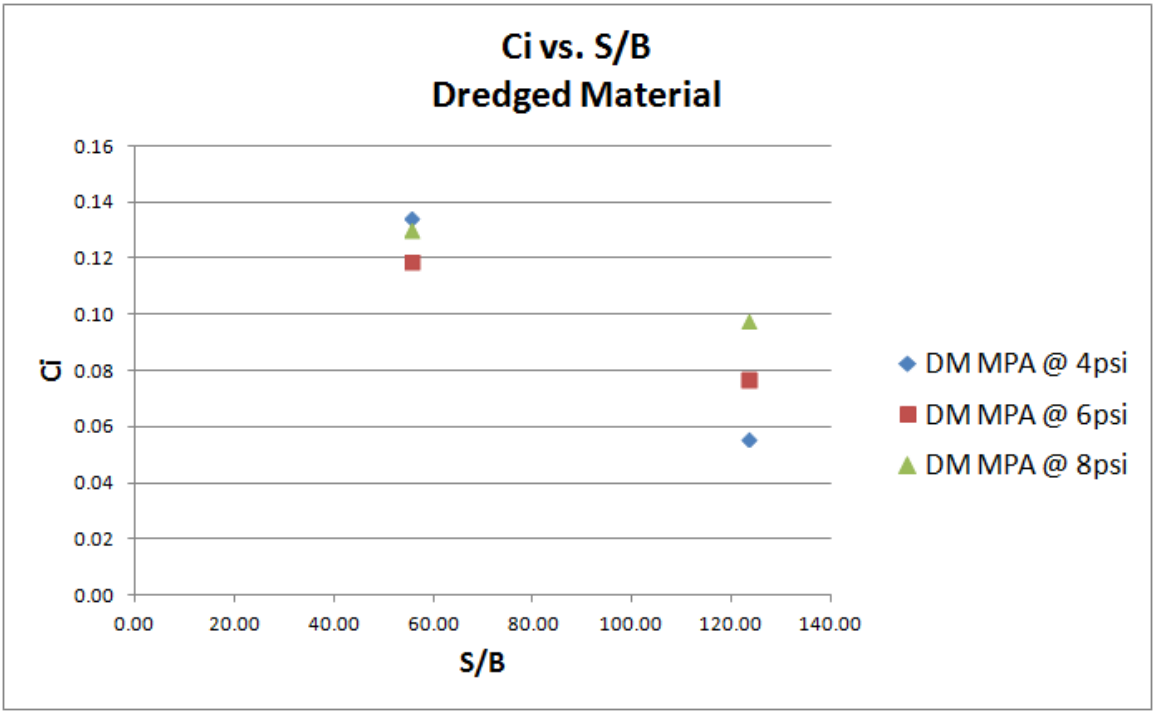

Figure 4.25: Ci versus transverse member spacing normalized by member thickness.

All of the UX1700 tests have a S/B ratio of 56 and the UX1400 have a ratio value of 124. Similar to the trend shown by the Monterey Sand results, a reduction in Ci is observed with an increasing S/B ratio. Since the transverse member spacing (S) is the same for both geogrids, the thickness of the member is what contributes to the decrease in Ci. The thicker transverse member for the UX1700 contributes more bearing resistance to the overall pullout force. A higher pullout force for the UX1700 results in a higher Ci value. Both the dredged materials and Monterey Sand results show that the transverse member spacing for both geogrids are past the optimum value of 45 millimeters.

4.4 PULLOUT TESTS WITH PHILADELPHIA DREDGED MATERIAL

The tests conducted on the Philadelphia dredged material are shown in Figures 4.26 to 4.31. The Tensar UX1400 and UX1700 geogrids were used with three different normal stresses: 4, 6, and 8 psi.

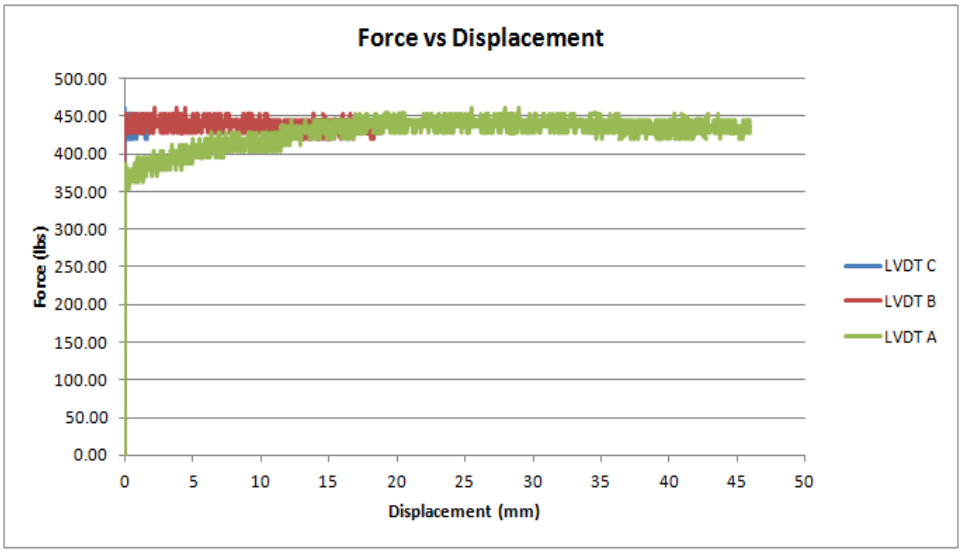

Figure 4.26: Dredged material from Philadelphia with a UX1400 under a normal stress of 4psi.

Figure 4.26 shows the results for Test 56. This test shows a pullout resistance of around 450 pounds. This is slightly higher than the MPA dredged material results, but significantly lower when compared to the Monterey Sand.

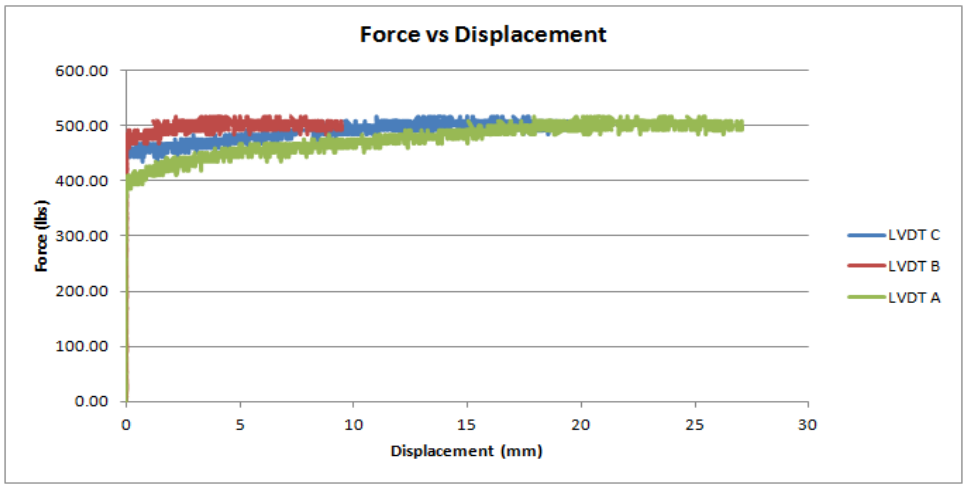

Figure 4.27: Dredged material from Philadelphia with a UX1400 under a normal stress of 6psi.

Figure 4.27 shows the results for Test 57. The pullout load plateaus at 500 lbs. for this test. This is only an increase of 50 lbs. when compared to Test 56. Similar to the Monterey Sand and the MPA dredged material, the increase in normal stress from 4 to 6 psi does not have a significant effect on the pullout load.

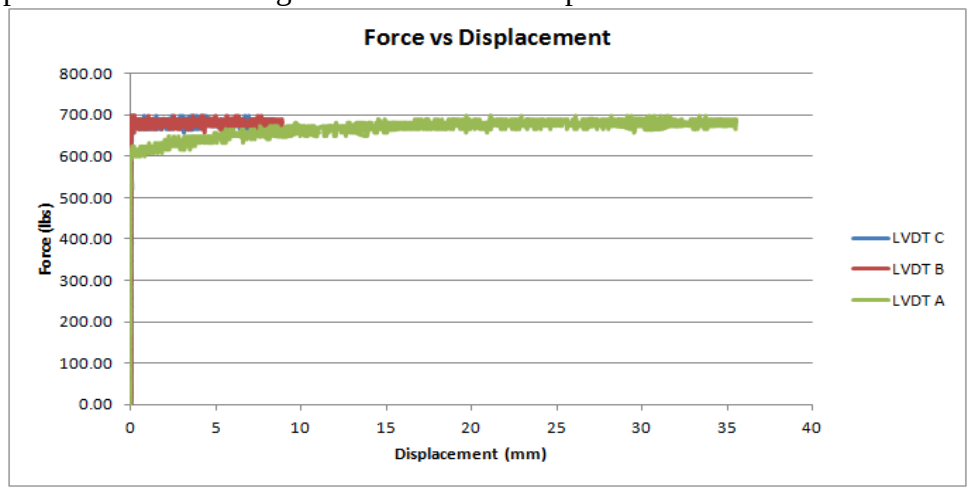

Figure 4.28: Dredged material from Philadelphia with a UX1400 under a normal stress of 8psi.

Figure 4.28 shows the results for Test 58. The pullout load for this test is approximately 700 pounds. There is a 200 lb. increase when compared to Test 57. The total range in pullout load for the UX1400 tested with the Philadelphia dredged material is from 450 to 700 pounds. This is similar to the pullout load range for the UX1400 tested with the MPA dredged material.

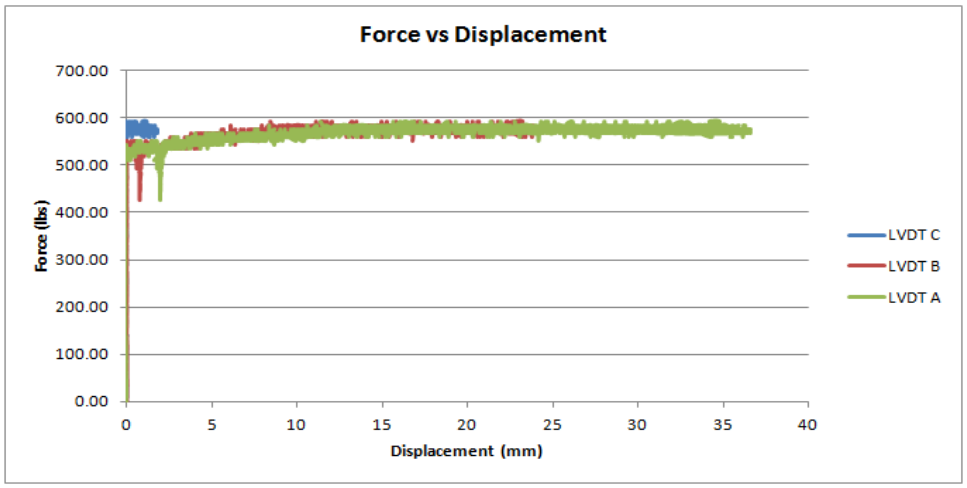

Figure 4.29: Dredged material from Philadelphia with a UX1700 under a normal stress of 4psi.

Figure 4.29 shows the results for Test 59. The pullout load reaches just below 600 lbs. for this test. This is 200 lbs. lower than Test 50 for the MPA dredged material.

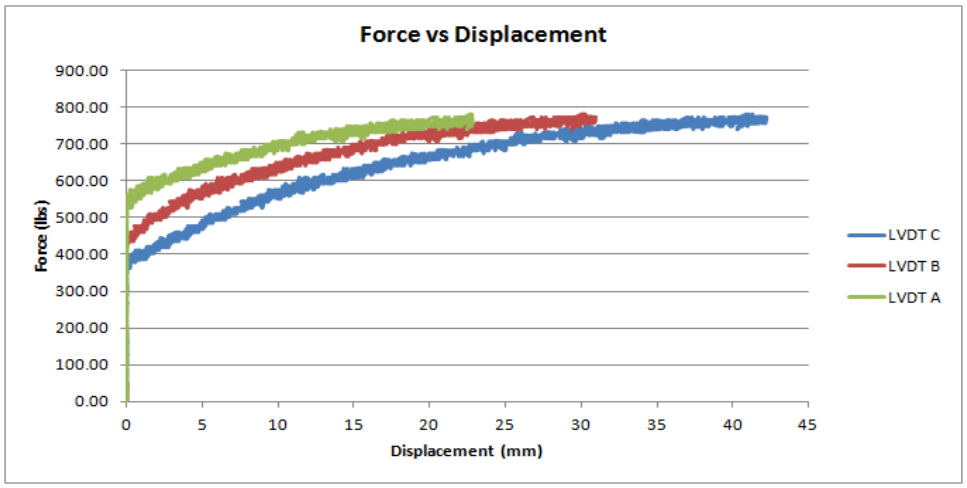

Figure 4.30: Dredged material from Philadelphia with a UX1700 under a normal stress of 6psi.

Figure 4.30 shows the results for Test 60. The pullout load reaches a plateau around 750 pounds. This is a 150 lb. increase from Test 59.

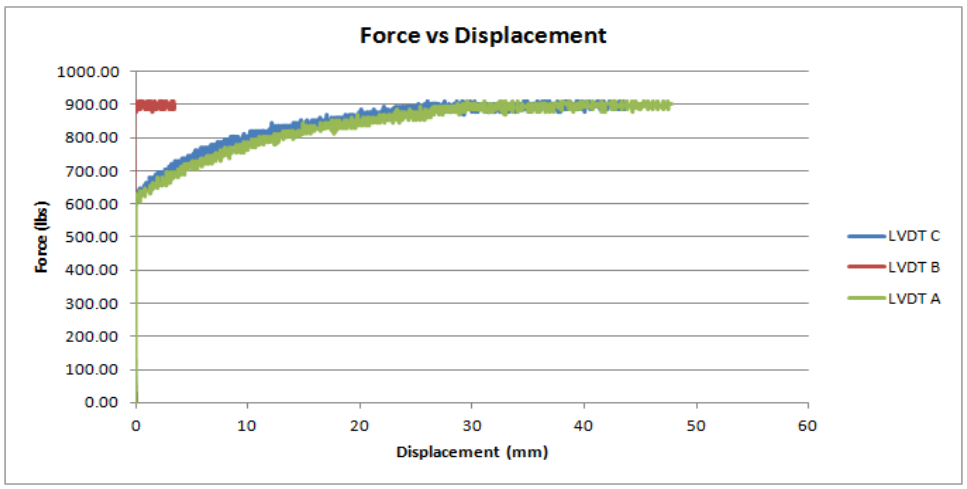

Figure 4.31: Dredged material from Philadelphia with a UX1700 under a normal stress of 8psi.

Figure 4.31 shows the results for Test 61. The pullout load reaches 900 lbs. for this test. When compared to the MPA dredged material, the Philadelphia dredged

material test had a lower pullout load. This is the last of the tests for the Philadelphia dredged material.

4.4.1 Analysis of the Pullout Parameters of Philadelphia Dredged Material

Figures 4.32 and 4.33 show the pullout results and Ci values with increasing normal stresses.

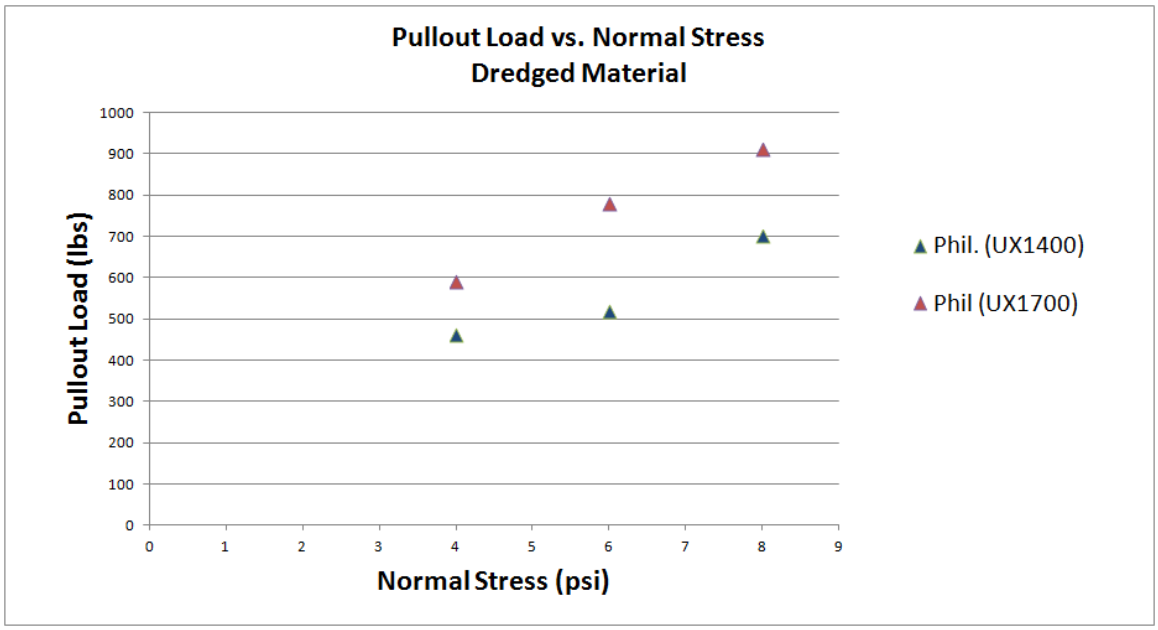

Figure 4.32: Pullout load versus normal stress for Philadelphia dredged material.

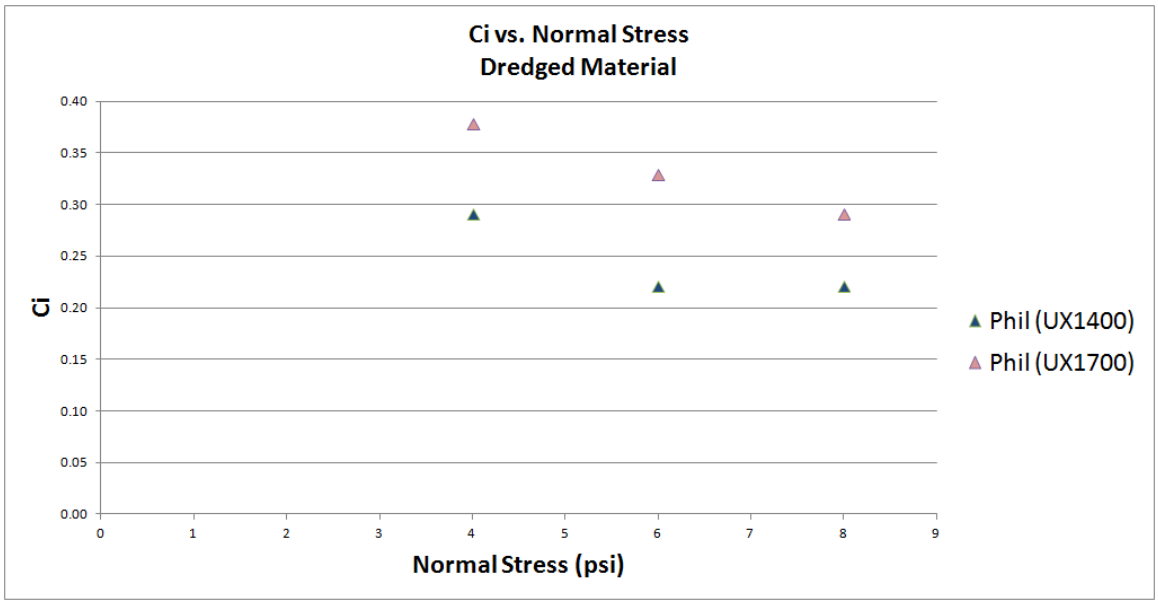

Figure 4.33: Ci versus normal stress for Philadelphia dredged material.

The Philadelphia dredged material has a similar trend in both pullout load and Ci when compared with the MPA dredged material. The pullout load from Figure 4.32 shows an approximately linear trend with an adhesion intercept. The change in pullout resistance with increasing normal stresses ranging from 4 to 8 psi seems to be the same for both the UX1400 and UX1700 geogrids. This change in pullout resistance is relatively small when compared to that shown by the Monterey Sand. The coefficient of interaction for the Philadelphia dredged material decreases with increasing normal stress. This trend is similar to the Ci results from the MPA dredged material. The decreasing Ci trend is due to the adhesion intercept shown in Figure 4.33. Also, similar to the MPA dredged material, the small change in pullout resistance within the 4 to 8 psi normal stress range can be characterized as an undrained behavior. This undrained behavior is most likely due to the Philadelphia dredged material having a moisture content in excess of the optimum value.

Comparison of the pullout results using the Philadelphia dredged material to those from Figure 2.12 (Abu-Faraskh et. al., 2006) reveals a significant difference in the pullout resistance results. The pullout resistance for the Philadelphia DM do not exceed 1,000 lbs/ft. whereas Abu-Faraskh et. al. (2006) show pullout results greater than 2,000 lbs/ft. Similar to the MPA DM, the Philadelphia DM was tested with a moisture content that was wet of OMC. The moisture content for the Philadelphia DM was at 50%, but the optimum moisture content was 28%. The Philadelphia DM moisture content is comparatively wetter in relation to the MPA DM. This helps to explain why the pullout resistance for the Philadelphia DM was below that of the MPA DM. The moisture content for the Philadelphia DM can also explain why there is a significant difference in pullout resistance results between Abu-Faraskh et. al. (2006) and the Philadelphia DM. Since the clay soil from Abu-Faraskh et. al. (2006) was tested at OMC, the pullout resistance is expected to be higher than the Philadelphia DM.

The Philadelphia dredged material also shows a significantly higher pullout resistance for the UX1700 when compared to the UX1400. The UX1700 also develops a higher Ci value. Figure 4.34 shows that the higher S/B ratio for the UX1400 results in a lower Ci value. These results are consistent with those obtained for the MPA dredged material.

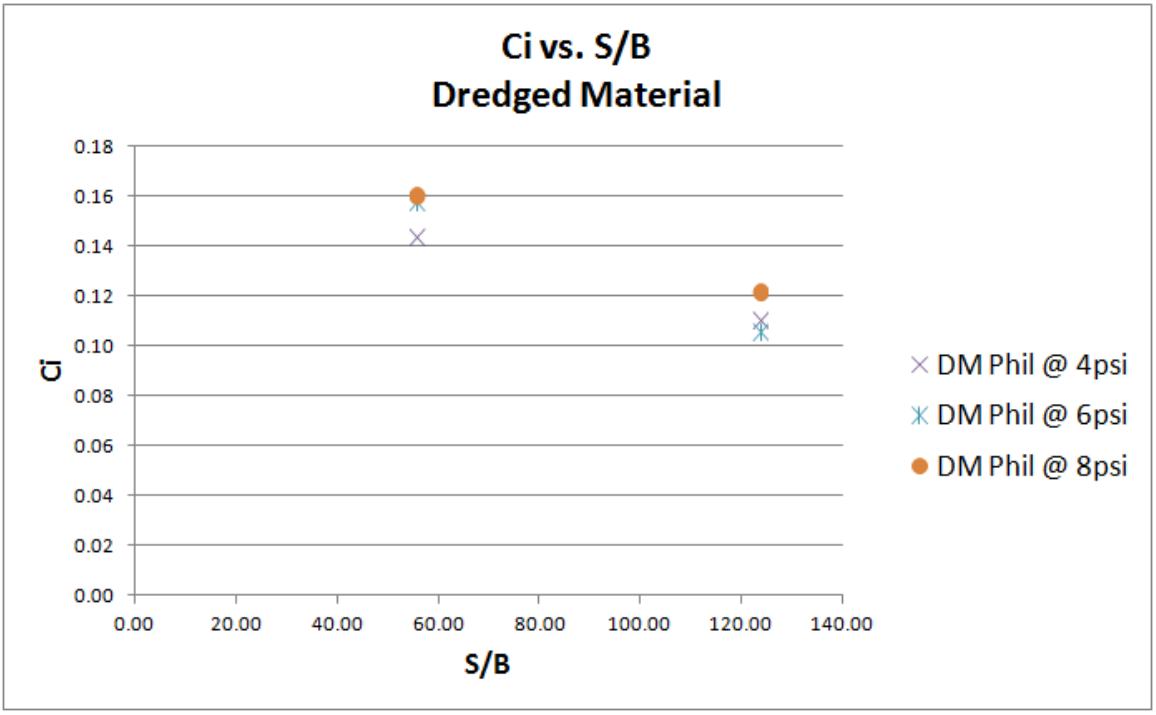

Figure 4.34: Ci versus transverse member spacing normalized by member thickness.

4.5 COMPARISON OF PULLOUT RESULTS OF MPA AND PHILADELPHIA DREDGED MATERIALS

The MPA and Philadelphia showed similar physical properties, but had different undrained shear strengths for the as-received moisture contents. The modified proctor curves for the dredged materials shows that the Philadelphia dredged material has a higher maximum dry density and a lower optimum moisture content than the MPA dredged material. The actual moisture content used for the pullout test's as-received moisture content was not the optimum value. The MPA was tested with a moisture content averaging 40% while the Philadelphia dredged material was tested with a moisture content averaging 50%. Both dredged materials were tested wet of optimum, but the Philadelphia dredged material was further away from its optimum moisture

content. This could be a contributing factor that explains the lower pullout resistances obtained for the Philadelphia DM when compared to the MPA DM. Figure 4.35 shows that the Philadelphia dredged material has a slightly lower pullout load in comparison to the MPA dredged material.

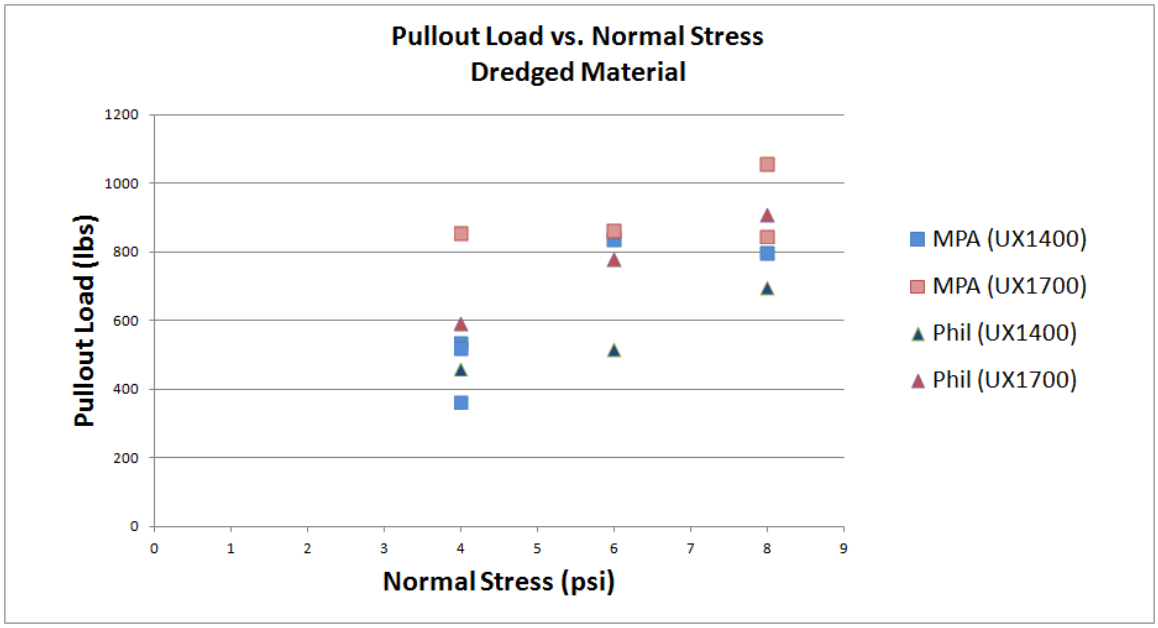

Figure 4.35: Ci versus transverse member spacing normalized by member thickness.

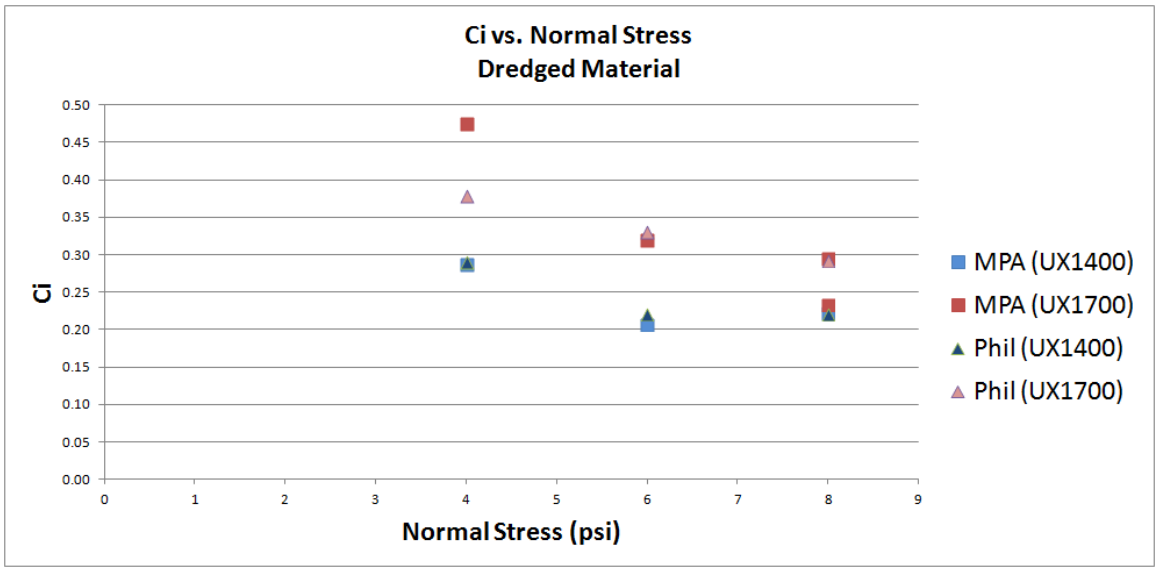

Figure 4.36: Ci versus transverse member spacing normalized by member thickness.

Even with the difference in pullout resistance between the MPA DM and Philadelphia DM, the coefficient of interaction for both dredged materials seem to be very similar. Figure 4.36 shows a slight difference in Ci values from the two dredged materials tested with the UX1700 under a normal stress of 4 psi. However, the Ci values seem to be the same with the same normal stress tested with the UX1400.

The MPA and Philadelphia dredged material have similar physical properties, but different undrained shear strengths and maximum dry densities. The Philadelphia dredged material showed a lower pullout resistance, but similar Ci values when compared to the MPA dredged material. The lower pullout resistances could be attributed to the Philadelphia dredged material having a higher moisture content. Since the physical properties and shear strengths of dredged materials may vary greatly, the pullout results of the dredged materials tested in this thesis may not represent the properties of dredged materials found in other regions. Yet, it is worth noting the similarity in the Ci values obtained for the two dredged materials tested in this investigation.

Chapter 5: Conclusions and Recommendations

5.1 CONCLUSION

The results of laboratory pullout tests on two geogrid reinforcements embedded in dredged material backfill were presented in this study. The dredged material for all of the pullout tests was compacted at similar densities and moisture contents. Two geogrids were tested at different confining stresses, different lengths, and using three soils. Comparison was made between the laboratory pullout test results and previous results identified in the literature. The measured pullout loads were used to calculate the coefficient of interaction between soil and geogrid. Based on the results, the following conclusions can be drawn:

- The presence of an adhesion component in the pullout load versus normal stress graphs for the dredged material result in a decreasing trend in the coefficient of interaction with increasing normal stress. The presence of an adhesion component suggests an undrained response of the dredged material for the moisture conditions used in the tests. In addition to an adhesion intercept, which is present in the results obtained in dredged material but not in the Monterey Sand, these tests also show a comparatively smaller rate of increase in pullout resistance (compared to that in sand) with increasing normal stress.
- The reinforcement length of the geogrid was found not to affect the coefficient of interaction, unless where the results are affected by proximity of the geogrid to the box boundary. Reinforcement lengths tested below 4.5 ft. showed a constant Ci. Reinforcement lengths greater than 4.5 ft. produced an intercept on the maximum pullout load vs. reinforcement length curve suggesting that there exists some influence by the pullout box boundaries. This influence of the pullout box

boundaries caused the pullout results for the larger reinforcement lengths to decrease thereby decreasing the coefficient of interaction.

- Dredged materials tested wet of optimum produced a lower rate of increase in pullout resistance with increasing normal stress when compared to the Monterey Sand. This comparatively low rate of change is consistent with an undrained behavior. When compared to the Monterey Sand the dredged material results in pullout resistance values that are three to four times lower and in values of Ci that are also significantly lower.
- The pullout resistance results, as well as the coefficient of interaction, was found to be considerably higher for the UX1700 geogrid compared to the UX1400. This was found to be the case for both sand and dredged materials. The two dredged materials had Ci values of .2 to .3 for the UX1400 and .3 to .4 for the UX1700. The Monterey Sand had a higher Ci value for the UX1700 as well. The values were .4 for the UX1400 and .8 for the UX1700. The pullout loads were higher for the UX1700 for both the Monterey Sand and the two dredged materials. The two dredged materials had pullout loads ranging from 400 to 800 lbs. for the UX1400 and 600 to 1,000 lbs. for the UX1700. The Monterey Sand had pullout loads of 1,000 to 3,000 lbs. for the UX1400 and 2,000 to 5,000 lbs. for the UX1700.

5.2 RECOMMENDATIONS

Recommendations are offered based on the experiences and results from this research program. The recommendations aim at optimizing both the efficiency of pullout testing as well as the quality of the results.

- A wider range of normal stresses should be tested to understand the full characteristics of the pullout results for each soil type. Suggested normal stresses range from the dead load of the system to 12psi.
- Additional tests should be conducted that allow for the consolidation of the dredged material before interface shearing takes place. The pullout rate for these consolidated tests should also be tested to represent both drained and undrained conditions. This will help show results more consistent with field conditions.
- Multiple earth pressure cells should be used in order to verify the correct normal stress.
- Additional testing should be completed to determine the degree of interference, DI, between bearing members. Different arrangements of the earth pressure cells in relation to the transverse members could help identify interference between bearing members.
- Biaxial and triaxial geogrids could be tested to verify the effect of different S/B ratios on the coefficient of interaction.
- Variations with the reinforcement length could be tested in a small pullout box as well as in the field. This will help clearly identify any influence of the boundary conditions.

Appendix A: Monterey Sand Pullout Test Results

Appendix A is a collection of all the Monterey Sand pullout test results. The results are summarized into two pages. The first page has the testing information at the top. Below this is the description of the geogrid that is being tested as well as the dimensions of the pullout box. After this is the material properties which shows the properties of the soil being tested. To the right of the material properties is the amount of normal stress being applied and the rate of pullout.

The results are the last section on this page. Within the results section are the values for the pullout resistance and the coefficient of interaction. The maximum displacement of the lvdts are also listed as well as a graph of the pullout force vs. displacement. At the bottom of the page is a comments section. This section is where the operator records any problems or any information worth noting for that particular test.

The second page has three figures. The first figure is a diagram of the geogrid inside the pullout box. The diagram shows the locations of the lvdts in relation to the geogrid. The second figure is a graph of the pullout force versus time. The last figure is a graph of the earth pressure cell reading versus the lvdt displacements.

TEST 103

Large Pullout Test

Test details :		
	Test Name	UX1400-sand-.5psi
	Date	1/9/2013
	Member	Jacob

Box Dimensions (inch)	Length	Width	Depth	Area (in2)	Height from base to sleeve
	60	24	11	1440	5

Geogrid Details	Manufactur	Product	Ultimate Tensile Strength
	Tensar	UX1400	12000 lb/ft

Specimen Information(ft)	Width	Embedment Length (Le)
	1	2.97

Material Properties	
Material Name	Monterey Sand
Friction Angle (ϕ')	35
Moisture Content (%)	0%
Y'd,max (pcf)	99.3
Target Compaction	1
Weight of each Lift	201
No. of Lifts	4

Test Details	
Normal Stress σ' (psi)	Rate of Pullout (in/min)
0.5	0.04

Maximum Displacements	
LVDT	Disp (mm)
A	21.242
B	15.955
C	22.649

RESULTS

Maximum Load (lb)	140.00	
Pullout Resisatnce (lb/ft)	140.00	
Coefficient of Interaction, ci	$\frac{Pr}{2(Le)(c + \sigma' \tan(\phi'))}$	0.468

Average EPC reading (psi)	-2.857

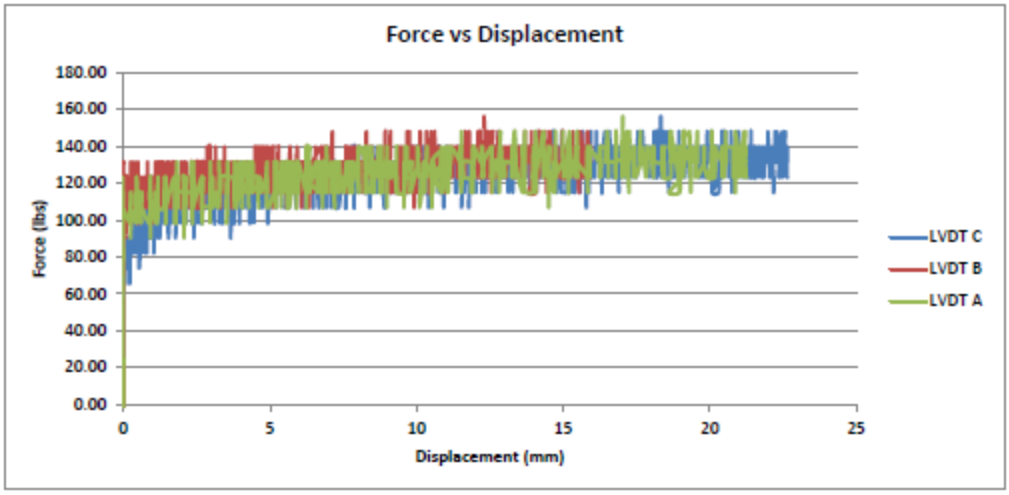

Comments:

TEST 103 CONTINUED

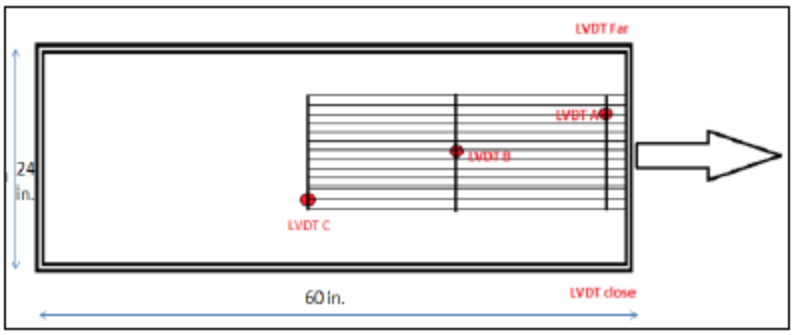

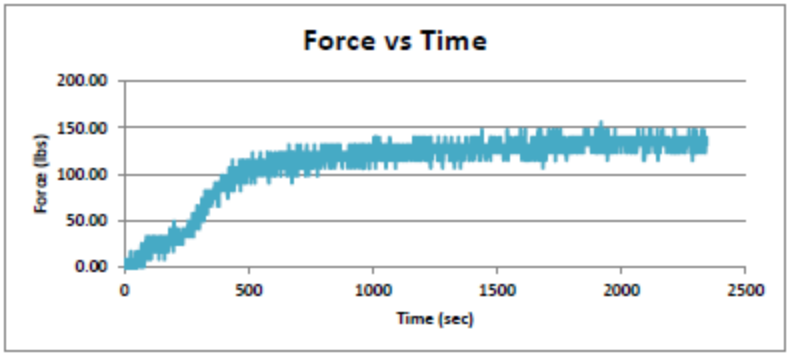

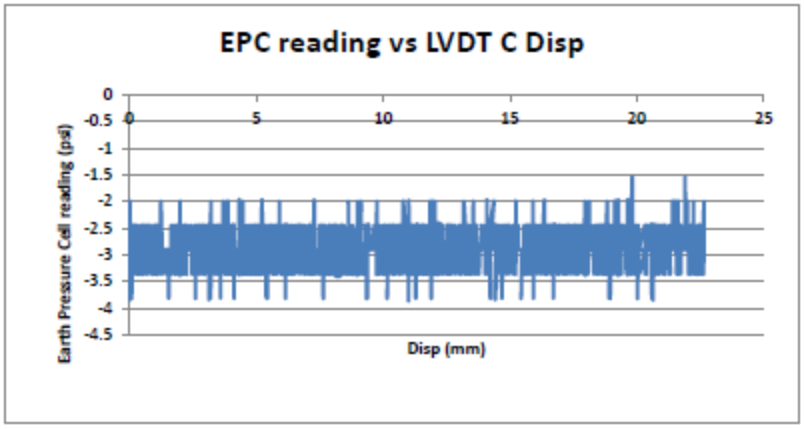

TEST 104

Large Pullout Test

Test details :		
	Test Name	UX1700-sand-.5psi
	Date	1/18/2013
	Member	Jacob

Box Dimensions (inch)	Length	Width	Depth	Area (in2)	Height from base to sleeve
	60	24	11	1440	5

Geogrid Details	Manufactur	Product	Ultimate Tensile Strength
	Tensar	UX1700	12000 lb/ft

Specimen Information(ft)	Width	Embedment Length (Le)
	1	2.904

Material Properties	
Material Name	Monterey Sand
Friction Angle (ϕ')	35
Moisture Content (%)	1%
Y'd,max (pcf)	99.3
Target Compaction	1
Weight of each Lift	201
No. of Lifts	4

Test Details	
Normal Stress σ' (psi)	Rate of Pullout (in/min)
0.5	0.04

Maximum Displacements	
LVDT	Disp (mm)
A	39.170
B	44.119
C	46.761

RESULTS

Maximum Load (lb)	222.67	
Pullout Resisatnce (lb/ft)	222.67	
Coefficient of Interaction, ci	$\frac{Pr}{2(Le)(c + \sigma' \tan(\phi'))}$	0.760

Average EPC reading (psi)	-1.967

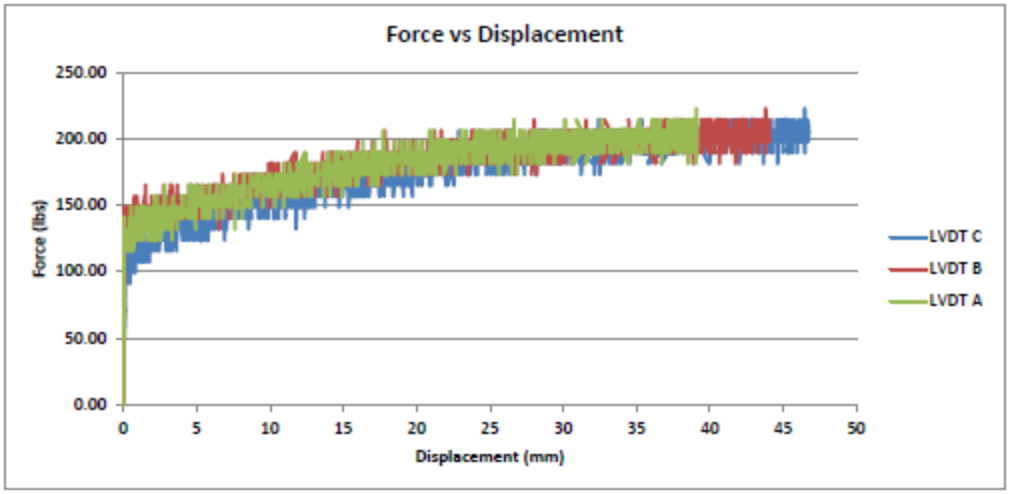

Comments:

TEST 104 CONTINUED

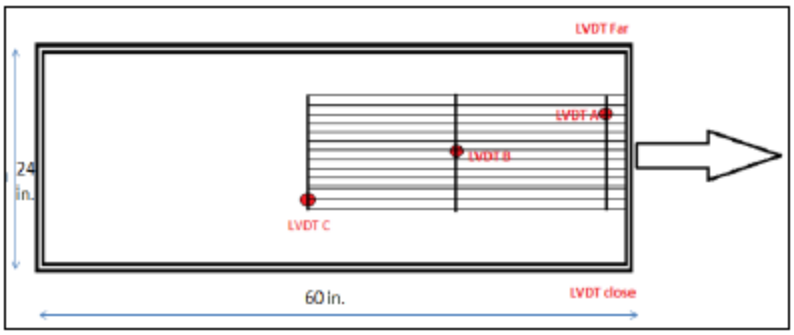

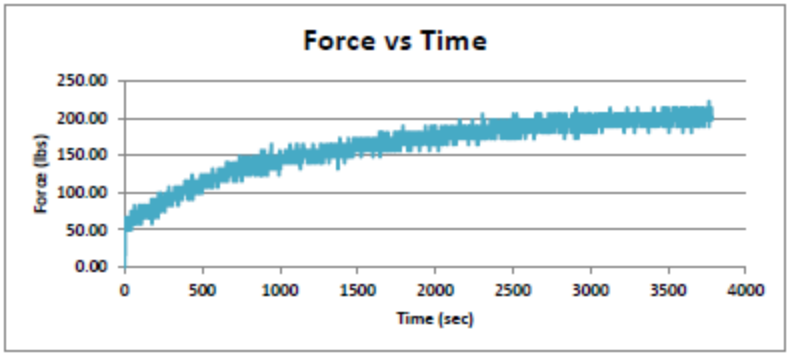

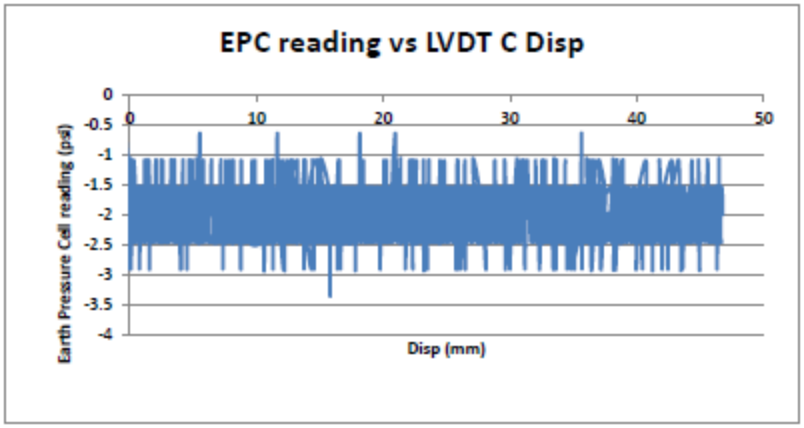

TEST 37

Large Pullout Test

Test details :		
	Test Name	UX1400-Monterey Sand-4psi
	Date	4/2/2012
	Member	Kemp

Box Dimensions (inch)	Length	Width	Depth	Area (in2)	Height from base to sleeve
	60	24	11	1440	5

Geogrid Details	Manufactur	Product	Ultimate Tensile Strength
	Tensar	UX1400	4800 lb/ft

Specimen Information(ft)	Width	Embedment Length (Le)
	1.5	2.97

Material Properties	
Material Name	Monterey San
Friction Angle (ϕ')	35
Moisture Content (%)	1.5
Y'd,max (pcf)	99
Target Compaction	100%
Weight of each Lift (lbs)	134
No. of Lifts	6

Test Details	
Normal Stress σ' (psi)	Rate of Pullout (in/min)
4	0.04

Maximum Displacements	
LVDT	Disp (mm)
A	99.468
B	108.321
C	109.136

RESULTS

Maximum Load (lb)	1660.63	
Pullout Resisatnce (lb/ft)	1107.09	
Coefficient of Interaction, ci	$\frac{Pr}{2(Le)(c + \sigma' \tan(\phi'))}$	0.462

Average EPC reading (psi)	3.389

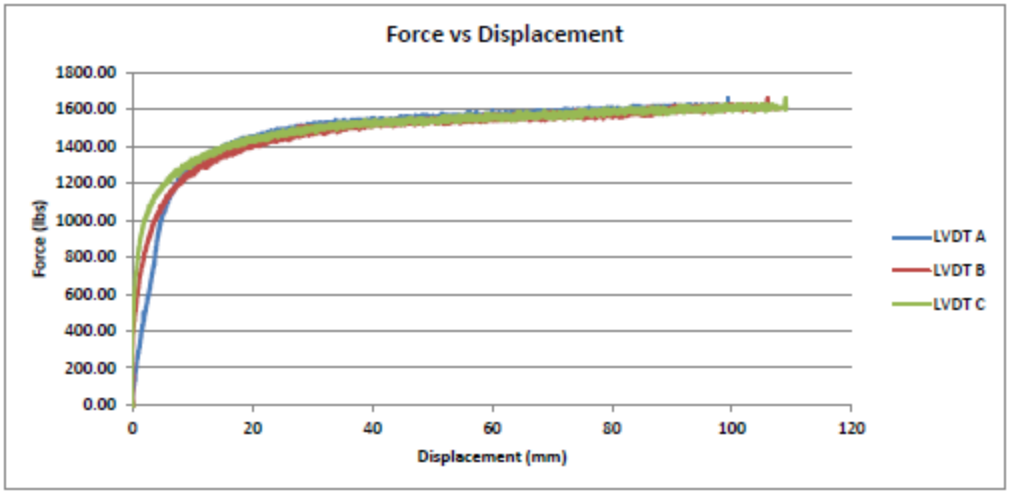

Comments:
Test Duration: *3.52 hours*
Plateau observed

TEST 37 CONTINUED

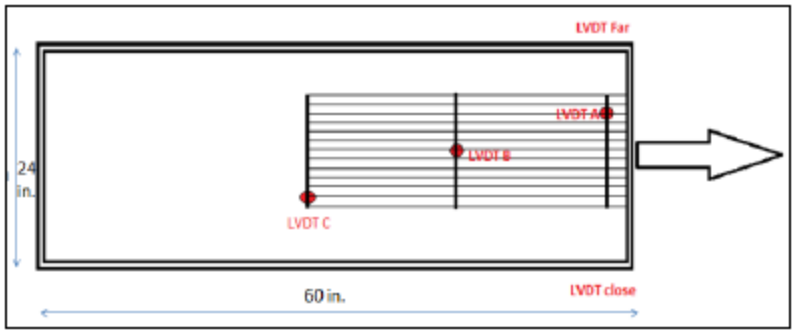

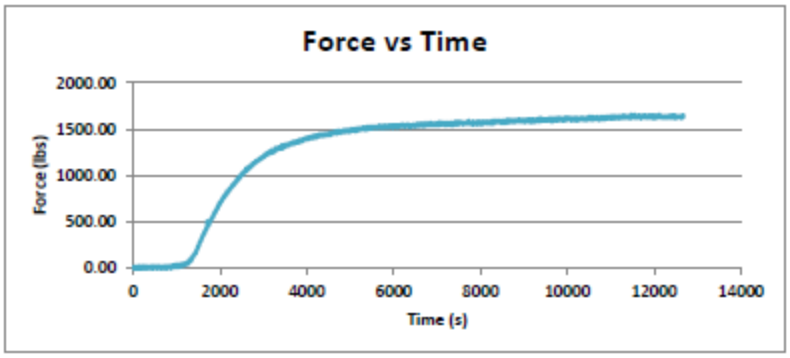

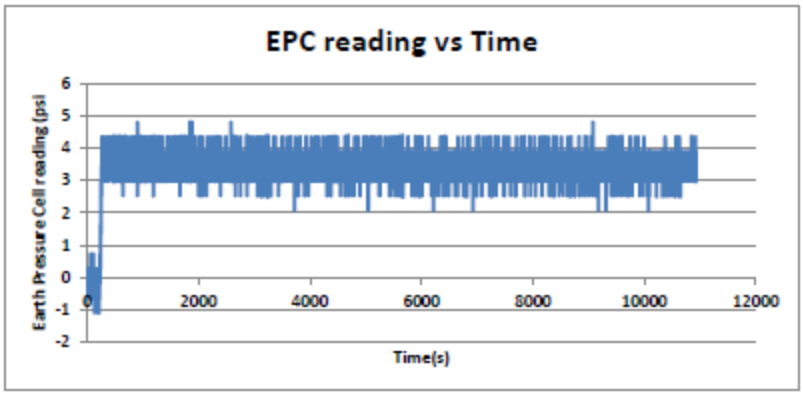

TEST 34

Large Pullout Test

Test details :		
	Test Name	UX1700-Monterey Sand-4psi
	Date	3/28/2012
	Member	Sangy

Box Dimensions (inch)	Length	Width	Depth	Area (in2)	Height from base to sleeve
	60	24	11	1440	5

Geogrid Details	Manufactur	Product	Ultimate Tensile Strength
	Tensar	UX1700	11900 lb/ft

Specimen Information(ft)	Width	Embedment Length (Le)
	1.5	2.87

Material Properties	
Material Name	Monterey San
Friction Angle (ϕ')	35
Moisture Content (%)	1.5
Y'd,max (pcf)	99
Target Compaction	100%
Weight of each Lift (lbs)	134
No. of Lifts	6

Test Details	
Normal Stress σ' (psi)	Rate of Pullout (in/min)
4	0.04

Maximum Displacements	
LVDT	Disp (mm)
A	54.327
B	0.008
C	83.730

RESULTS

Maximum Load (lb)	2605.40	
Pullout Resisatnce (lb/ft)	1736.93	
Coefficient of Interaction, ci	$\frac{Pr}{2(Le)(c + \sigma' \tan(\phi'))}$	0.750

Average EPC reading (psi)	-0.411

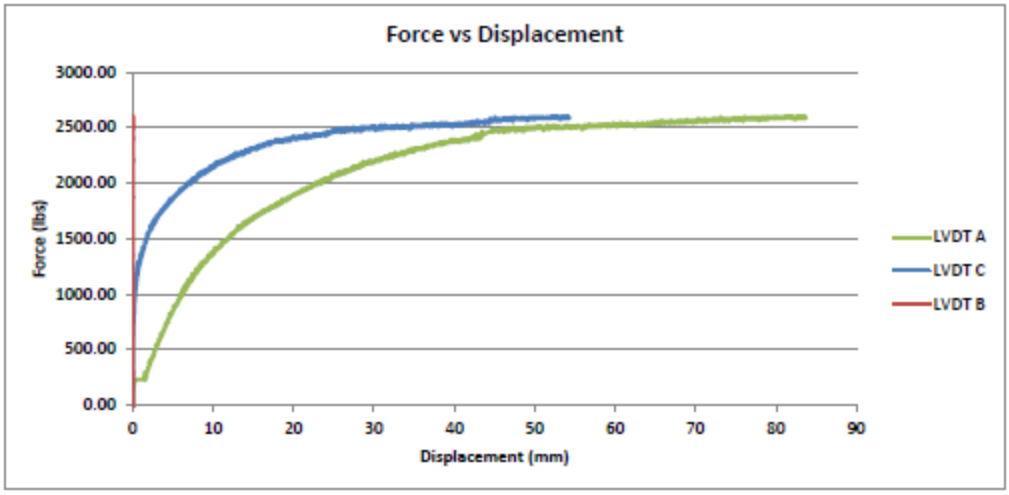

Comments:
Test Duration: 1.99 hours
1 LVDT not working, Load cell stopped working thrice, computer had to be restarted
Plateau observed

TEST 34 CONTINUED

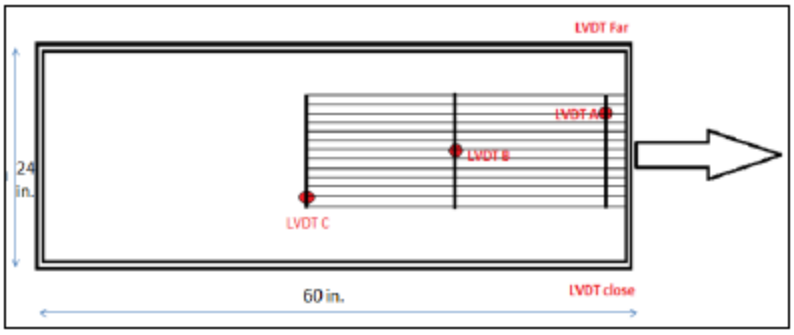

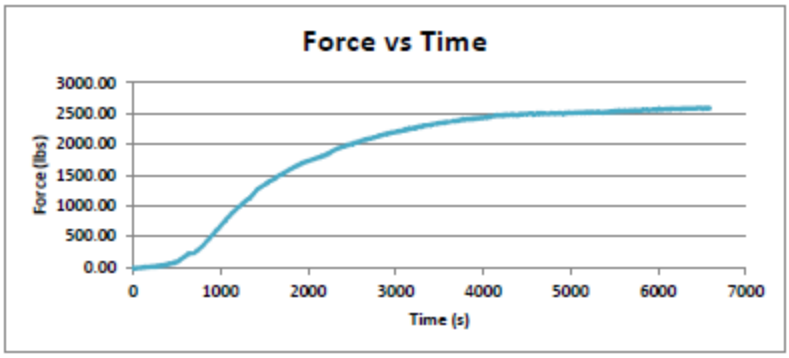

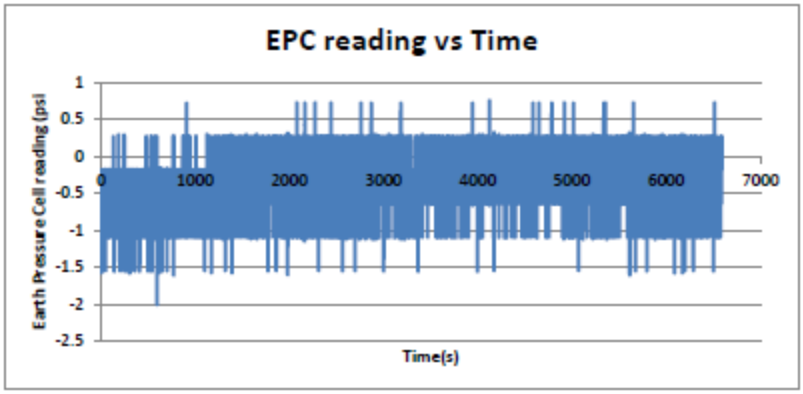

TEST 90

Large Pullout Test

Test details :		
	Test Name	UX1400-Monterey Sand-4psi
	Date	7/19/2012
	Member	Kemp

Box Dimensions (inch)	Length	Width	Depth	Area (in2)	Height from base to sleeve
	60	24	11	1440	5

Geogrid Details	Manufactur	Product	Ultimate Tensile Strength
	Tensar	UX1400	4800 lb/ft

Specimen Information(ft)	Width	Embedment Length (Le)
	1	2.87

Material Properties	
Material Name	Monterey San
Friction Angle (ϕ')	35
Moisture Content (%)	1.5
Y'd,max (pcf)	99
Target Compaction	100%
Weight of each Lift (lbs)	134
No. of Lifts	6

Test Details	
Normal Stress σ' (psi)	Rate of Pullout (in/min)
4	0.04

Maximum Displacements	
LVDT	Disp (mm)
A	29.661
B	8.134
C	42.598

RESULTS

Maximum Load (lb)	1019.15	
Pullout Resisatnce (lb/ft)	1019.15	
Coefficient of Interaction, ci	$\frac{Pr}{2(Le)(c + \sigma' \tan(\phi'))}$	0.440

Average EPC reading (psi)	1.135

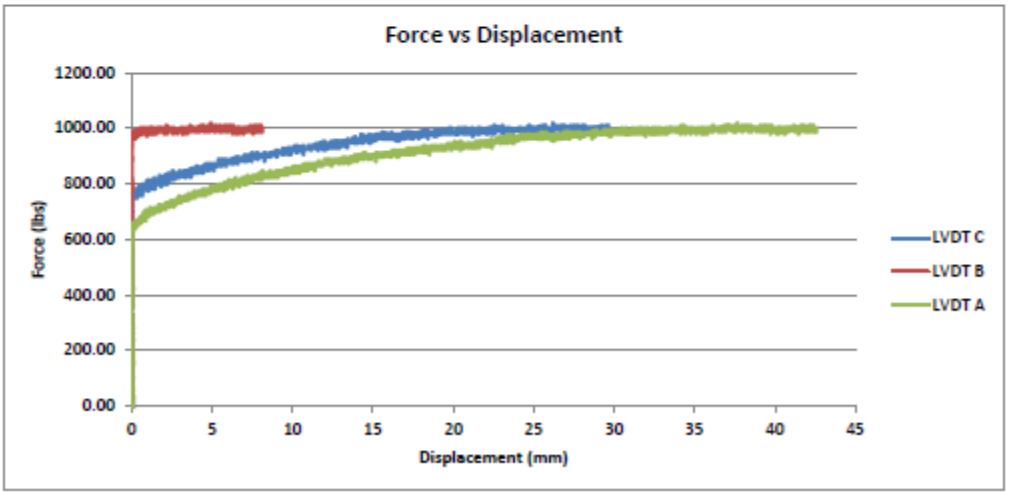

Comments:
Test Duration: 1.58 hours
Plateau observed
LVDT B moved latest

TEST 90 CONTINUED

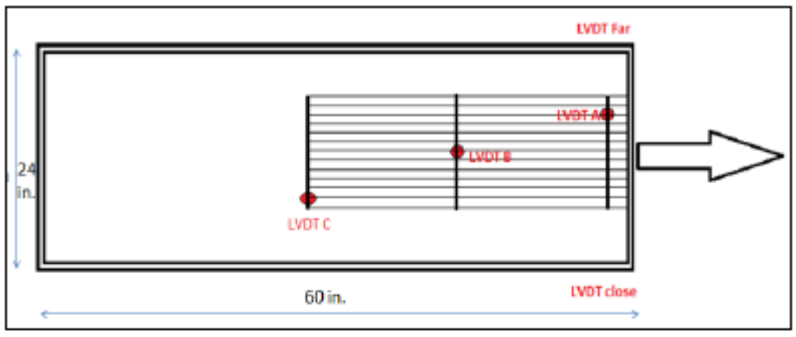

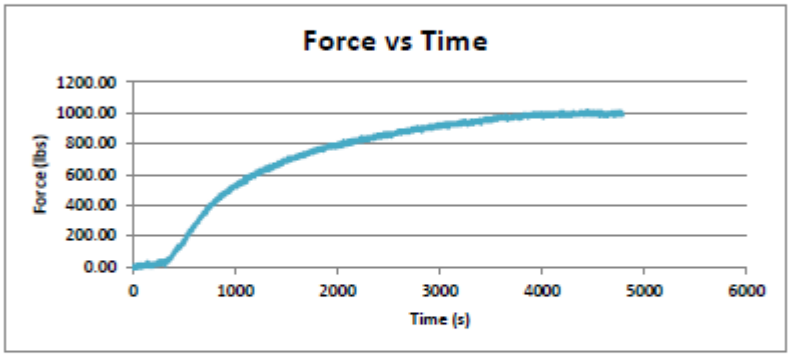

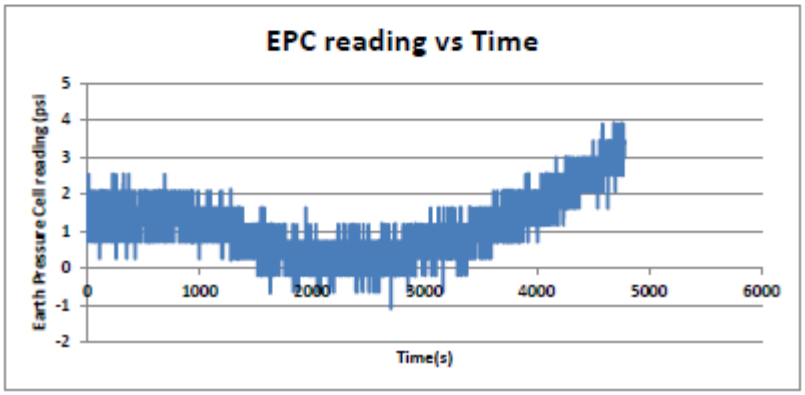

TEST 85

Large Pullout Test

Test details :		
	Test Name	UX1700-Monterey Sand-4psi
	Date	7/17/2012
	Member	Kemp

Box Dimensions (inch)	Length	Width	Depth	Area (in2)	Height from base to sleeve
	60	24	11	1440	5

Geogrid Details	Manufactur	Product	Ultimate Tensile Strength
	Tensar	UX1700	11900 lb/ft

Specimen Information(ft)	Width	Embedment Length (Le)
	1	2.87

Material Properties	
Material Name	Monterey San
Friction Angle (ϕ')	35
Moisture Content (%)	1.5
Y'd,max (pcf)	99
Target Compaction	100%
Weight of each Lift (lbs)	134
No. of Lifts	6

Test Details	
Normal Stress σ' (psi)	Rate of Pullout (in/min)
4	0.04

Maximum Displacements	
LVDT	Disp (mm)
A	33.008
B	22.551
C	49.419

RESULTS

Maximum Load (lb)	2046.51	
Pullout Resisatnce (lb/ft)	2046.51	
Coefficient of Interaction, ci	$\frac{Pr}{2(Le)(c + \sigma' \tan(\phi'))}$	0.884

Average EPC reading (psi)	2.320

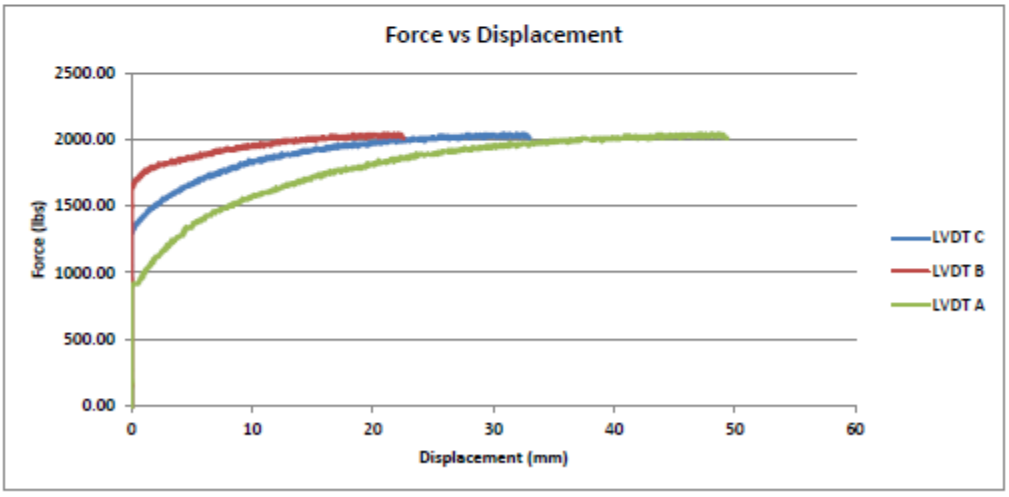

Comments:
Test Duration: *1.48 hours*
Lvdt B moves latest

TEST 85 CONTINUED

Large Pullout Test

Test details :		
	Test Name	UX1700-Monterey Sand-4psi
	Date	7/17/2012
	Member	Kemp

Box Dimensions (inch)	Length	Width	Depth	Area (in2)	Height from base to sleeve
	60	24	11	1440	5

Geogrid Details	Manufactur	Product	Ultimate Tensile Strength
	Tensar	UX1700	11900 lb/ft

Specimen Information(ft)	Width	Embedment Length (Le)
	1	2.87

Material Properties	
Material Name	Monterey San
Friction Angle (ϕ')	35
Moisture Content (%)	1.5
Y'd,max (pcf)	99
Target Compaction	100%
Weight of each Lift (lbs)	134
No. of Lifts	6

Test Details	
Normal Stress σ' (psi)	Rate of Pullout (in/min)
4	0.04

Maximum Displacements	
LVDT	Disp (mm)
A	33.008
B	22.551
C	49.419

RESULTS

Maximum Load (lb)	2046.51	
Pullout Resisatnce (lb/ft)	2046.51	
Coefficient of Interaction, ci	$\frac{Pr}{2(Le)(c + \sigma' \tan(\phi'))}$	0.884

Average EPC reading (psi)	2.320

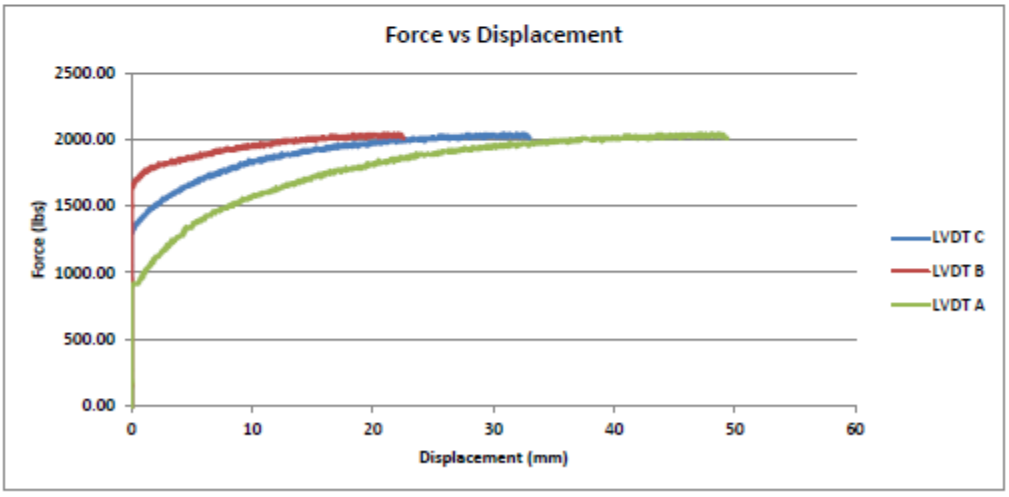

Comments:
Test Duration: *1.48 hours*
Lvdt B moves latest

TEST 105

Large Pullout Test

Test details :		
	Test Name	UX1400-Monterey Sand-6psi
	Date	1/24/2013
	Member	Jacob

Box Dimensions (inch)	Length	Width	Depth	Area (in2)	Height from base to sleeve
	60	24	11	1440	5

Geogrid Details	Manufactur	Product	Ultimate Tensile Strength
	Tensar	UX1400	12000 lb/ft

Specimen Information(ft)	Width	Embedment Length (Le)
	1	4.323

Material Properties	
Material Name	Monterey Sand
Friction Angle (ϕ')	35
Moisture Content (%)	1%
Y'd,max (pcf)	99.3
Target Compaction	1
Weight of each Lift	201
No. of Lifts	4

Test Details	
Normal Stress σ' (psi)	Rate of Pullout (in/min)
6	0.04

Maximum Displacements	
LVDT	Disp (mm)
A	66.559
B	48.251
C	38.581

RESULTS

Maximum Load (lb)	1939.67	
Pullout Resisatnce (lb/ft)	1939.67	
Coefficient of Interaction, ci	$\frac{Pr}{2(Le)(c + \sigma' \tan(\phi'))}$	0.371

Average EPC reading (psi)	4.954

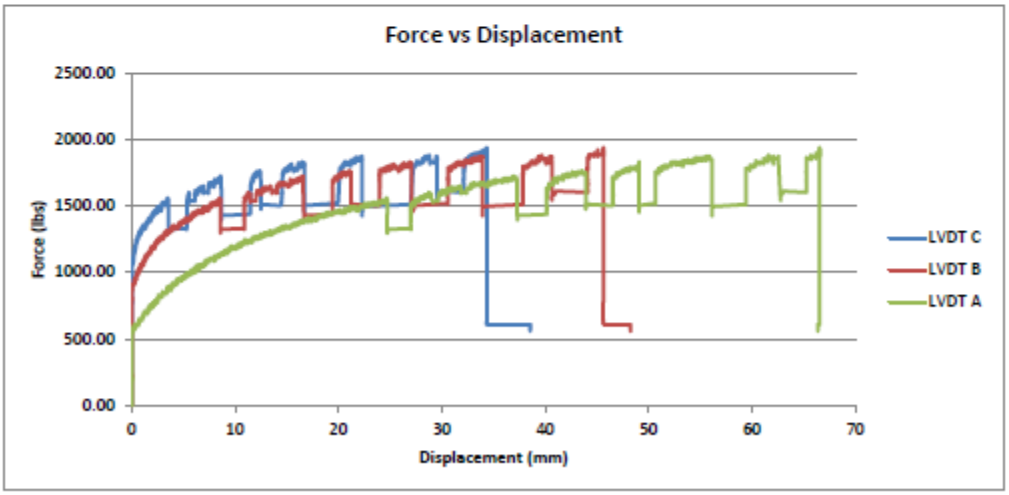

Comments:

TEST 105 CONTINUED

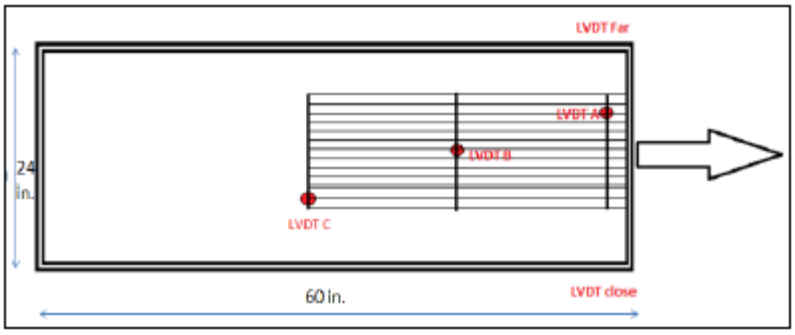

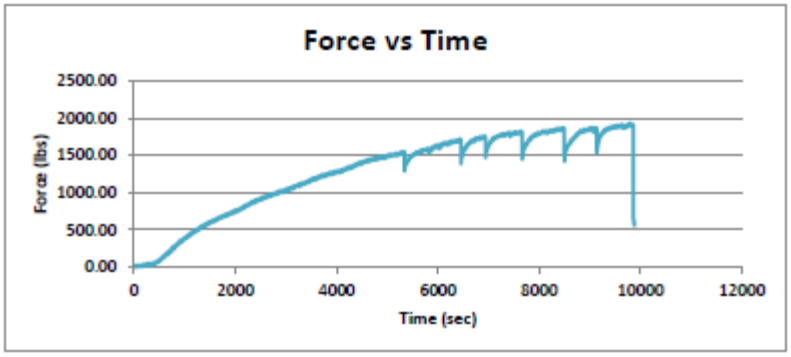

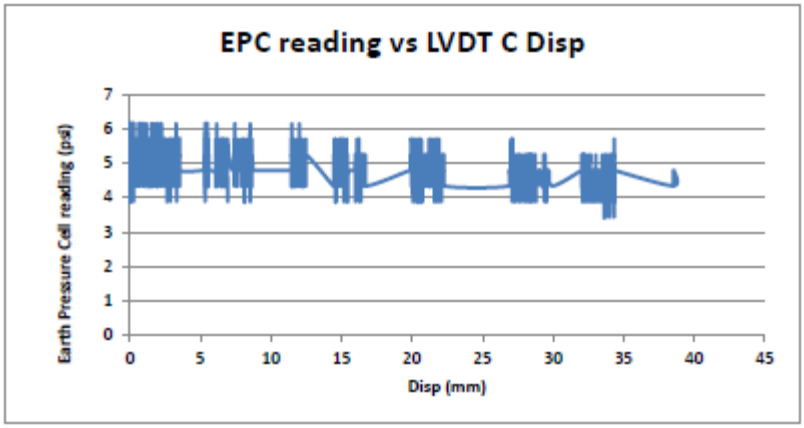

TEST 33

Large Pullout Test

Test details :		
	Test Name	UX1400-Monterey Sand-6psi
	Date	3/27/2012
	Member	Jake

Box Dimensions (inch)	Length	Width	Depth	Area (in2)	Height from base to sleeve
	60	24	11	1440	5

Geogrid Details	Manufactur	Product	Ultimate Tensile Strength
	Tensar	UX1400	4800 lb/ft

Specimen Information(ft)	Width	Embedment Length (Le)
	1.5	3.14

Material Properties	
Material Name	Monterey San
Friction Angle (ϕ')	35
Moisture Content (%)	1.5
Y'd,max (pcf)	99
Target Compaction	100%
Weight of each Lift (lbs)	134
No. of Lifts	6

Test Details	
Normal Stress σ' (psi)	Rate of Pullout (in/min)
6	0.04

Maximum Displacements	
LVDT	Disp (mm)
A	39.480
B	21.230
C	8.719

RESULTS

Maximum Load (lb)	1538.25	
Pullout Resisatnce (lb/ft)	1025.50	
Coefficient of Interaction, ci	$\frac{Pr}{2(Le)(c + \sigma' \tan(\phi'))}$	0.270

Average EPC reading (psi)	6.078

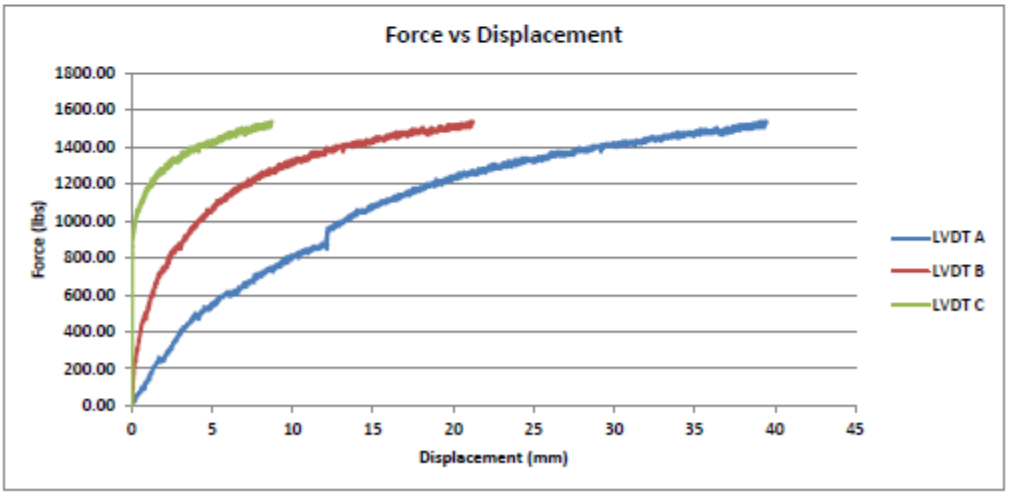

Comments:
Test Duration: 1.16 hours
Stopped early because clamp bar ran into piston
Was repeated

TEST 33 CONTINUED

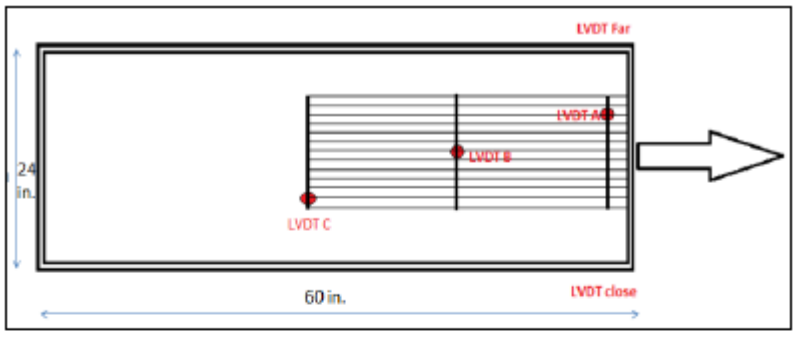

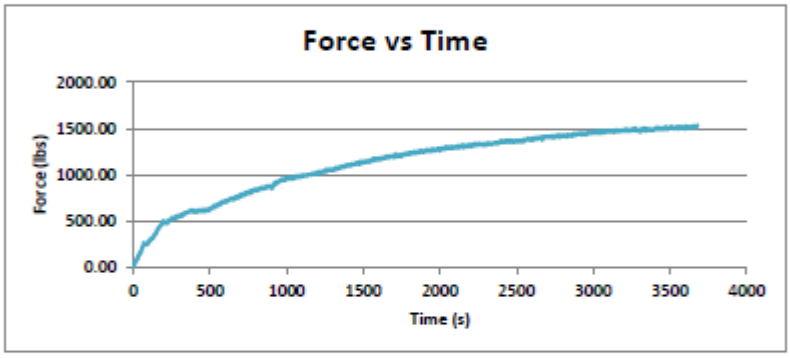

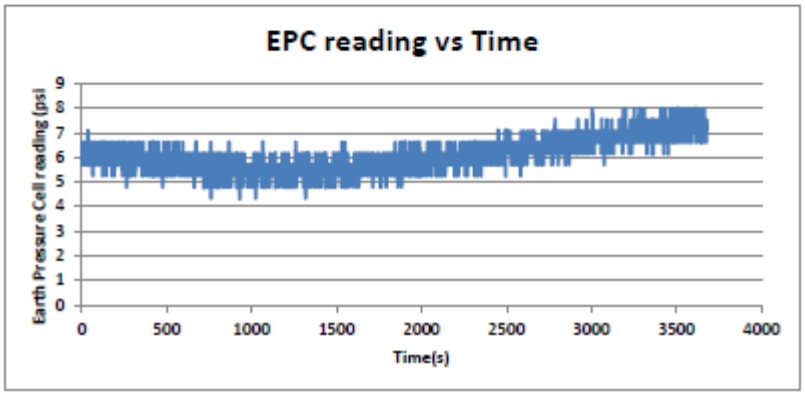

TEST 91

Large Pullout Test

Test details :		
	Test Name	UX1400-Monterey Sand-6psi
	Date	7/19/2012
	Member	Fabrizio,Kemp

Box Dimensions (inch)	Length	Width	Depth	Area (in2)	Height from base to sleeve
	60	24	11	1440	5

Geogrid Details	Manufactur	Product	Ultimate Tensile Strength
	Tensar	UX1400	4800 lb/ft

Specimen Information(ft)	Width	Embedment Length (Le)
	1	2.87

Material Properties	
Material Name	Monterey San
Friction Angle (ϕ')	35
Moisture Content (%)	1.5
Y'd,max (pcf)	99
Target Compaction	100%
Weight of each Lift (lbs)	134
No. of Lifts	6

Test Details	
Normal Stress σ' (psi)	Rate of Pullout (in/min)
6	0.04

Maximum Displacements	
LVDT	Disp (mm)
A	142.515
B	98.135
C	170.540

RESULTS

Maximum Load (lb)	1347.90	
Pullout Resisatnce (lb/ft)	1347.90	
Coefficient of Interaction, ci	$\frac{Pr}{2(Le)\,(c + \sigma' \tan(\phi'))}$	0.388

Average EPC reading (psi)	1.676

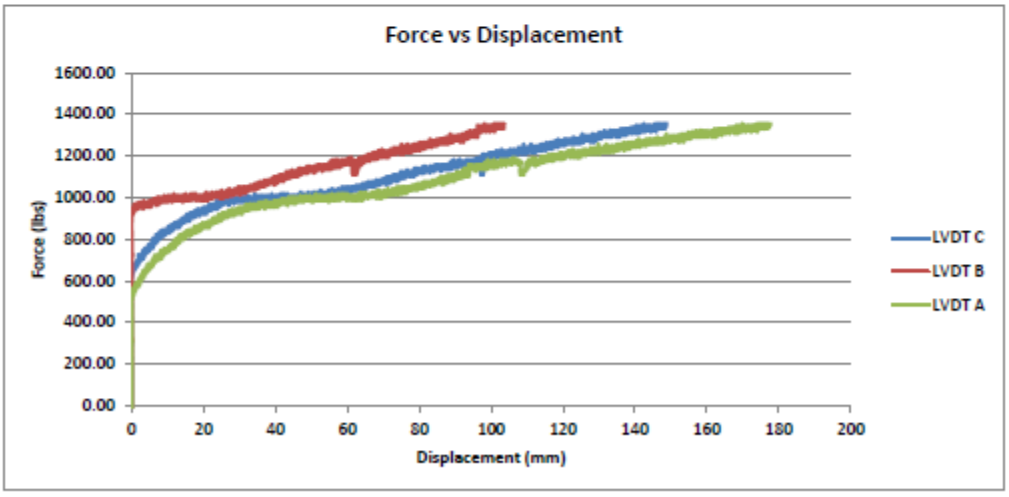

Comments:
Test Duration: 4.37 hours
No plateau observed
LVDT B moved latest

TEST 91 CONTINUED

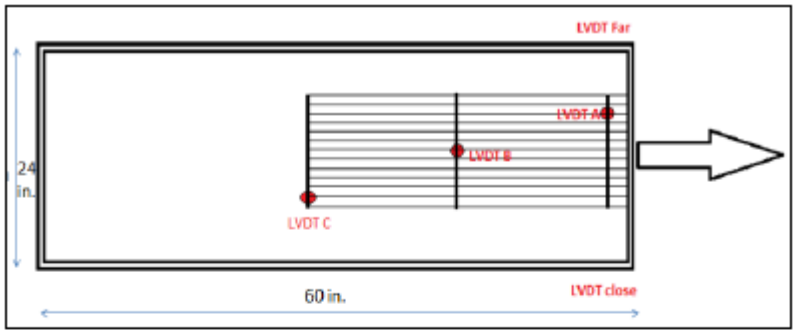

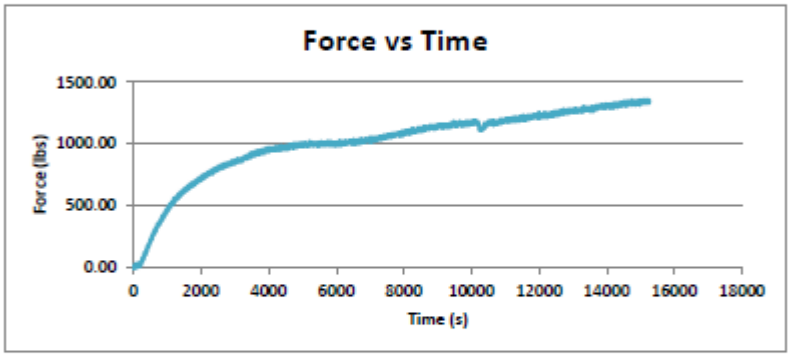

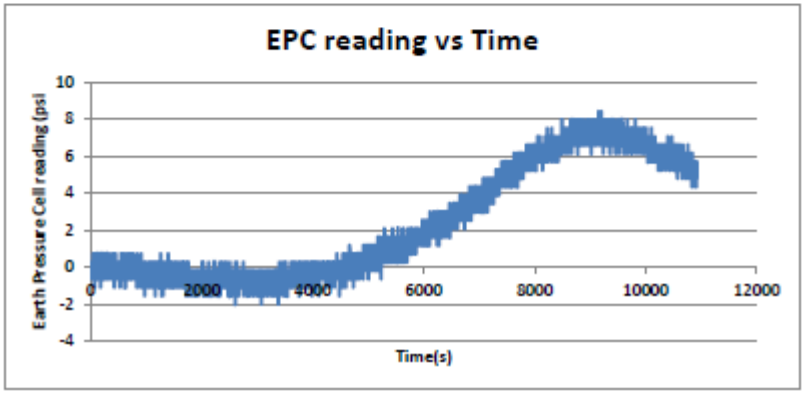

TEST 87

Large Pullout Test

Test details :		
	Test Name	UX1700-Monterey Sand-6psi
	Date	7/17/2012
	Member	Kemp

Box Dimensions (inch)	Length	Width	Depth	Area (in2)	Height from base to sleeve
	60	24	11	1440	5

Geogrid Details	Manufactur	Product	Ultimate Tensile Strength
	Tensar	UX1700	11900 lb/ft

Specimen Information(ft)	Width	Embedment Length (Le)
	1	2.87

Material Properties	
Material Name	Monterey San
Friction Angle (ϕ')	35
Moisture Content (%)	1.5
Ɣd,max (pcf)	99
Target Compaction	100%
Weight of each Lift (lbs)	134
No. of Lifts	6

Test Details	
Normal Stress σ' (psi)	Rate of Pullout (in/min)
6	0.04

Maximum Displacements	
LVDT	Disp (mm)
A	116.424
B	108.508
C	172.050

RESULTS

Maximum Load (lb)	2423.21	
Pullout Resisatnce (lb/ft)	2423.21	
Coefficient of Interaction, ci	$\frac{Pr}{2(Le)(c + \sigma' \tan(\phi'))}$	0.698

Average EPC reading (psi)	1.578

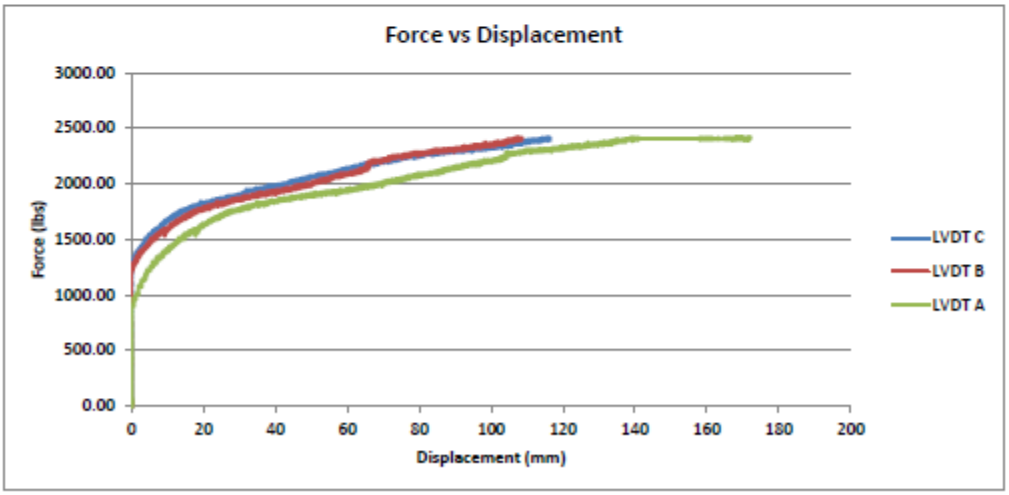

Comments:
Test Duration: *4.02 hours*

TEST 87 CONTINUED

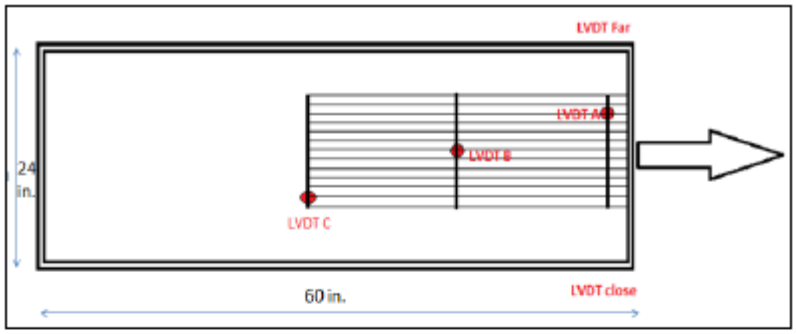

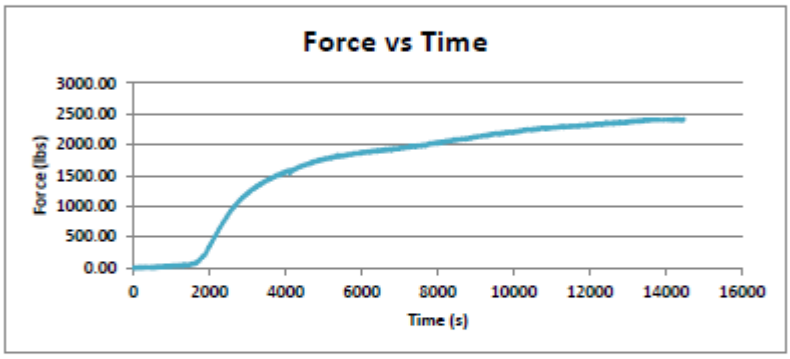

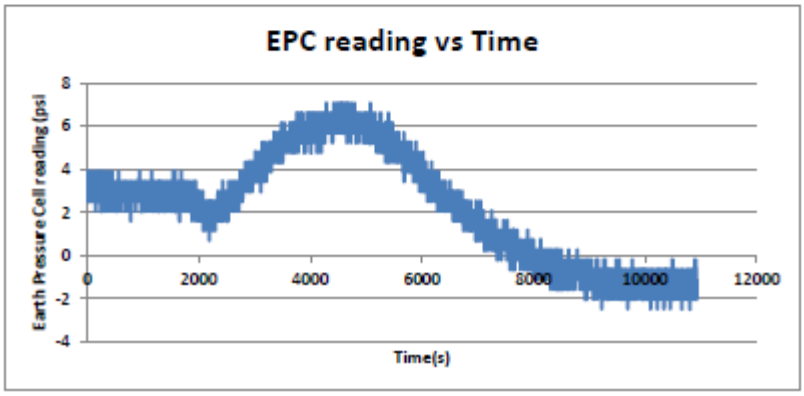

TEST 32

Large Pullout Test

Test details :		
	Test Name	UX1400-Monterey Sand-8psi
	Date	3/26/2012
	Member	Kemp

Box Dimensions (inch)	Length	Width	Depth	Area (in2)	Height from base to sleeve
	60	24	11	1440	5

Geogrid Details	Manufactur	Product	Ultimate Tensile Strength
	Tensar	UX1400	4800 lb/ft

Specimen Information(ft)	Width	Embedment Length (Le)
	1.5	2.97

Material Properties	
Material Name	Monterey San
Friction Angle (ϕ')	35
Moisture Content (%)	1.5
Ɣd,max (pcf)	99
Target Compaction	100%
Weight of each Lift (lbs)	134
No. of Lifts	6

Test Details	
Normal Stress σ' (psi)	Rate of Pullout (in/min)
8	0.04

Maximum Displacements	
LVDT	Disp (mm)
A	6.184
B	0.002
C	0.021

RESULTS

Maximum Load (lb)	3041.00	
Pullout Resisatnce (lb/ft)	2027.34	
Coefficient of Interaction, ci	$\frac{Pr}{2(Le)(c + \sigma' \tan(\phi'))}$	0.423

Average EPC reading (psi)	4.609

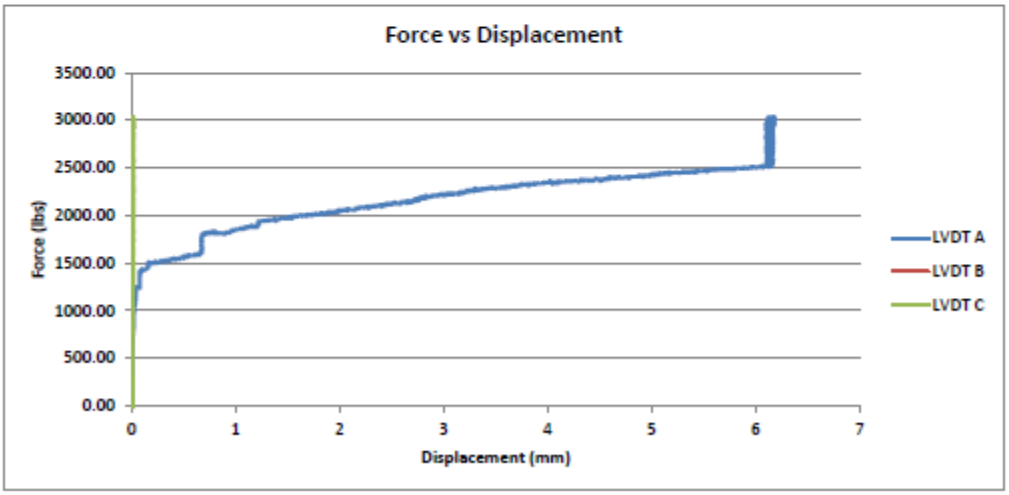

Comments:
Test Duration: 2.27 hours
Stopped early because clamp bar ran into piston
Was repeated

TEST 32 CONTINUED

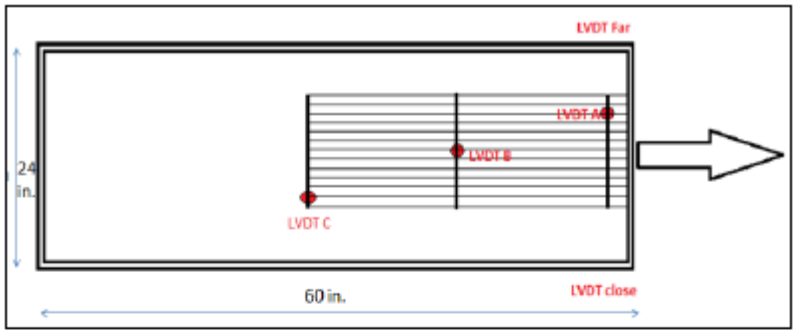

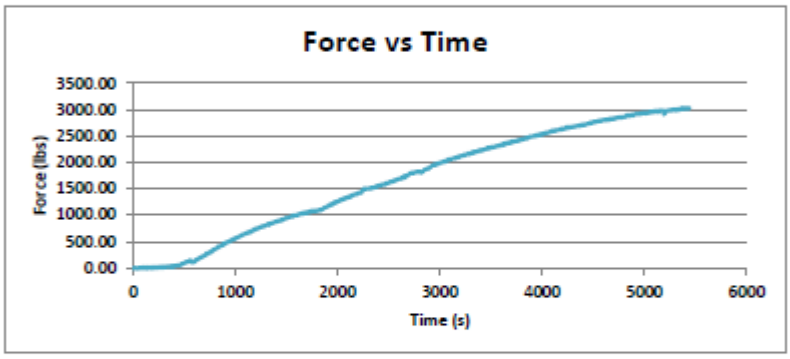

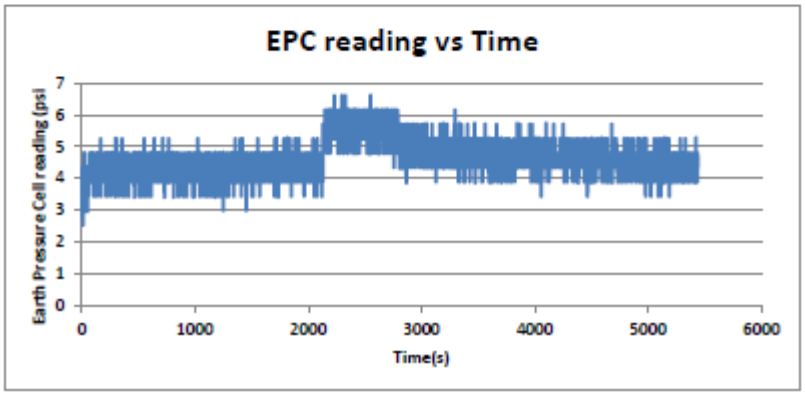

TEST 35

Large Pullout Test

Test details :		
	Test Name	UX1700-Monterey Sand-8psi
	Date	3/29/2012
	Member	Alan

Box Dimensions (inch)	Length	Width	Depth	Area (in2)	Height from base to sleeve
	60	24	11	1440	5

Geogrid Details	Manufactur	Product	Ultimate Tensile Strength
	Tensar	UX1700	11900 lb/ft

Specimen Information(ft)	Width	Embedment Length (Le)
	1.5	2.97

Material Properties	
Material Name	Monterey San
Friction Angle (ϕ')	35
Moisture Content (%)	1.5
Ɣd,max (pcf)	99
Target Compaction	100%
Weight of each Lift (lbs)	134
No. of Lifts	6

Test Details	
Normal Stress σ' (psi)	Rate of Pullout (in/min)
8	0.04

Maximum Displacements	
LVDT	Disp (mm)
A	125.269
B	114.944
C	132.896

RESULTS

Maximum Load (lb)	5449.15	
Pullout Resisatnce (lb/ft)	3632.77	
Coefficient of Interaction, ci	$\frac{Pr}{2(Le)(c + \sigma' \tan(\phi'))}$	0.758

Average EPC reading (psi)	4.899

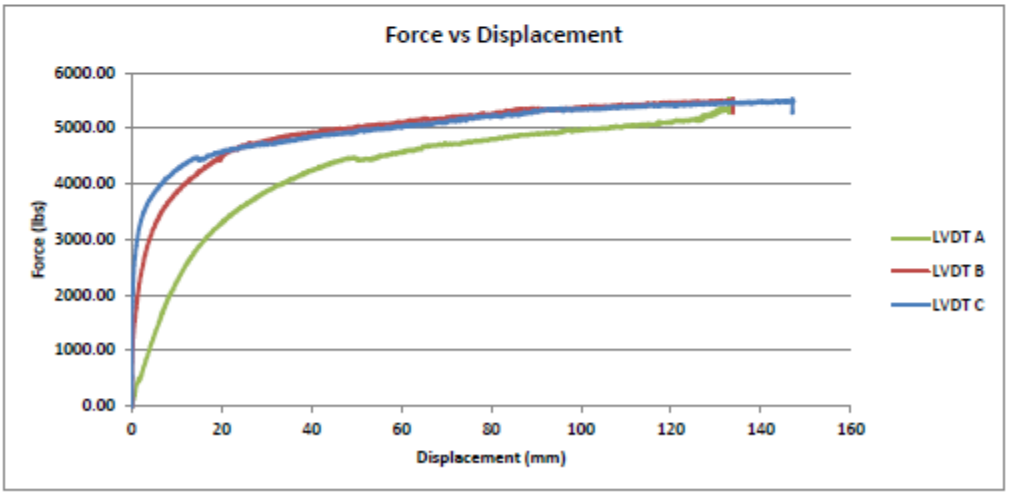

Comments:
Test Duration: *5.45 hours*

Plateau observed

TEST 35 CONTINUED

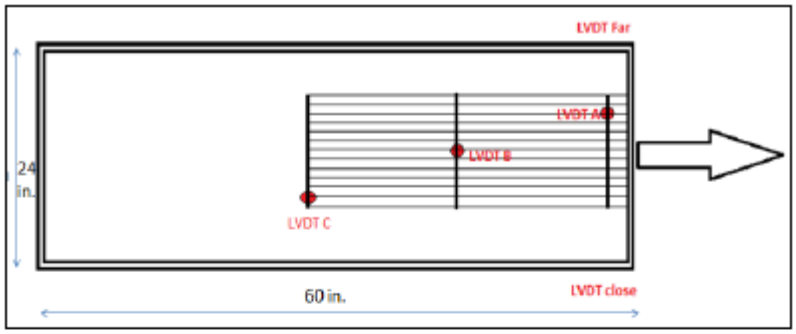

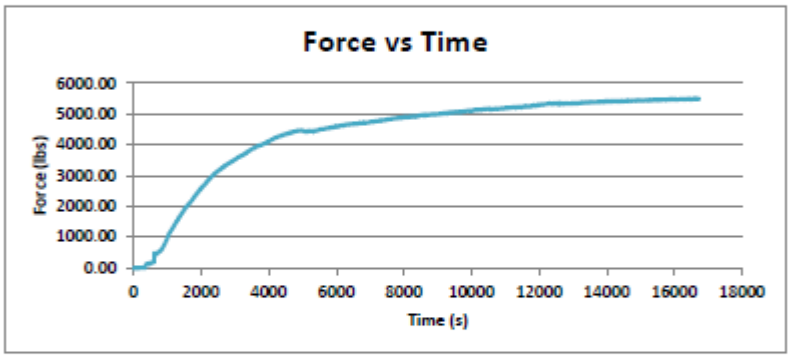

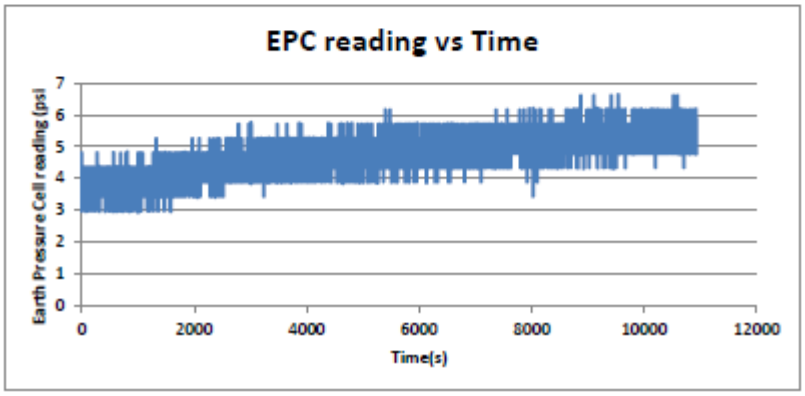

TEST 92

Large Pullout Test

Test details :		
	Test Name	UX1700-Monterey Sand-8psi
	Date	7/20/2012
	Member	Kemp

Box Dimensions (inch)	Length	Width	Depth	Area (in2)	Height from base to sleeve
	60	24	11	1440	5

Geogrid Details	Manufactur	Product	Ultimate Tensile Strength
	Tensar	UX1700	11900 lb/ft

Specimen Information(ft)	Width	Embedment Length (Le)
	1	2.87

Material Properties	
Material Name	Monterey San
Friction Angle (ϕ')	35
Moisture Content (%)	1.5
Ɣd,max (pcf)	99
Target Compaction	100%
Weight of each Lift (lbs)	134
No. of Lifts	6

Test Details	
Normal Stress σ' (psi)	Rate of Pullout (in/min)
8	0.04

Maximum Displacements	
LVDT	Disp (mm)
A	69.451
B	63.579
C	103.889

RESULTS

Maximum Load (lb)	4060.15	
Pullout Resisatnce (lb/ft)	4060.15	
Coefficient of Interaction, ci	$\frac{Pr}{2(Le)\,(c + \sigma' \tan(\phi'))}$	0.877

Average EPC reading (psi)	8.636

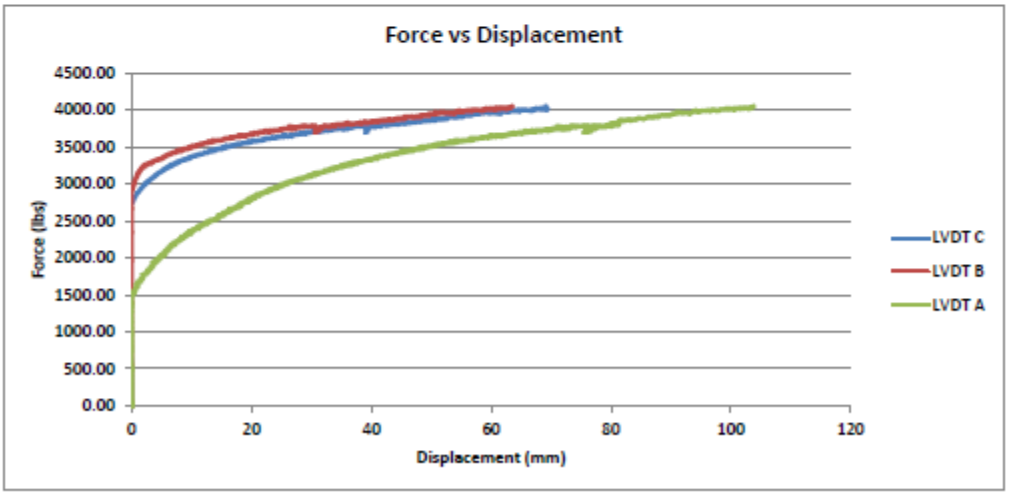

Comments:
Test Duration: *3.81 hours*

TEST 92 CONTINUED

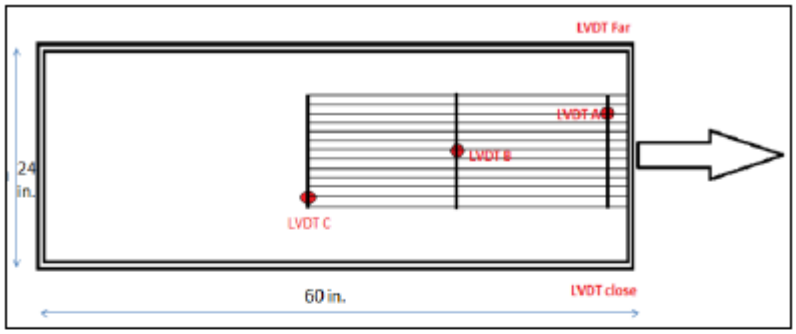

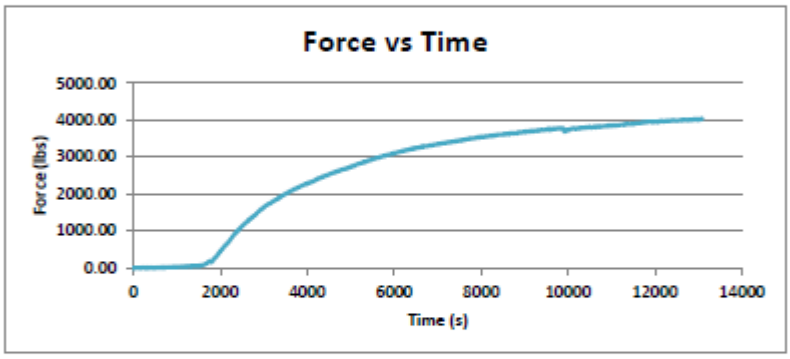

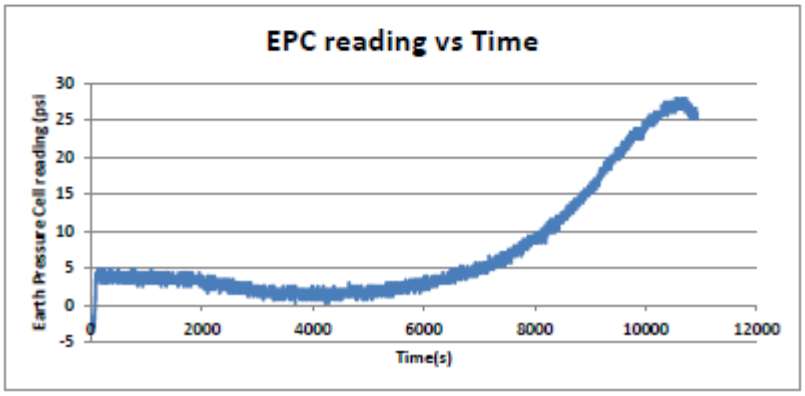

TEST 38

Large Pullout Test

Test details :		
	Test Name	UX1700-Monterey Sand-10psi
	Date	4/3/2012
	Member	Jake

Box Dimensions (inch)	Length	Width	Depth	Area (in2)	Height from base to sleeve
	60	24	11	1440	5

Geogrid Details	Manufactur	Product	Ultimate Tensile Strength
	Tensar	UX1700	11900 lb/ft

Specimen Information(ft)	Width	Embedment Length (Le)
	1.5	2.97

Material Properties	
Material Name	Monterey San
Friction Angle (ϕ')	35
Moisture Content (%)	1.5
Ɣd,max (pcf)	99
Target Compaction	100%
Weight of each Lift (lbs)	134
No. of Lifts	6

Test Details	
Normal Stress σ' (psi)	Rate of Pullout (in/min)
10	0.04

Maximum Displacements	
LVDT	Disp (mm)
A	67.483
B	54.127
C	54.904

RESULTS

Maximum Load (lb)	4923.14	
Pullout Resisatnce (lb/ft)	3282.09	
Coefficient of Interaction, ci	$\frac{Pr}{2(Le)(c + \sigma' \tan(\phi'))}$	0.548

Average EPC reading (psi)	6.370

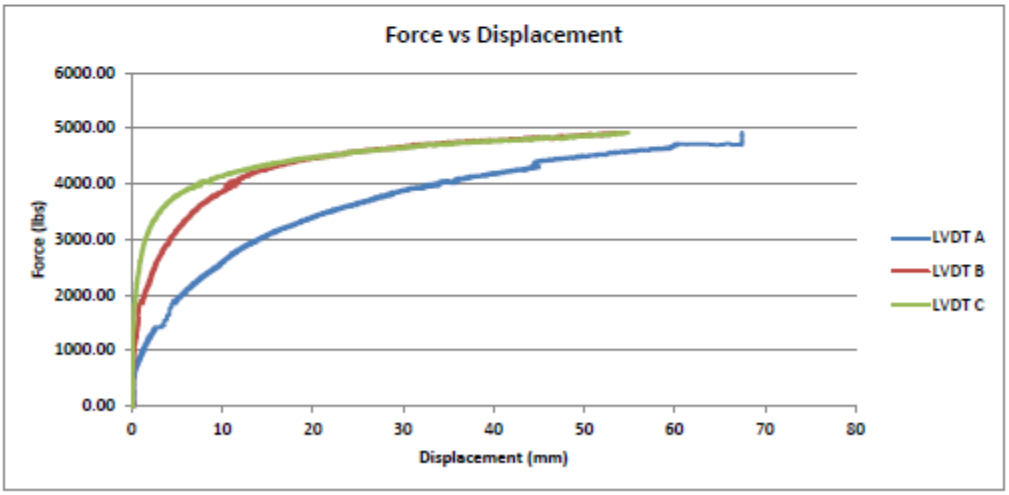

Comments:
Test Duration: 2.89 hours
Load cell stopped working once in between, computer was restarted

TEST 38 CONTINUED

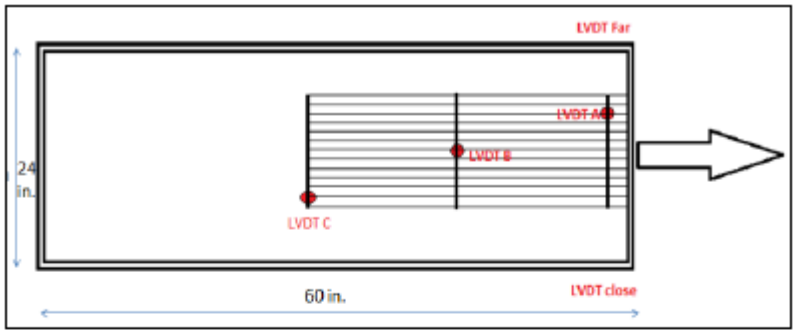

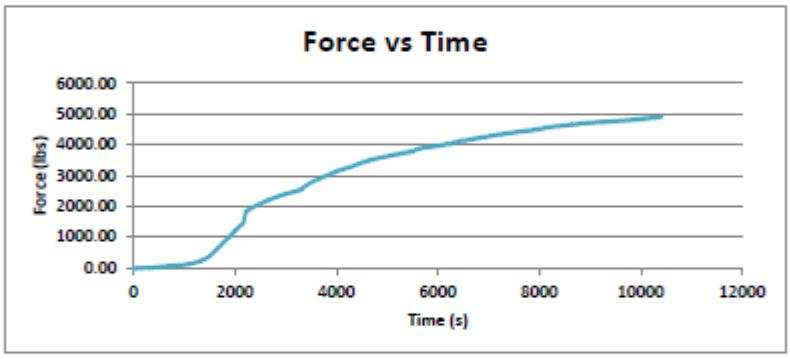

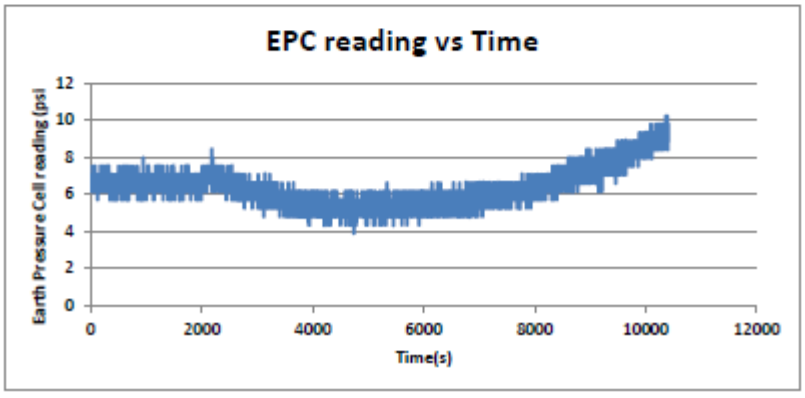

TEST 36

Large Pullout Test

Test details :		
	Test Name	UX1700-Monterey Sand-12psi
	Date	4/1/2012
	Member	Fabrizio

Box Dimensions (inch)	Length	Width	Depth	Area (in2)	Height from base to sleeve
	60	24	11	1440	5

Geogrid Details	Manufactur	Product	Ultimate Tensile Strength
	Tensar	UX1700	11900 lb/ft

Specimen Information(ft)	Width	Embedment Length (Le)
	1	2.97

Material Properties	
Material Name	Monterey San
Friction Angle (ϕ')	35
Moisture Content (%)	1.5
Ɣd,max (pcf)	99
Target Compaction	100%
Weight of each Lift (lbs)	134
No. of Lifts	6

Test Details	
Normal Stress σ' (psi)	Rate of Pullout (in/min)
12	0.04

Maximum Displacements	
LVDT	Disp (mm)
A	89.213
B	35.404
C	0.005

RESULTS

Maximum Load (lb)	5671.06	
Pullout Resisatnce (lb/ft)	5671.06	
Coefficient of Interaction, ci	$\frac{Pr}{2(Le)(c + \sigma' \tan(\phi'))}$	0.789

Average EPC reading (psi)	10.899

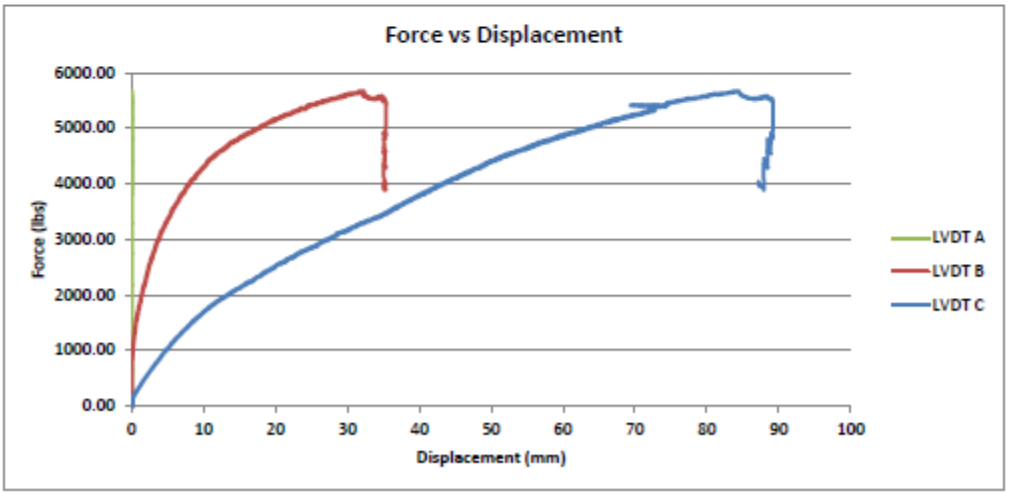

Comments:
Test Duration: 3.19 hours
Stopped early, as load cell lost contact on sensor surface

TEST 36 CONTINUED

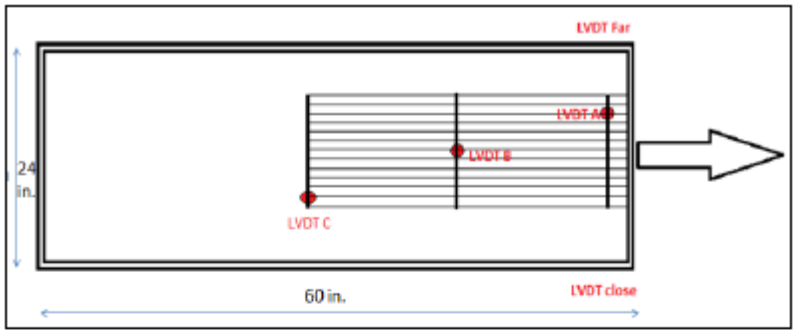

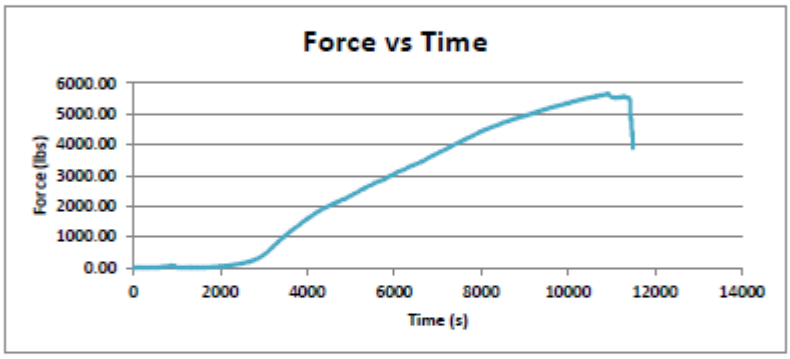

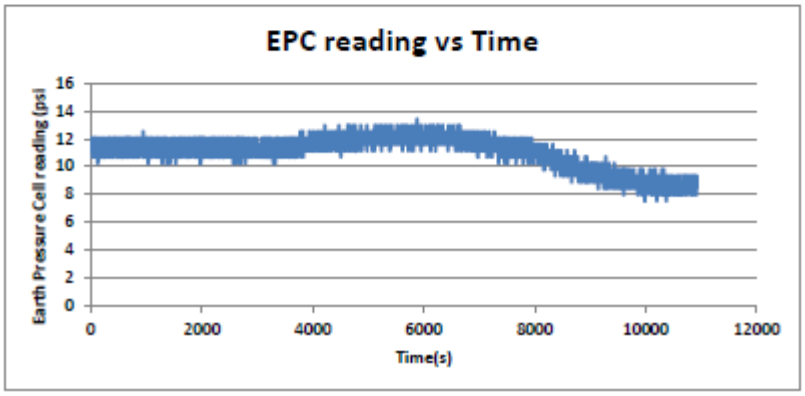

Appendix B: Dredged Material Pullout Test Results

Appendix B is a collection of all the Dredged Material pullout test results. The results are summarized similar to Appendix A. The first half of Appendix B is the results of the MPA dredged material pullout tests and the second half is for the Philadelphia dredged material.

TEST 47

Large Pullout Test

Test details :		
	Test Name	UX1400-100%DM(MPA)-4psi
	Date	4/25/2012
	Member	Kemp

Box Dimensions (inch)	Length	Width	Depth	Area (in2)	Height from base to sleeve
	60	24	11	1440	5

Geogrid Details	Manufactur	Product	Ultimate Tensile Strength
	Tensar	UX1400	4800 lb/ft

Specimen Information(ft)	Width	Embedment Length (Le)
	1	2.97

Material Properties	
Material Name	100% DM (MPA)
Friction Angle (ϕ')	27.7
cohesion, c (psf)	770.4
Moisture Content (%)	43
Ɣd,max (pcf)	85
Target Compaction	80%
Weight of each Lift (lbs)	190
No. of Lifts	4

Test Details	
Normal Stress σ' (psi)	Rate of Pullout (in/min)
4	0.04

Maximum Displacements	
LVDT	Disp (mm)
A	21.301
B	8.345
C	4.948

RESULTS

Maximum Load (lb)	517.79	
Pullout Resisatnce (lb/ft)	517.79	
Coefficient of Interaction, ci	$\frac{Pr}{2(Le)\,(c + \sigma' \tan(\phi'))}$	0.081

Average EPC reading (psi)	4.564

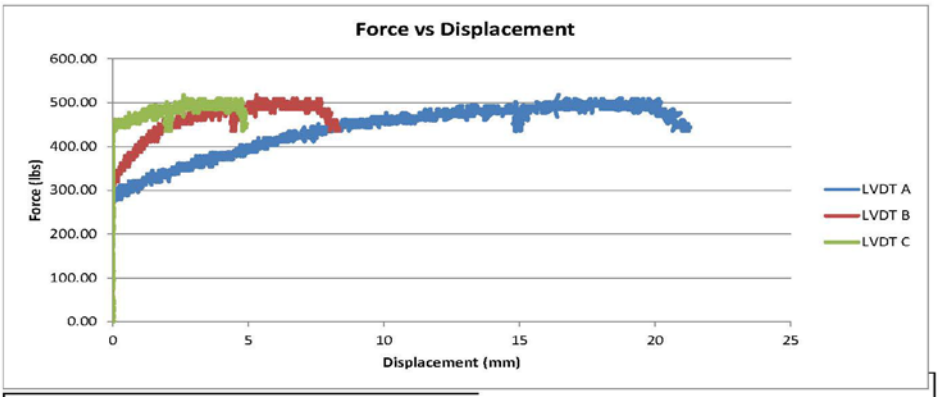

Comments:
Test Duration: 0.91 hours
Plateau observed, load drops

TEST 47 CONTINUED

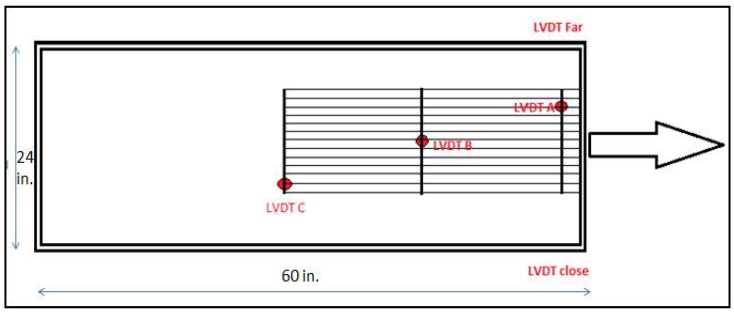

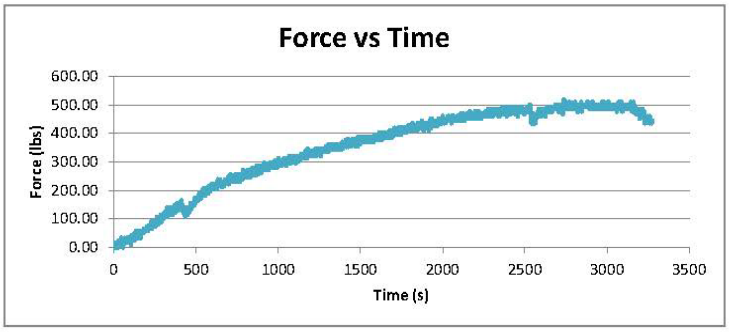

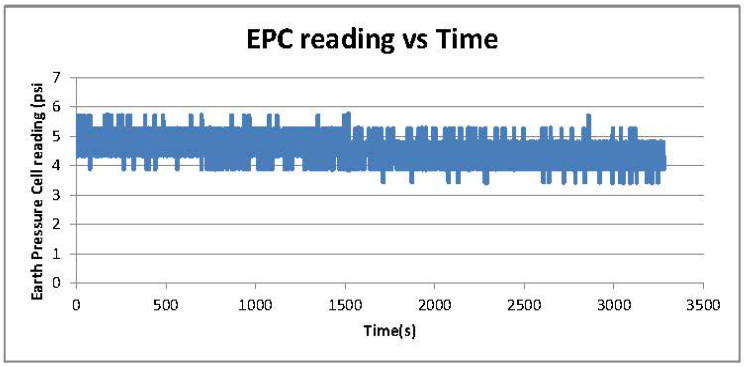

TEST 48

Large Pullout Test

Test details :		
	Test Name	UX1400-100%DM(MPA)-8psi
	Date	4/28/2012
	Member	Sangy

Box Dimensions (inch)	Length	Width	Depth	Area (in2)	Height from base to sleeve
	60	24	11	1440	5

Geogrid Details	Manufactur	Product	Ultimate Tensile Strength
	Tensar	UX1400	4800 lb/ft

Specimen Information(ft)	Width	Embedment Length (Le)
	1	2.97

Material Properties	
Material Name	100% DM (MPA)
Friction Angle (ϕ')	27.7
cohesion, c (psf)	770.4
Moisture Content (%)	43
Ɣd,max (pcf)	85
Target Compaction	80%
Weight of each Lift (lbs)	190
No. of Lifts	4

Test Details	
Normal Stress σ' (psi)	Rate of Pullout (in/min)
8	0.04

Maximum Displacements	
LVDT	Disp (mm)
A	13.353
B	4.377
C	7.115

RESULTS

Maximum Load (lb)	797.24	
Pullout Resisatnce (lb/ft)	797.24	
Coefficient of Interaction, ci	$\frac{Pr}{2(Le)\,(c + \sigma' \tan(\phi'))}$	0.098

Average EPC reading (psi)	9.457

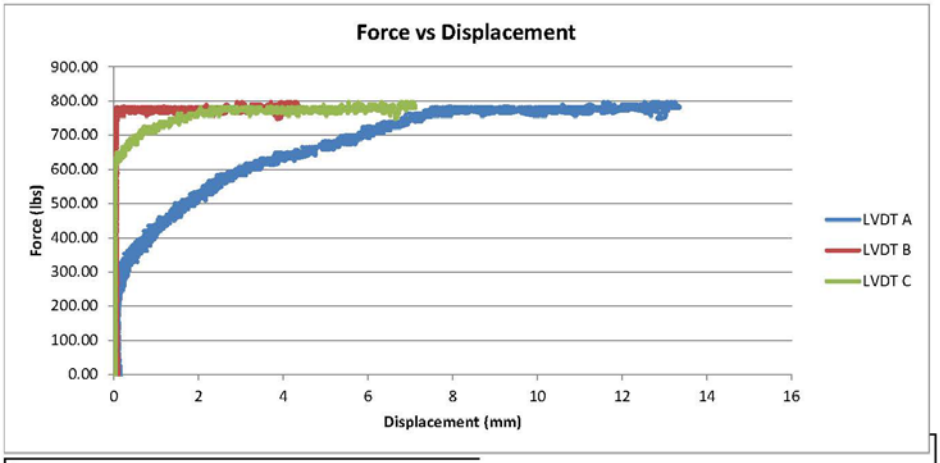

Comments:
Test Duration: 0.68 hours
Plateau observed, LVDT B moves latest

TEST 48 CONTINUED

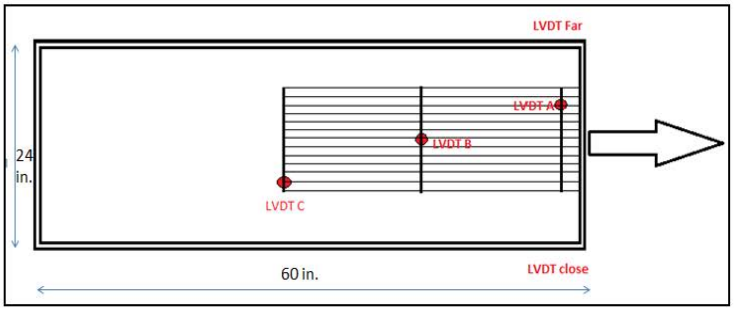

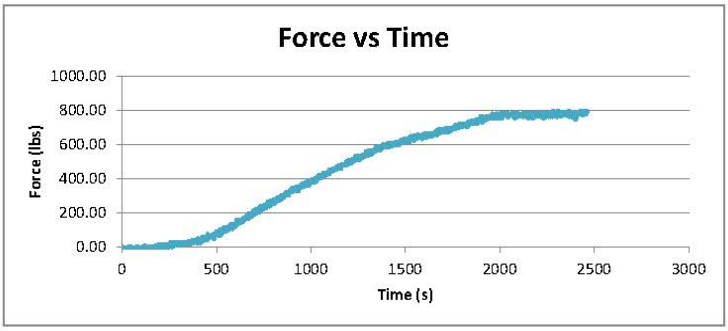

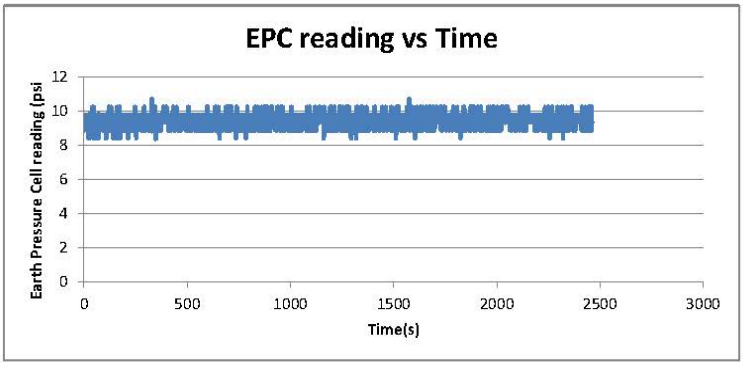

TEST 49

Large Pullout Test

Test details :		
	Test Name	UX1400-100%DM(MPA)-6psi
	Date	4/29/2012
	Member	Fabrizio

Box Dimensions (inch)	Length	Width	Depth	Area (in2)	Height from base to sleeve
	60	24	11	1440	5

Geogrid Details	Manufactur	Product	Ultimate Tensile Strength
	Tensar	UX1400	4800 lb/ft

Specimen Information(ft)	Width	Embedment Length (Le)
	1.5	2.97

Material Properties	
Material Name	100% DM (MPA)
Friction Angle (ϕ')	27.7
cohesion, c (psf)	770.4
Moisture Content (%)	43
Ɣd,max (pcf)	85
Target Compaction	80%
Weight of each Lift (lbs)	190
No. of Lifts	4

Test Details	
Normal Stress σ' (psi)	Rate of Pullout (in/min)
6	0.04

Maximum Displacements	
LVDT	Disp (mm)
A	8.657
B	5.942
C	9.336

RESULTS

Maximum Load (lb)	838.33
Pullout Resisatnce (lb/ft)	558.89
Coefficient of Interaction, ci	$\frac{Pr}{2(Le)(c + \sigma' \tan(\phi'))}$ = 0.077

Average EPC reading (psi)	-2.019

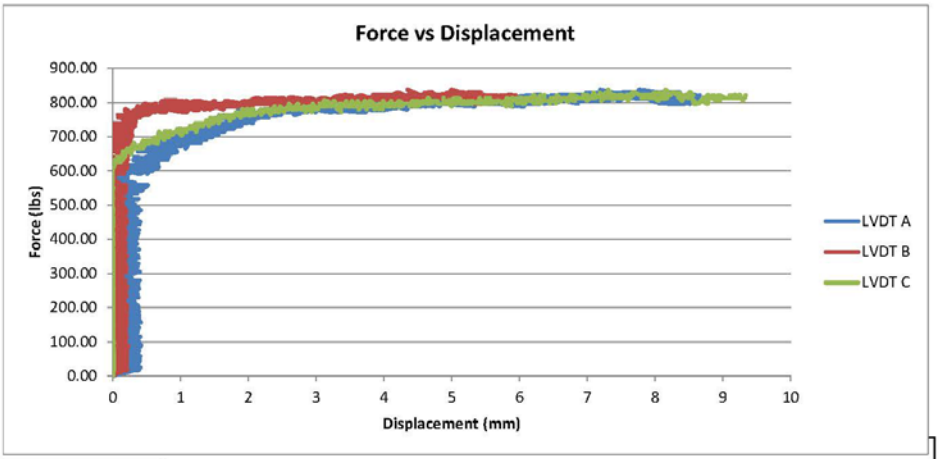

Comments: *Plateau observed, LVDT B moves latest*
Test Duration: *0.67 hours*
Earth Pressure cell reading and location :

TEST 49 CONTINUED

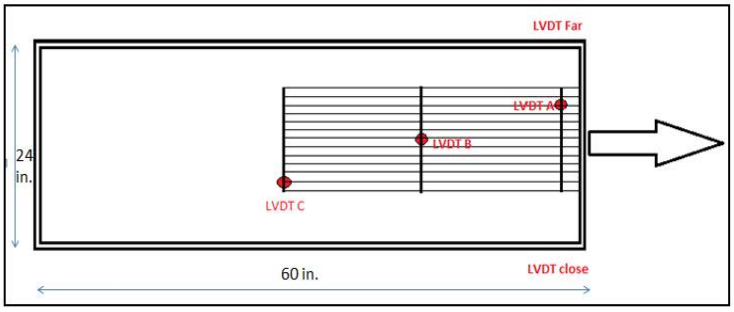

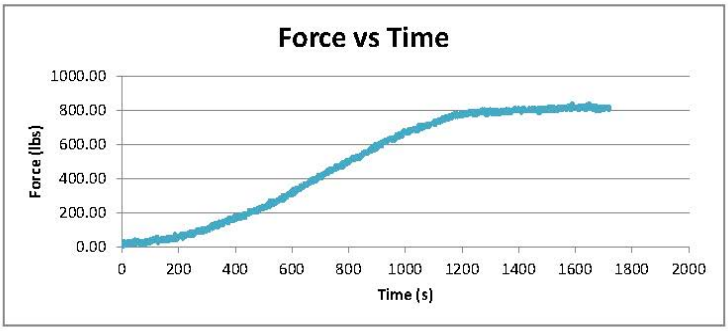

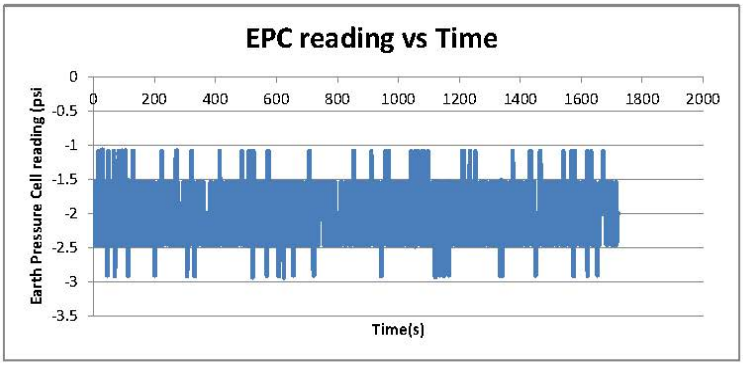

TEST 50

Large Pullout Test

Test details :		
	Test Name	UX1700-100%DM(MPA)-4psi
	Date	4/30/2012
	Member	Kemp

Box Dimensions (inch)	Length	Width	Depth	Area (in2)	Height from base to sleeve
	60	24	11	1440	5

Geogrid Details	Manufactur	Product	Ultimate Tensile Strength
	Tensar	UX1700	11900 lb/ft

Specimen Information(ft)	Width	Embedment Length (Le)
	1	2.97

Material Properties	
Material Name	100% DM (MPA)
Friction Angle (ϕ')	27.7
cohesion, c (psf)	770.4
Moisture Content (%)	43
Ɣd,max (pcf)	85
Target Compaction	80%
Weight of each Lift (lbs)	190
No. of Lifts	4

Test Details	
Normal Stress σ' (psi)	Rate of Pullout (in/min)
4	0.04

Maximum Displacements	
LVDT	Disp (mm)
A	37.661
B	36.600
C	36.181

RESULTS

Maximum Load (lb)	854.77	
Pullout Resisatnce (lb/ft)	854.77	
Coefficient of Interaction, ci	$\frac{Pr}{2(Le)(c + \sigma' \tan(\phi'))}$	0.134

Average EPC reading (psi)	2.658

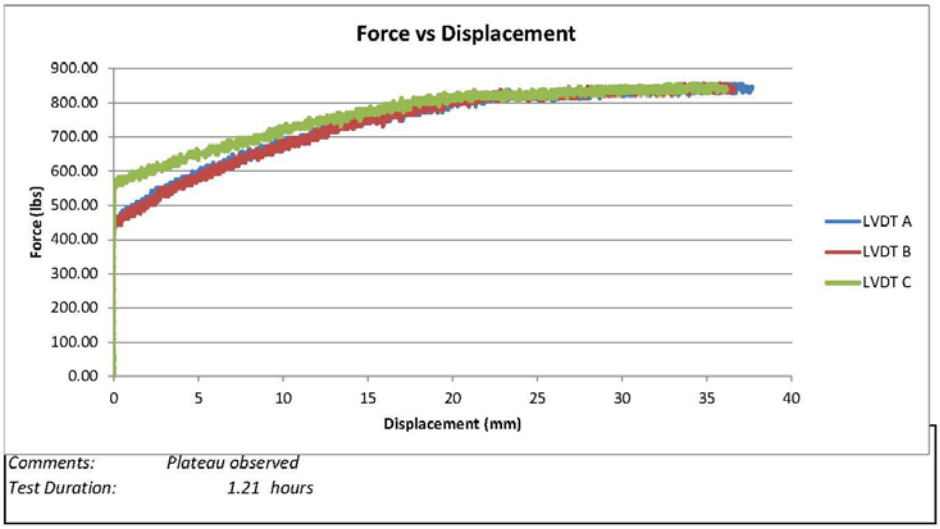

Comments: *Plateau observed*

Test Duration: *1.21 hours*

TEST 50 CONTINUED

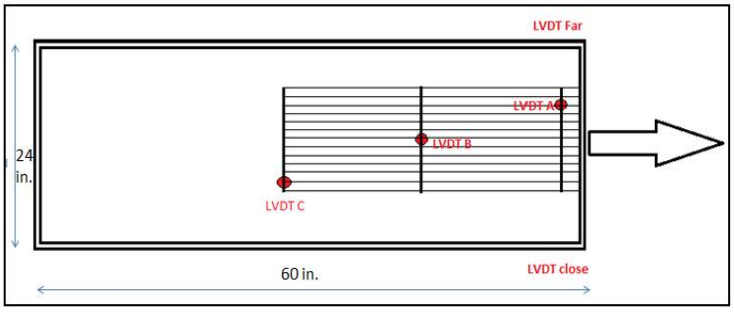

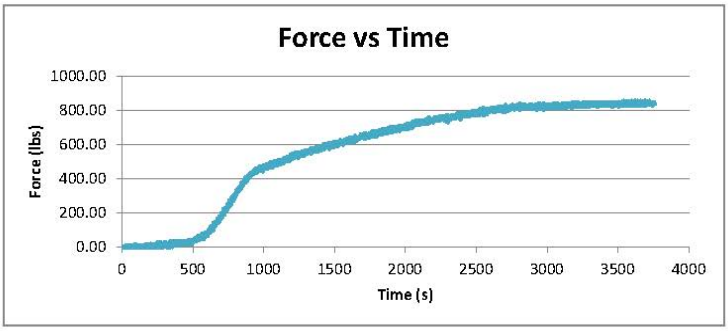

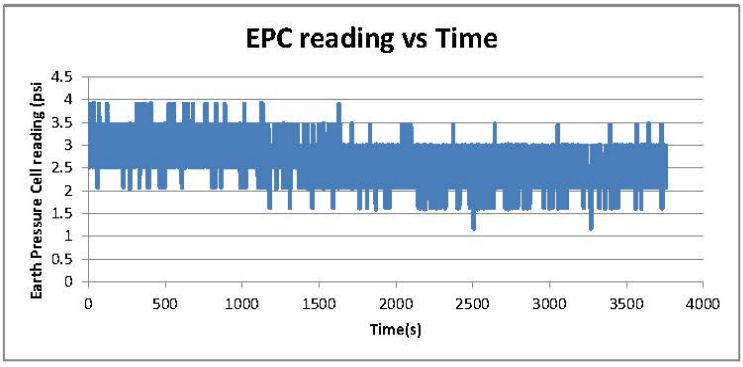

TEST 51

Large Pullout Test

Test details :		
	Test Name	UX1700-100%DM(MPA)-8psi
	Date	5/1/2012
	Member	Jake

Box Dimensions (inch)	Length	Width	Depth	Area (in2)	Height from base to sleeve
	60	24	11	1440	5
Geogrid Details	Manufactur	Product	Ultimate Tensile Strength		
	Tensar	UX1700	11900 lb/ft		
Specimen Information(ft)	Width	Embedment Length (Le)			
	1	3			

Material Properties	
Material Name	100% DM (MPA)
Friction Angle (ϕ')	27.7
cohesion, c (psf)	770.4
Moisture Content (%)	43
Ɣd,max (pcf)	85
Target Compaction	80%
Weight of each Lift (lbs)	190
No. of Lifts	4

Test Details	
Normal Stress σ' (psi)	Rate of Pullout (in/min)
8	0.04

Maximum Displacements	
LVDT	Disp (mm)
A	41.530
B	34.353
C	37.719

RESULTS

Maximum Load (lb)	846.55	
Pullout Resisatnce (lb/ft)	846.55	
Coefficient of Interaction, ci	$\frac{Pr}{2(Le)(c + \sigma' \tan(\phi'))}$	0.103

Average EPC reading (psi)	7.396

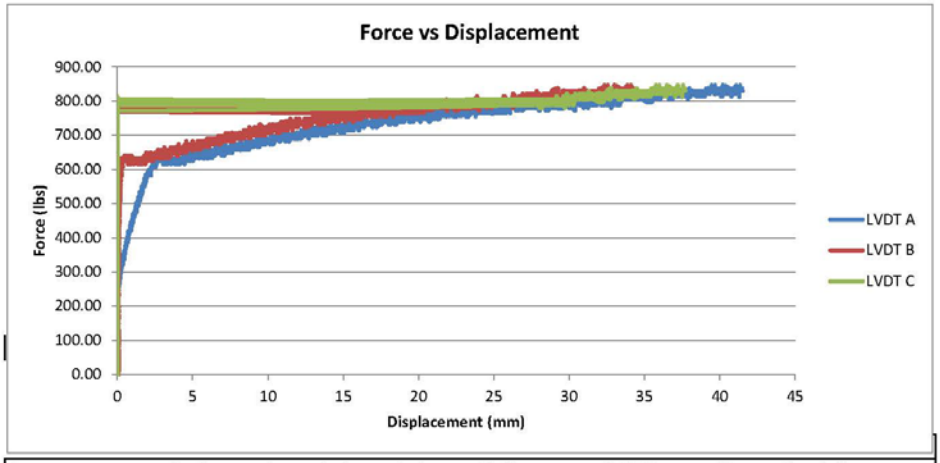

Comments: *No Plateau observed, change in slope at 610lbs* *LVDT C not working until end of test*

Test Duration: *1.25 hours*

TEST 51 CONTINUED

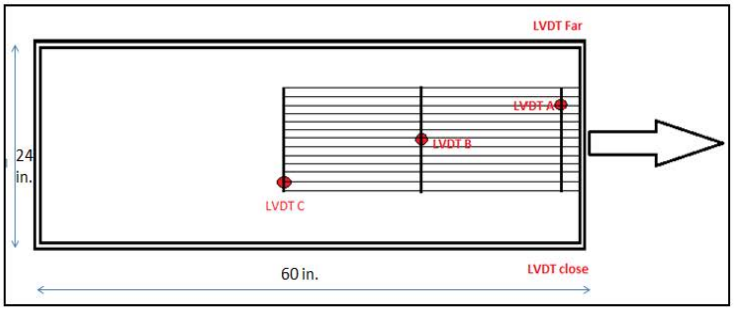

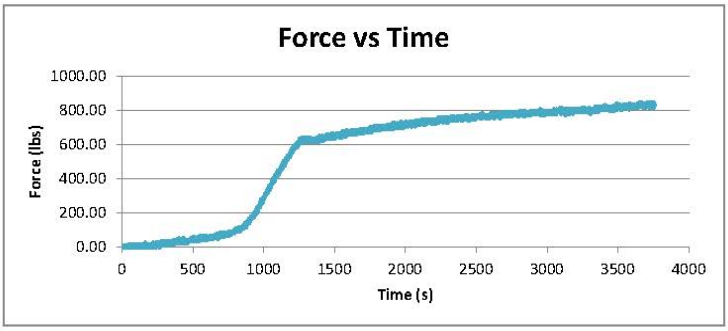

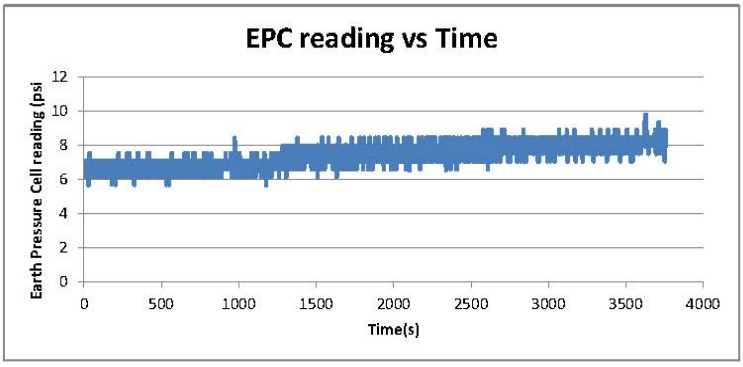

TEST 52

Large Pullout Test

Test details :		
	Test Name	UX1700-100%DM(MPA)-12psi
	Date	5/3/2012
	Member	Sangy

Box Dimensions (inch)	Length	Width	Depth	Area (in2)	Height from base to sleeve
	60	24	11	1440	5

Geogrid Details	Manufactur	Product	Ultimate Tensile Strength
	Tensar	UX1700	11900 lb/ft

Specimen Information(ft)	Width	Embedment Length (Le)
	1	2.871

Material Properties	
Material Name	100% DM (MPA)
Friction Angle (ϕ')	27.7
cohesion, c (psf)	770.4
Moisture Content (%)	43
Ɣd,max (pcf)	85
Target Compaction	80%
Weight of each Lift (lbs)	190
No. of Lifts	4

Test Details	
Normal Stress σ' (psi)	Rate of Pullout (in/min)
12	0.04

Maximum Displacements	
LVDT	Disp (mm)
A	9.893
B	10.085
C	18.020

RESULTS

Maximum Load (lb)	1027.37	
Pullout Resisatnce (lb/ft)	1027.37	
Coefficient of Interaction, ci	$\frac{Pr}{2(Le)(c + \sigma' \tan(\phi'))}$	0.107

Average EPC reading (psi)	16.417

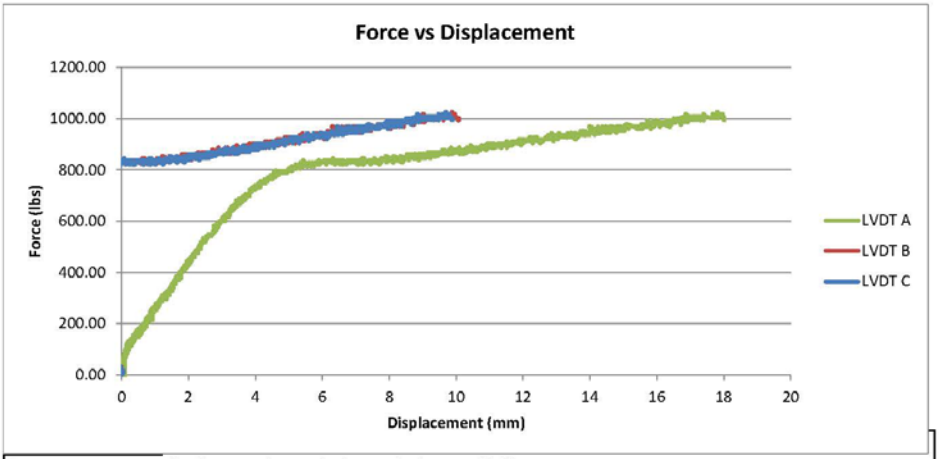

Comments: *No Plateau observed, change in slope at 810lbs*

Test Duration: *1.03 hours*

TEST 52 CONTINUED

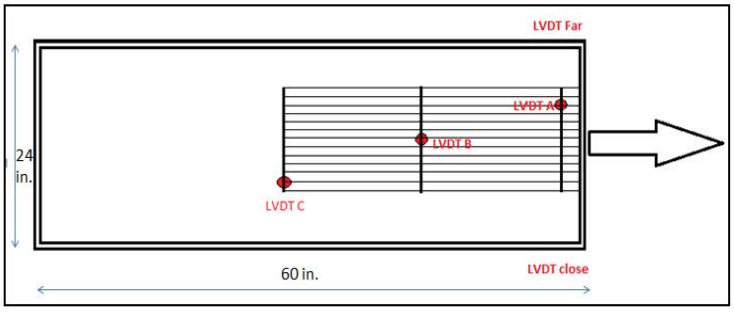

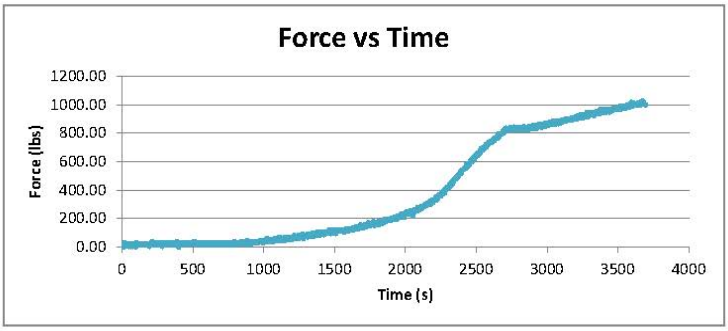

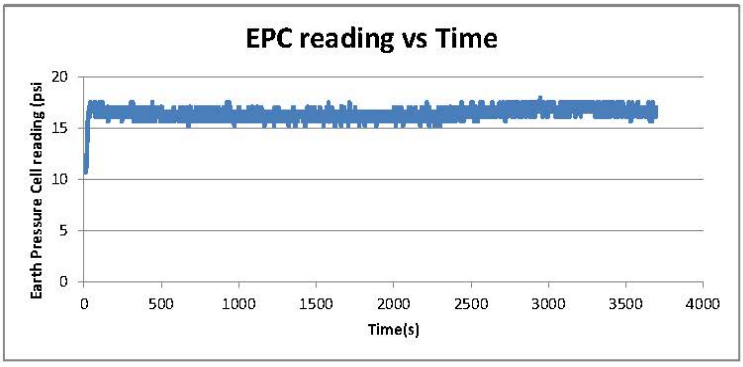

TEST 95

Large Pullout Test

Test details :		
	Test Name	UX1700-100%DM(MPA)-6psi
	Date	10/19/2012
	Member	Jake

Box Dimensions (inch)	Length	Width	Depth	Area (in2)	Height from base to sleeve
	60	24	11	1440	5

Geogrid Details	Manufactur	Product	Ultimate Tensile Strength
	Tensar	UX1700	11900 lb/ft

Specimen Information(ft)	Width	Embedment Length (Le)
	1	2.97

Material Properties	
Material Name	100% DM (MPA)
Friction Angle (ϕ')	27.7
cohesion, c (psf)	770.4
Moisture Content (%)	43
Ɣd,max (pcf)	85
Target Compaction	80%
Weight of each Lift (lbs)	190
No. of Lifts	4

Test Details	
Normal Stress σ' (psi)	Rate of Pullout (in/min)
6	0.04

Maximum Displacements	
LVDT	Disp (mm)
A	44.349
B	44.560
C	45.675

RESULTS

Maximum Load (lb)	862.99	
Pullout Resisatnce (lb/ft)	862.99	
Coefficient of Interaction, ci	$\frac{Pr}{2(Le)\,(c + \sigma' \tan(\phi'))}$	0.119

Average EPC reading (psi)	2.847

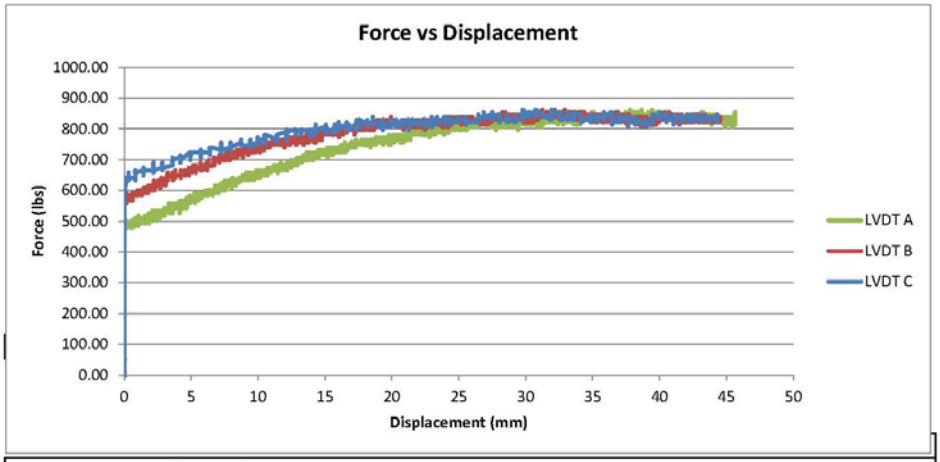

Comments: *Plateau observed*
Test Duration: *1.38 hours*

TEST 95 CONTINUED

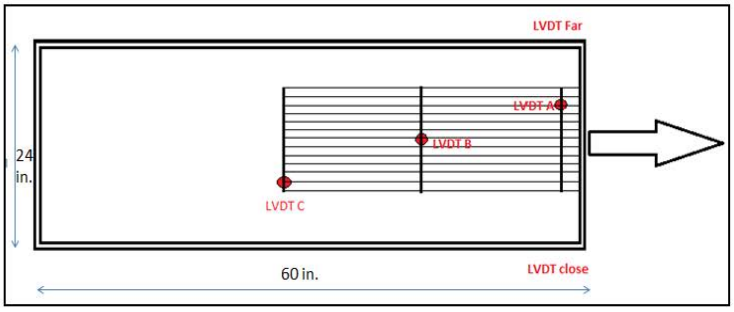

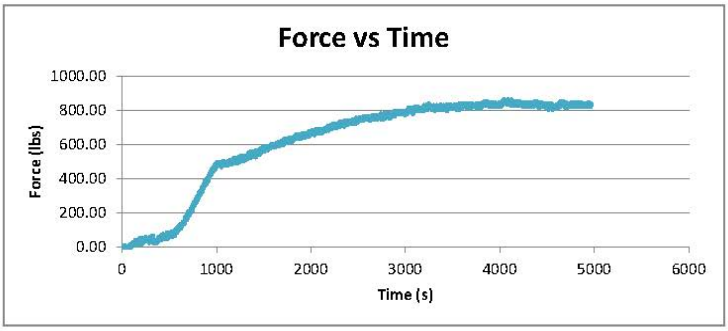

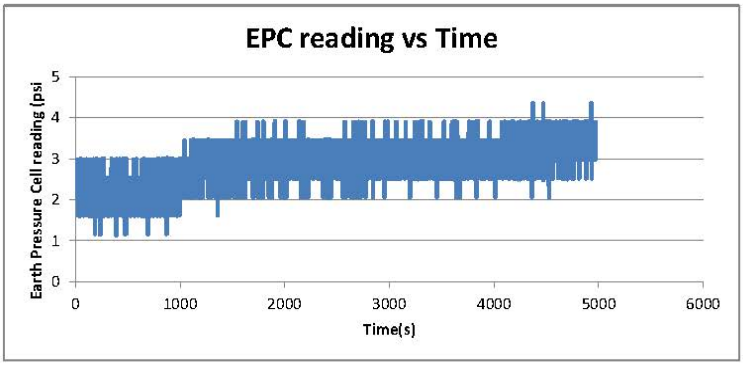

TEST 96

Large Pullout Test

Test details :		
	Test Name	UX1700-100%DM(MPA)-8psi
	Date	10/30/2012
	Member	Jake

Box Dimensions (inch)	Length	Width	Depth	Area (in2)	Height from base to sleeve
	60	24	11	1440	5

Geogrid Details	Manufactur	Product	Ultimate Tensile Strength
	Tensar	UX1700	11900 lb/ft

Specimen Information(ft)	Width	Embedment Length (Le)
	1	2.97

Material Properties	
Material Name	100% DM (MPA)
Friction Angle (ϕ')	27.7
cohesion, c (psf)	770.4
Moisture Content (%)	43
Ɣd,max (pcf)	85
Target Compaction	80%
Weight of each Lift (lbs)	190
No. of Lifts	4

Test Details	
Normal Stress σ' (psi)	Rate of Pullout (in/min)
8	0.04

Maximum Displacements	
LVDT	Disp (mm)
A	57.731
B	38.829
C	50.732

RESULTS

Maximum Load (lb)	1060.24	
Pullout Resisatnce (lb/ft)	1060.24	
Coefficient of Interaction, ci	$\frac{Pr}{2(Le)(c + \sigma' \tan(\phi'))}$	0.130

Average EPC reading (psi)	6.580

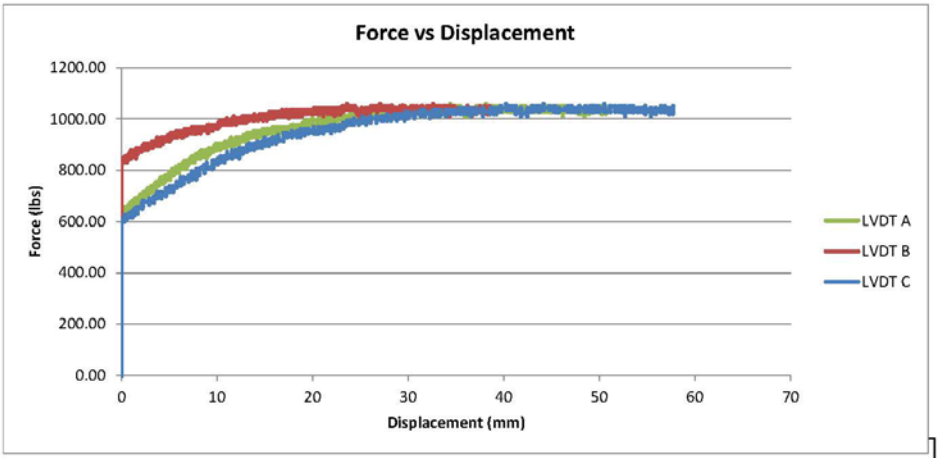

Comments: *Plateau observed*
Test Duration: *1.69 hours*

TEST 96 CONTINUED

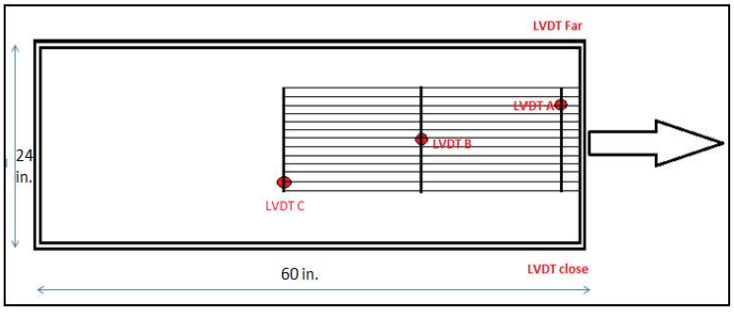

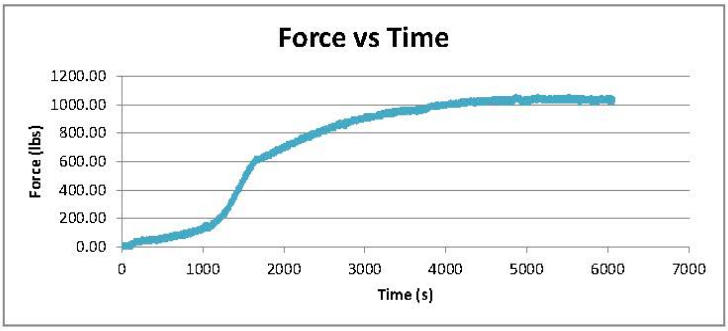

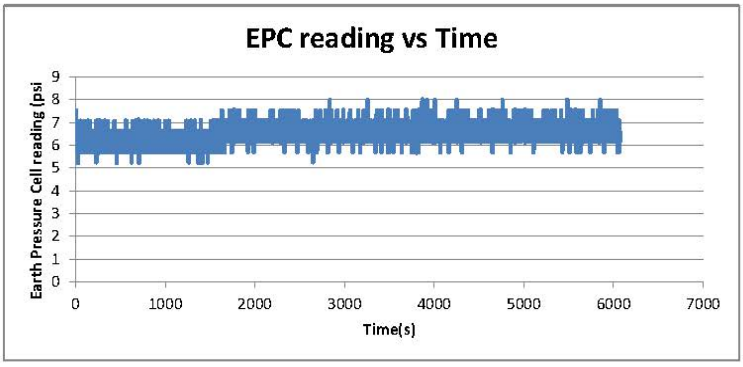

TEST 97

Large Pullout Test

Test details :		
	Test Name	UX1400-100%DM(MPA)-4psi
	Date	11/2/2012
	Member	Jake

Box Dimensions (inch)	Length	Width	Depth	Area (in2)	Height from base to sleeve
	60	24	11	1440	5

Geogrid Details	Manufactur	Product	Ultimate Tensile Strength
	Tensar	UX1400	4800 lb/ft

Specimen Information(ft)	Width	Embedment Length (Le)
	1	2.97

Material Properties	
Material Name	100% DM (MPA)
Friction Angle (ϕ')	27.7
cohesion, c (psf)	770.4
Moisture Content (%)	43
Ɣd,max (pcf)	85
Target Compaction	80%
Weight of each Lift (lbs)	190
No. of Lifts	4

Test Details	
Normal Stress σ' (psi)	Rate of Pullout (in/min)
4	0.04

Maximum Displacements	
LVDT	Disp (mm)
A	54.416
B	38.601
C	46.148

RESULTS

Maximum Load (lb)	361.63	
Pullout Resisatnce (lb/ft)	361.63	
Coefficient of Interaction, ci	$\frac{Pr}{2(Le)(c + \sigma' \tan(\phi'))}$	0.057

Average EPC reading (psi)	1.692

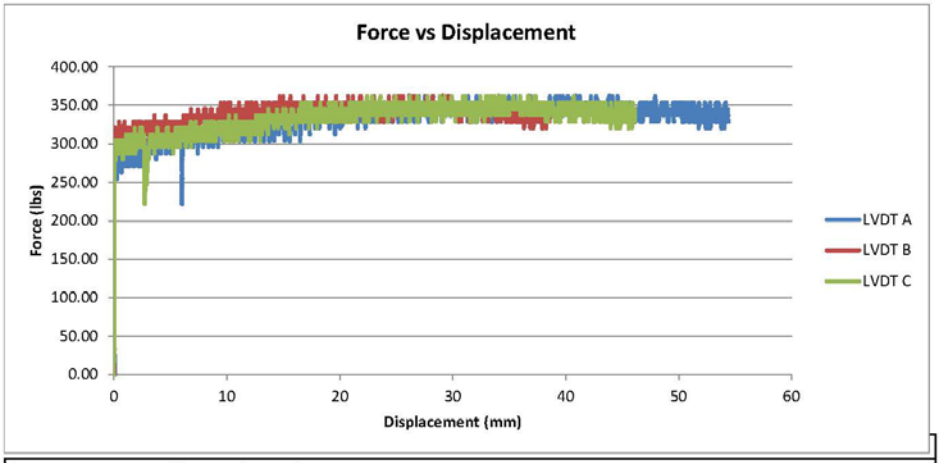

Comments: *Plateau observed*
Test Duration: *1.29 hours*

TEST 97 CONTINUED

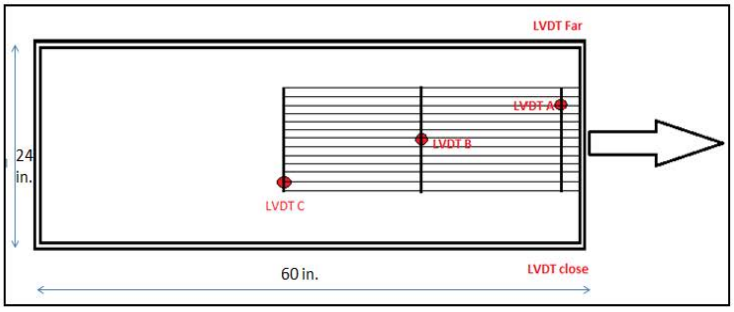

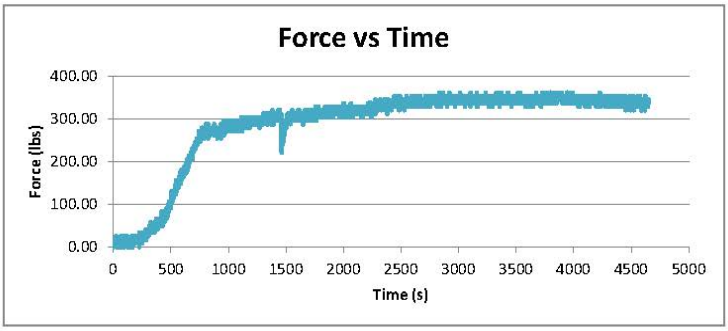

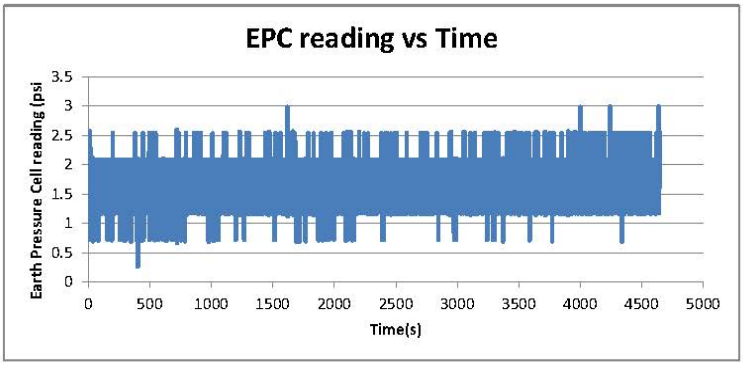

TEST 98

Large Pullout Test

Test details :		
	Test Name	UX1400-100%DM(MPA)-4psi (3 Transverse
	Date	11/11/2012
	Member	Jake

Box Dimensions (inch)	Length	Width	Depth	Area (in2)	Height from base to sleeve
	60	24	11	1440	5
Geogrid Details	Manufactur	Product	Ultimate Tensile Strength		
	Tensar	UX1400	4800 lb/ft		
Specimen Information(ft)	Width	Embedment Length (Le)			
	1	4.455			

Material Properties	
Material Name	100% DM (MPA)
Friction Angle (ϕ')	27.7
cohesion, c (psf)	770.4
Moisture Content (%)	43
Ɣd,max (pcf)	85
Target Compaction	80%
Weight of each Lift (lbs)	190
No. of Lifts	4

Test Details	
Normal Stress σ' (psi)	Rate of Pullout (in/min)
4	0.04

Maximum Displacements	
LVDT	Disp (mm)
A	50.850
B	44.260
C	46.465

RESULTS

Maximum Load (lb)	534.23	
Pullout Resisatnce (lb/ft)	534.23	
Coefficient of Interaction, ci	$\frac{Pr}{2(Le)(c + \sigma' \tan(\phi'))}$	0.056

Average EPC reading (psi)	3.194

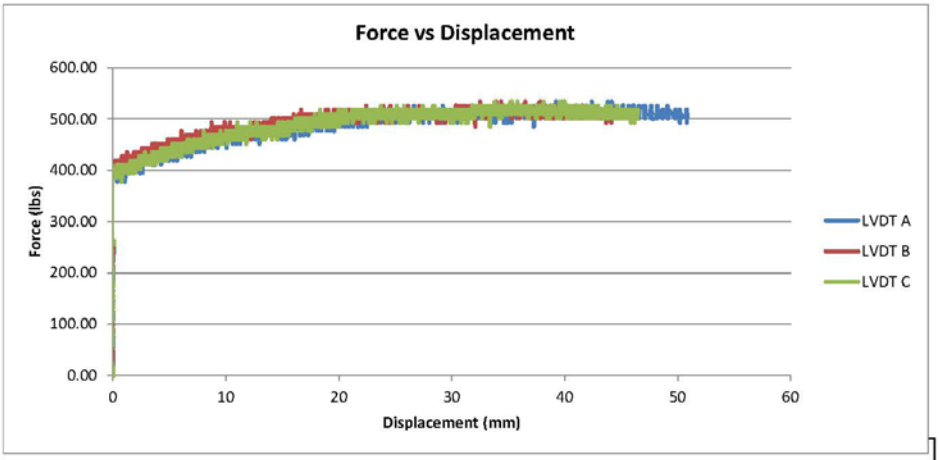

Comments: *Plateau observed*
Test Duration: *1.40 hours*

TEST 98 CONTINUED

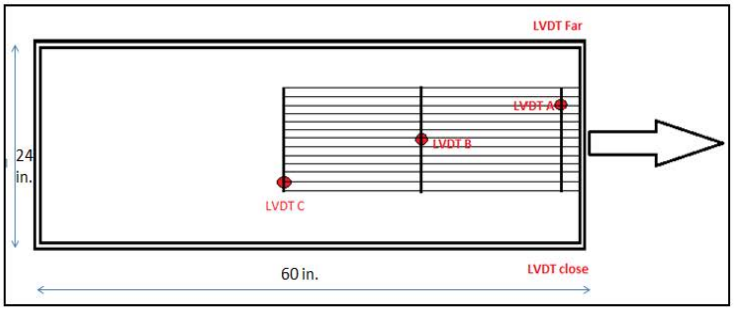

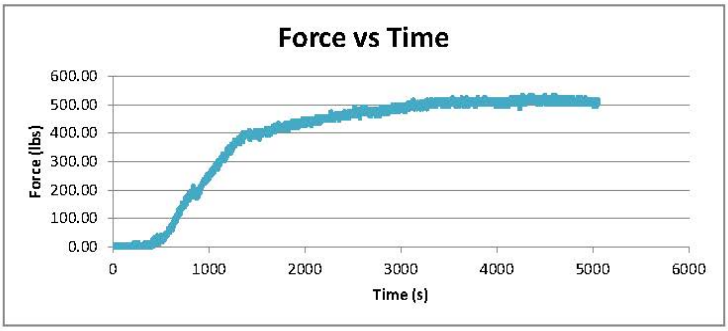

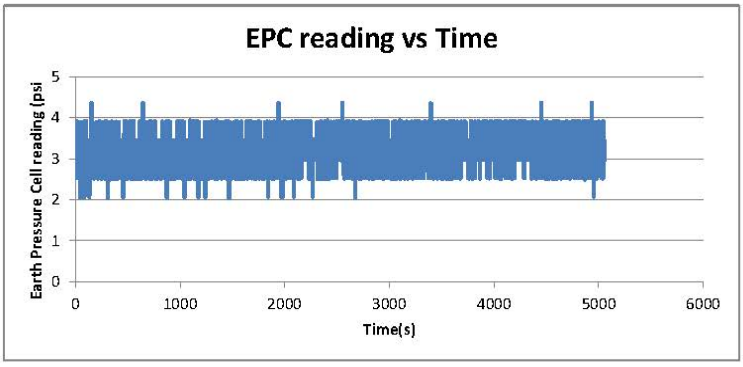

TEST 99

Large Pullout Test

Test details :		
	Test Name	UX1700-100%DM(MPA)-12psi
	Date	11/19/2012
	Member	Jake

Box Dimensions (inch)	Length	Width	Depth	Area (in2)	Height from base to sleeve
	60	24	11	1440	5
Geogrid Details	Manufactur	Product	Ultimate Tensile Strength		
	Tensar	UX1700	11900 lb/ft		
Specimen Information(ft)	Width	Embedment Length (Le)			
	1	2.97			

Material Properties	
Material Name	100% DM (MPA)
Friction Angle (ϕ')	27.7
cohesion, c (psf)	770.4
Moisture Content (%)	43
Ɣd,max (pcf)	85
Target Compaction	80%
Weight of each Lift (lbs)	190
No. of Lifts	4

Test Details	
Normal Stress σ' (psi)	Rate of Pullout (in/min)
12	0.04

Maximum Displacements	
LVDT	Disp (mm)
A	27.128
B	39.849
C	49.572

RESULTS

Maximum Load (lb)	1224.62	
Pullout Resisatnce (lb/ft)	1224.62	
Coefficient of Interaction, ci	$\frac{Pr}{2(Le)\,(c + \sigma' \tan(\phi'))}$	0.123

Average EPC reading (psi)	9.116

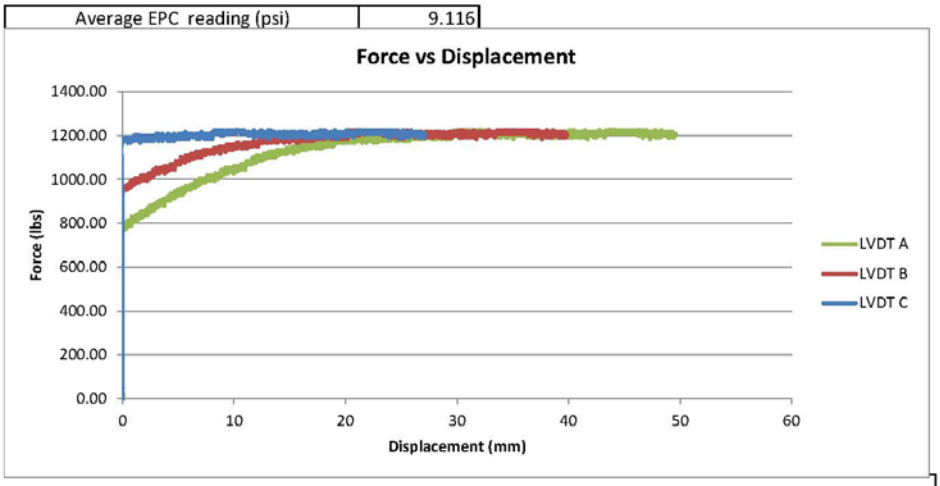

Comments: *Plateau observed*
Test Duration: *1.52 hours*

TEST 99 CONTINUED

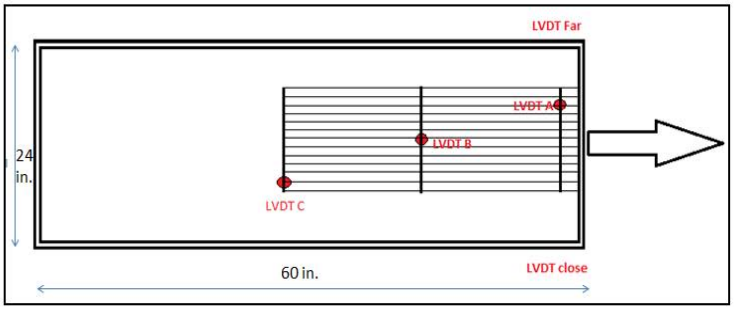

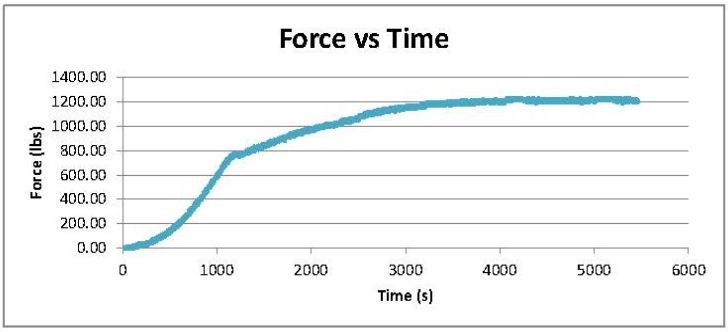

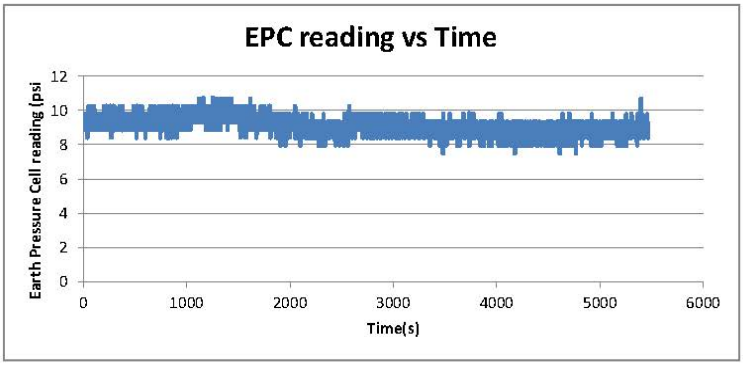

TEST 56

Large Pullout Test

Test details :		
	Test Name	UX1400-100%DM (phil)-4psi
	Date	7/4/2012
	Member	Kemp

Box Dimensions (inch)	Length	Width	Depth	Area (in2)	Height from base to sleeve
	60	24	11	1440	5
Geogrid Details	Manufactur	Product	Ultimate Tensile Strength		
	Tensar	UX1400	12000 lb/ft		
Specimen Information(ft)	Width	Embedment Length (Le)			
	1	2.871			

Material Properties	
Material Name	100%DM (Phil)
Friction Angle (ϕ')	25.5
Cohesion, c (psf)	449.28
Moisture Content (%)	50%
Ɣd,max (pcf)	75
Target Compaction	0.8
Weight of each Lift	180
No. of Lifts	4

Test Details	
Normal Stress σ' (psi)	Rate of Pullout (in/min)
4	0.04

Maximum Displacements	
LVDT	Disp (mm)
A	45.942
B	18.887
C	1.909

RESULTS

Maximum Load (lb)	460.26	
Pullout Resisatnce (lb/ft)	460.26	
Coefficient of Interaction, ci	$\frac{Pr}{2(Le)(c + \sigma' \tan(\phi'))}$	0.111

Average EPC reading (psi)	117.481

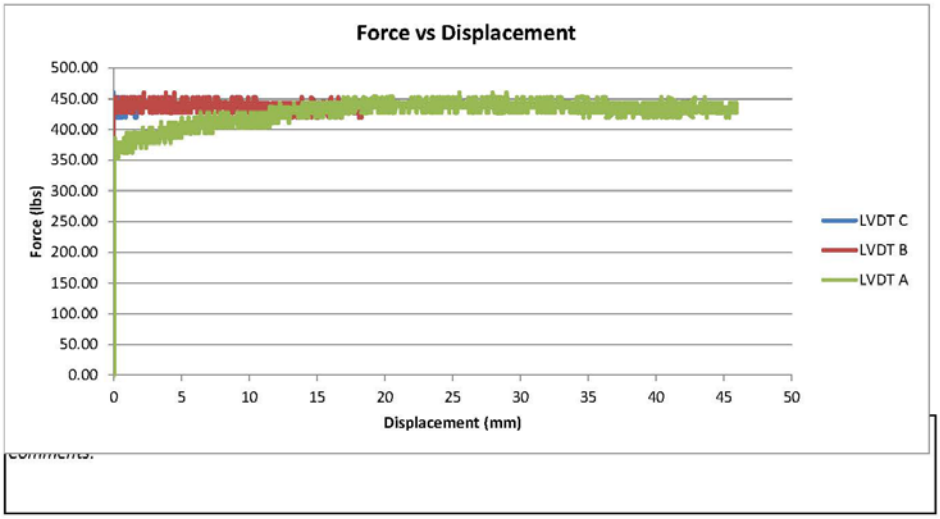

Comments:

TEST 56 CONTINUED

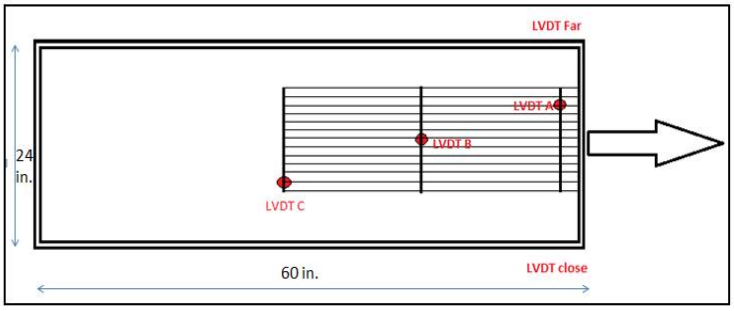

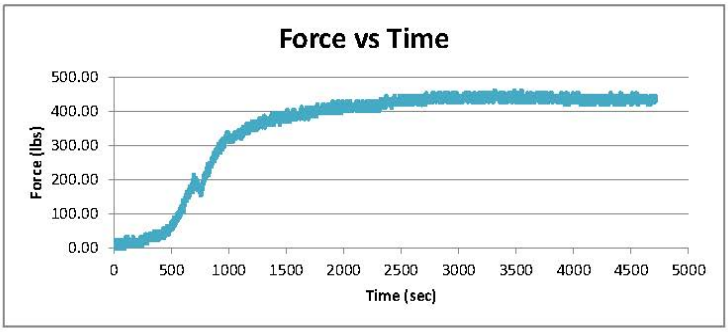

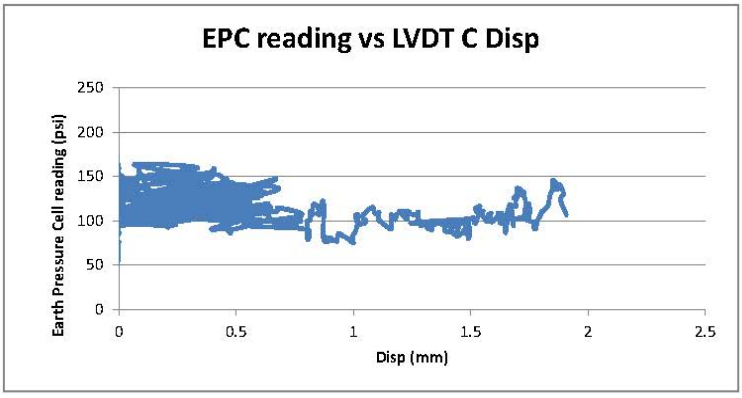

TEST 57

Large Pullout Test

Test details :		
	Test Name	UX1400-100%DM (phil)-6psi
	Date	7/5/2012
	Member	Kemp

Box Dimensions (inch)	Length	Width	Depth	Area (in2)	Height from base to sleeve
	60	24	11	1440	5

Geogrid Details	Manufactur	Product	Ultimate Tensile Strength
	Tensar	UX1400	12000 lb/ft

Specimen Information(ft)	Width	Embedment Length (Le)
	1	2.838

Material Properties	
Material Name	100%DM (Phil)
Friction Angle (ϕ')	25.5
Cohesion, c (psf)	449.28
Moisture Content (%)	50%
Ɣd,max (pcf)	75
Target Compaction	0.8
Weight of each Lift	180
No. of Lifts	4

Test Details	
Normal Stress σ' (psi)	Rate of Pullout (in/min)
6	0.04

Maximum Displacements	
LVDT	Disp (mm)
A	27.050
B	9.509
C	19.364

RESULTS

Maximum Load (lb)	517.79	
Pullout Resisatnce (lb/ft)	517.79	
Coefficient of Interaction, ci	$\frac{Pr}{2(Le)(c + \sigma' \tan(\phi'))}$	0.106

Average EPC reading (psi)	111.883

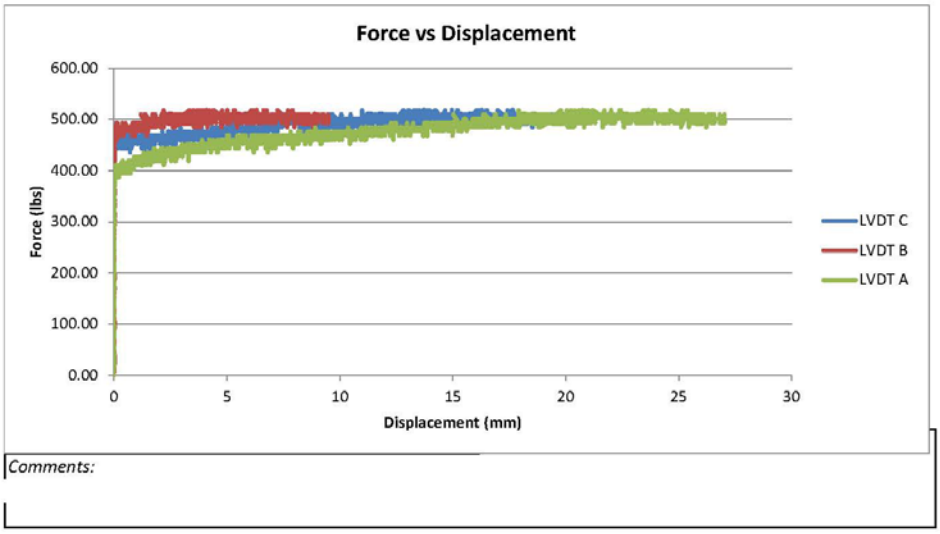

Comments:

TEST 57 CONTINUED

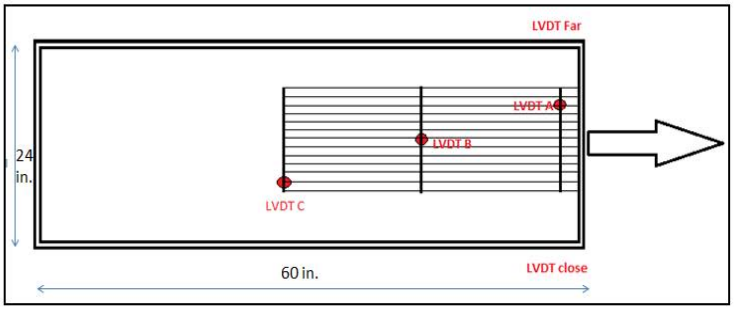

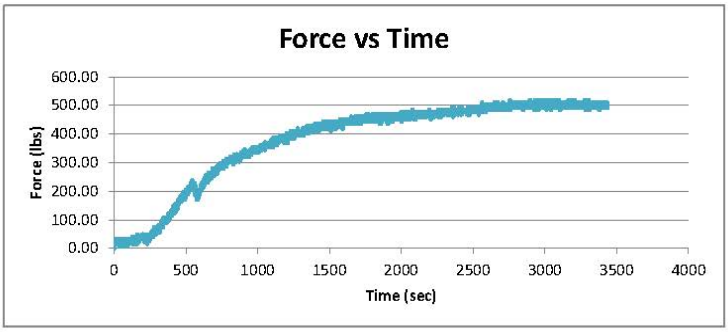

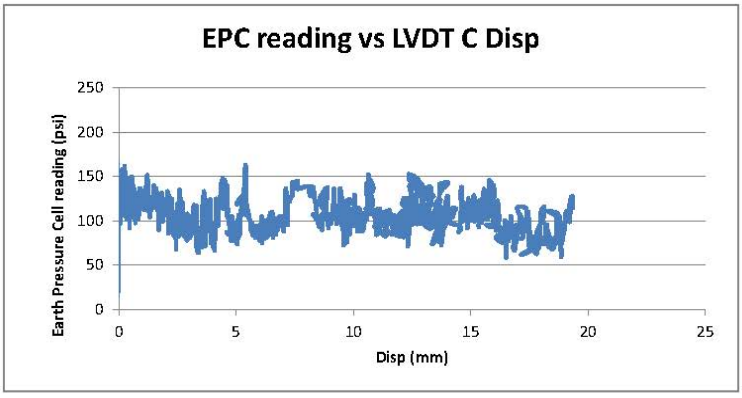

TEST 58

Large Pullout Test

Test details :		
	Test Name	UX1400-100%DM (phil)-8psi
	Date	7/6/2012
	Member	Kemp

Box Dimensions (inch)	Length	Width	Depth	Area (in2)	Height from base to sleeve
	60	24	11	1440	5

Geogrid Details	Manufactur	Product	Ultimate Tensile Strength
	Tensar	UX1400	12000 lb/ft

Specimen Information(ft)	Width	Embedment Length (Le)
	1	2.871

Material Properties	
Material Name	100%DM (Phil)
Friction Angle (ϕ')	25.5
Cohesion, c (psf)	449.28
Moisture Content (%)	50%
$\gamma_{d,max}$ (pcf)	75
Target Compaction	0.8
Weight of each Lift	180
No. of Lifts	4

Test Details	
Normal Stress σ' (psi)	Rate of Pullout (in/min)
8	0.04

Maximum Displacements	
LVDT	Disp (mm)
A	35.538
B	8.959
C	8.342

RESULTS

Maximum Load (lb)	698.61	
Pullout Resisatnce (lb/ft)	698.61	
Coefficient of Interaction, ci	$\frac{Pr}{2(Le)(c + \sigma' \tan(\phi'))}$	0.122

Average EPC reading (psi)	51.625

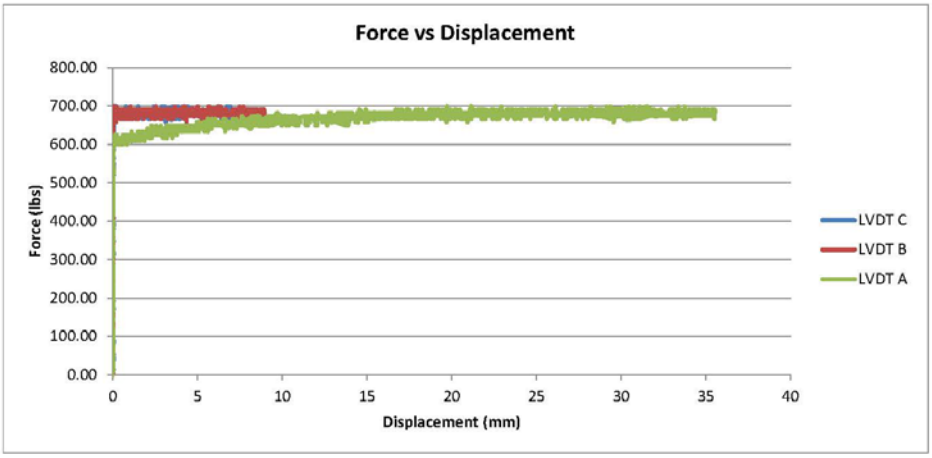

Comments:

TEST 58 CONTINUED

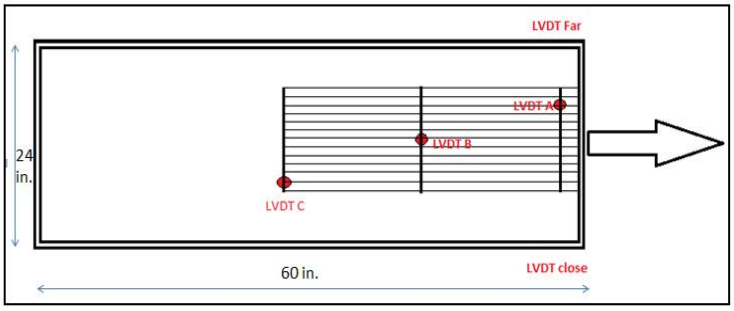

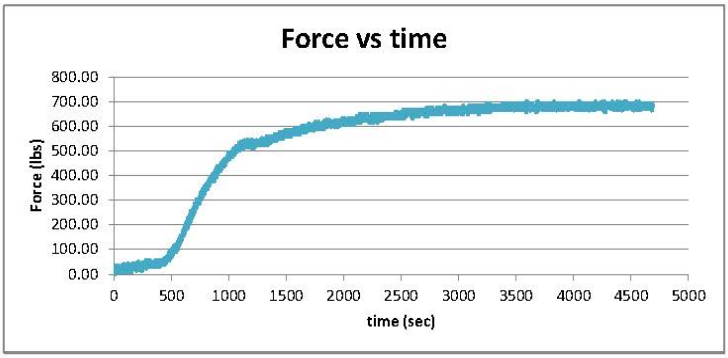

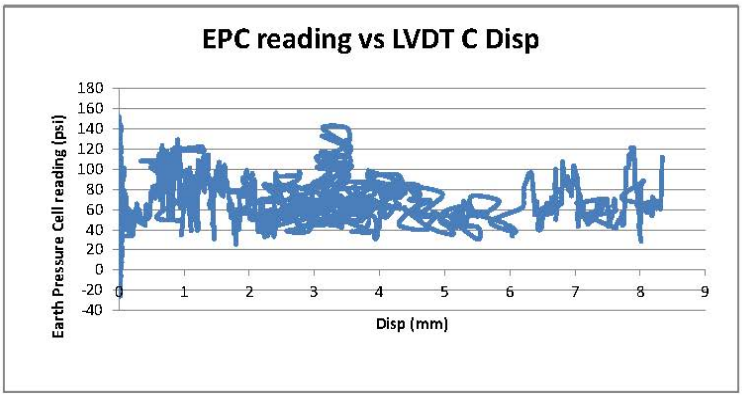

TEST 59

Large Pullout Test

Test details :		
	Test Name	UX1700-100%DM (phil)-4psi
	Date	7/6/2012
	Member	Kemp

Box Dimensions (inch)	Length	Width	Depth	Area (in2)	Height from base to sleeve
	60	24	11	1440	5

Geogrid Details	Manufactur	Product	Ultimate Tensile Strength
	Tensar	UX1700	12000 lb/ft

Specimen Information(ft)	Width	Embedment Length (Le)
	1	2.838

Material Properties	
Material Name	100%DM (Phil)
Friction Angle (ϕ')	25.5
Cohesion, c (psf)	449.28
Moisture Content (%)	50%
Ɣd,max (pcf)	75
Target Compaction	0.8
Weight of each Lift	180
No. of Lifts	4

Test Details	
Normal Stress σ' (psi)	Rate of Pullout (in/min)
4	0.04

Maximum Displacements	
LVDT	Disp (mm)
A	36.583
B	24.213
C	1.858

RESULTS

Maximum Load (lb)	591.76	
Pullout Resisatnce (lb/ft)	591.76	
Coefficient of Interaction, ci	$\frac{Pr}{2(Le)(c + \sigma' \tan(\phi'))}$	0.144

Average EPC reading (psi)	69.919

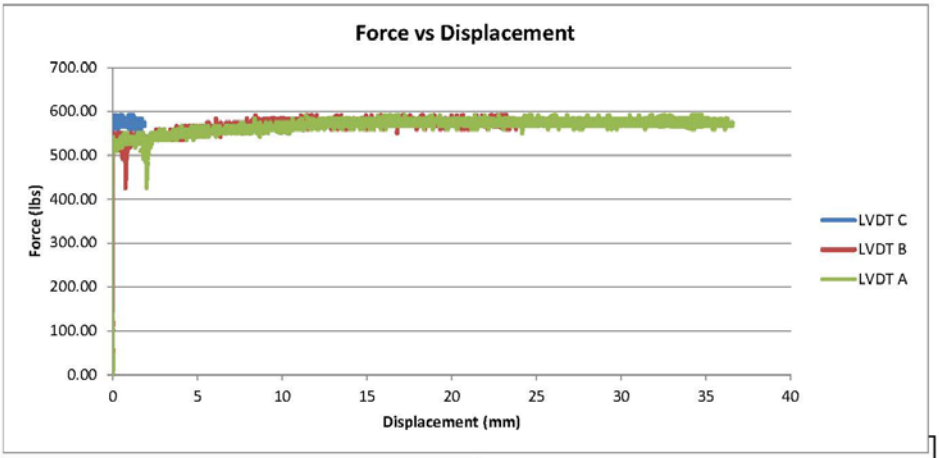

Comments:

TEST 59 CONTINUED

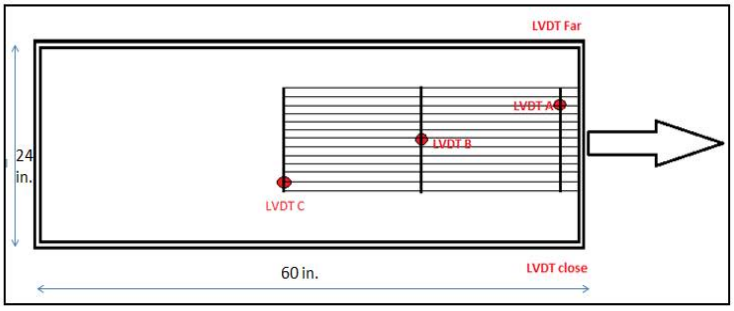

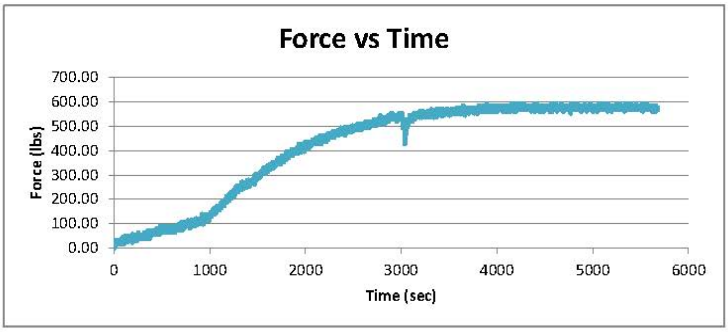

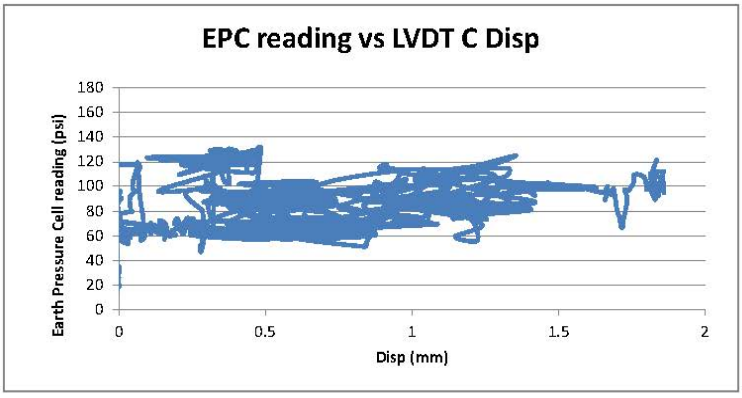

TEST 60

Large Pullout Test

Test details :		
	Test Name	UX1700-100%DM (phil)-6psi
	Date	7/7/2012
	Member	Kemp

Box Dimensions (inch)	Length	Width	Depth	Area (in2)	Height from base to sleeve
	60	24	11	1440	5

Geogrid Details	Manufactur	Product	Ultimate Tensile Strength
	Tensar	UX1700	12000 lb/ft

Specimen Information(ft)	Width	Embedment Length (Le)
	1	2.871

Material Properties	
Material Name	100%DM (Phil)
Friction Angle (ϕ')	25.5
Cohesion, c (psf)	449.28
Moisture Content (%)	50%
Ɣd,max (pcf)	75
Target Compaction	0.8
Weight of each Lift	180
No. of Lifts	4

Test Details	
Normal Stress σ' (psi)	Rate of Pullout (in/min)
6	0.04

Maximum Displacements	
LVDT	Disp (mm)
A	22.769
B	30.906
C	42.194

RESULTS

Maximum Load (lb)	780.80	
Pullout Resisatnce (lb/ft)	780.80	
Coefficient of Interaction, ci	$\frac{Pr}{2(Le)(c + \sigma' \tan(\phi'))}$	0.158

Average EPC reading (psi)	42.860

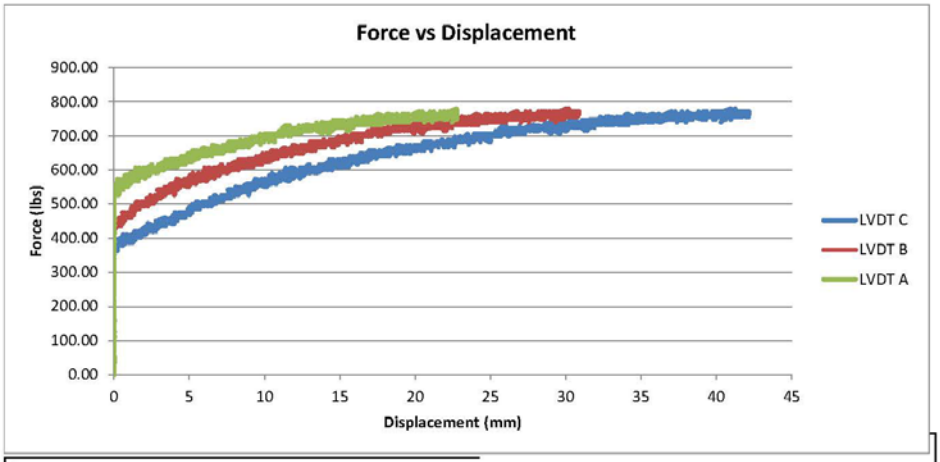

Comments:

TEST 60 CONTINUED

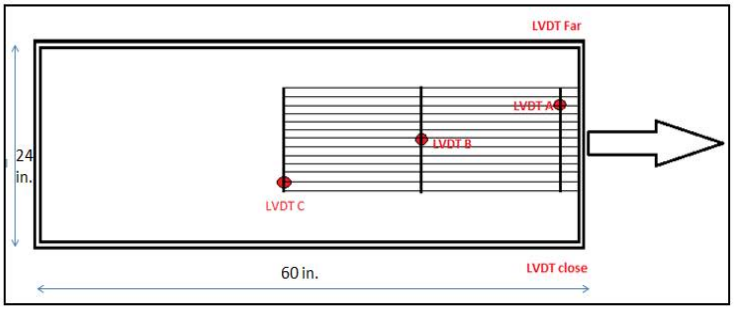

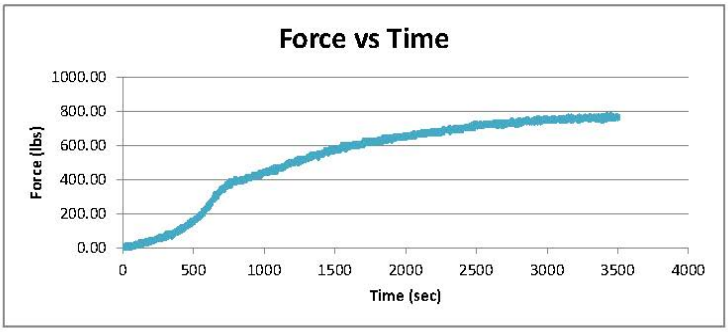

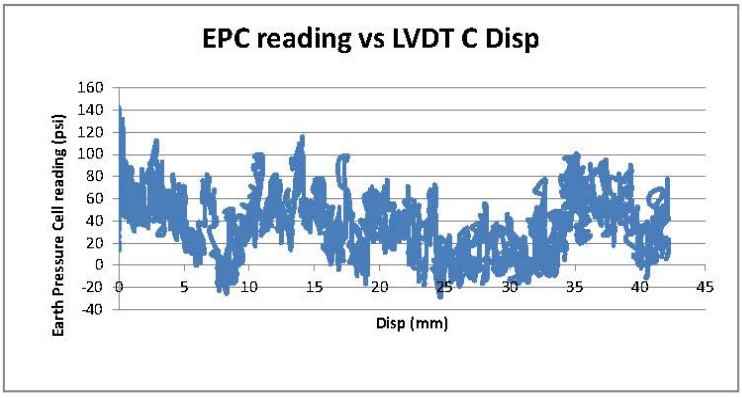

TEST 61

Large Pullout Test

Test details :		
	Test Name	UX1700-100%DM (phil)-8psi
	Date	7/9/2012
	Member	Kemp

Box Dimensions (inch)	Length	Width	Depth	Area (in2)	Height from base to sleeve
	60	24	11	1440	5

Geogrid Details	Manufactur	Product	Ultimate Tensile Strength
	Tensar	UX1700	12000 lb/ft

Specimen Information(ft)	Width	Embedment Length (Le)
	1	2.838

Material Properties	
Material Name	100%DM (Phil)
Friction Angle (ϕ')	25.5
Cohesion, c (psf)	449.28
Moisture Content (%)	50%
Ɣd,max (pcf)	75
Target Compaction	0.8
Weight of each Lift	180
No. of Lifts	4

Test Details	
Normal Stress σ' (psi)	Rate of Pullout (in/min)
8	0.04

Maximum Displacements	
LVDT	Disp (mm)
A	47.842
B	3.401
C	43.696

RESULTS

Maximum Load (lb)	912.30	
Pullout Resisatnce (lb/ft)	912.30	
Coefficient of Interaction, ci	$\frac{Pr}{2(Le)(c + \sigma' \tan(\phi'))}$	0.161

Average EPC reading (psi)	59.679

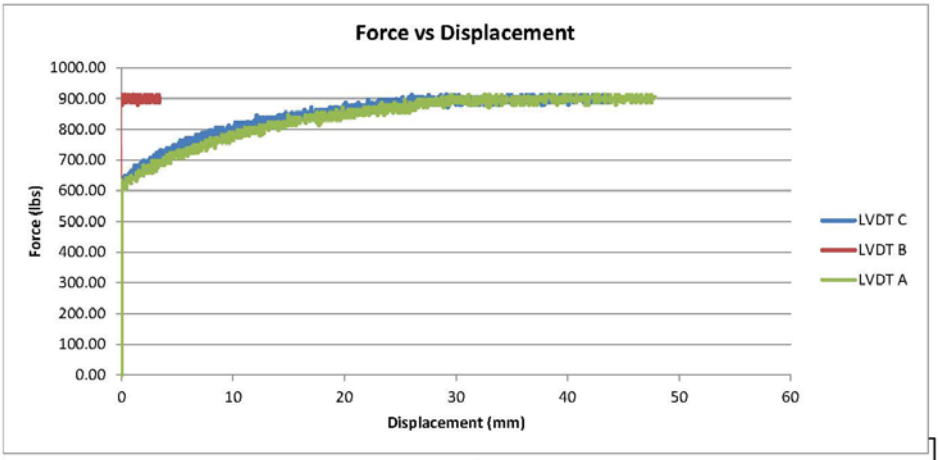

Comments:

TEST 61 CONTINUED

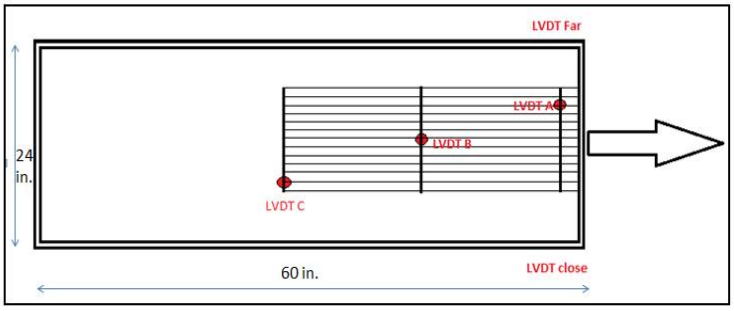

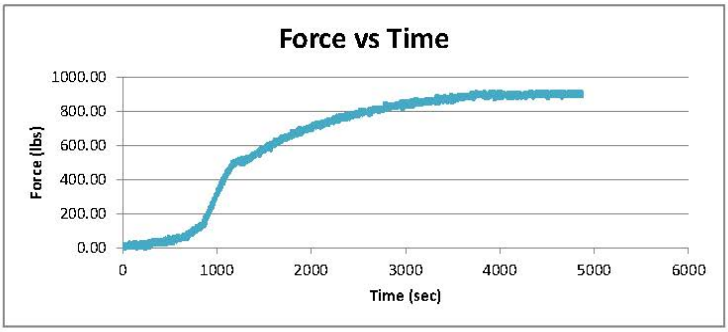

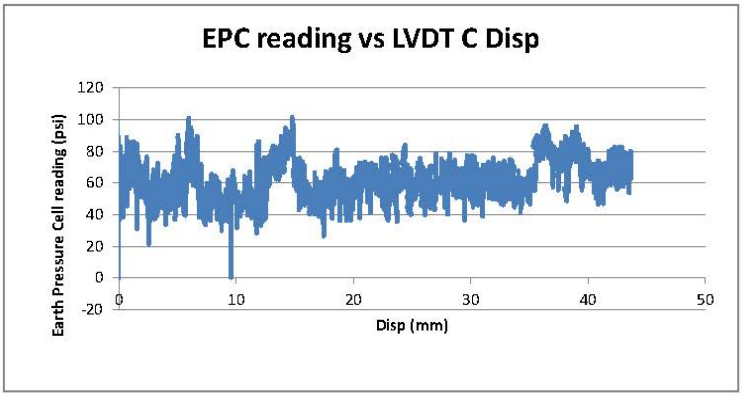

References

Abu-Farsakh, M. Y., Almoh'd I., and Farrag, K. (2006). "Comparison between Field and Laboratory Pullout Tests on Geosynthetics in Marginal Soils." *Journal of the Transportation Research Board,* No. 1975, 124 - 136.

ASTM D6706. (2003). "Standard Test Method for Measuring Geosynthetic Pullout Resistance in Soil", American Society for Testing and Materials, West Conshohocken, PA.

Bouazza, A., Zornberg, J. G., and Adam, D. (2002). "Geosynthetics in waste containment facilities: recent advances." *In Keynote paper, Proc. Seventh Intl. Conf. on Geosynthetics, Nice, France,* 22-27.

Christopher, B.R. and Berg, R.R. (1990). "Pullout Evaluation of Geosynthetics in Cohesive Soils." *Proceedings of the Fourth International Conference on Geotextiles, Geomembranes and Related Products, The Hague, Netherlands*, Vol. 2, 731-736.

Dias, A.C. (2003). "Numerical analyses of soil-geosynthetic interaction in pull-out tests." *MSc. Thesis, University of Brasilia, Brasilia, Brazil.*

"Earth Retaining Structures." Report No. FHWA-NHI-05-046. FHWA, U.S. Department of Transportation, 2005.

Grubb, D.D., Gallagher, P.M., Wartman, J., Carnivale, M., Ill, and Liu, Y. (2006). "Laboratory evaluation of crushed glass-dredged material blends." *J. Geotech. Geoenviron. Eng.*, 132(5), 562-576.

Grubb,D.G., Davis, A., Sands,S. C., Carnivale, M., Ill, Wartman, J., and Gallagher, P. M. (2006). "Field evaluation of crushed glass-dredged material blends." *J. Geotech. Geoenviron. Eng.*, 132(5), 577-590.

Grubb, D.G., Wartman, J., and Malasavage, N.E. (2008). "Aging of Crushed Glass-Dredged Material Blend Embankments." *J. Geotech. Geoenvrion. Eng.*, 134(11), 1676-1684.

Grubb, D.G., Wartman, J., Malasavage, N.E., and Mibroda, J.G. (2007). "Turning Mud Into Suitable Fill: Amending OH, ML-MH and CH Soils With Curbside-Collected Crushed Glass (CG)." *Proceedings of the Geo-Denver Conference on New Peaks in Geotechnics, Denver, CO, USA, February 2007*, 1-14.

Gurung, N. & Iwao, Y. (1999). "Comparative model study of geosynthetic pull-out response." *Geosynthetics International*, 6(1), 53-68.

Ingold, T.S. and Miller, K.S. (1982). "Analytical and Laboratory Investigation of Reinforced Clay." *Proceedings of Second International Conference on Geotextiles, IFAI, 1982, , Las Vegas, NV, USA*, Vol.2, 587-592.

Koerner, R.M. and Wilson-Fahmy, R.F. (1993). "Finite element modeling of soil-geogrid interaction with application t the behavior of geogrids in a pullout loading condition." *Geotextiles and Geomembranes*, 12(5), 479-501.

Milligan, G.W.E., Earl, R.F. & Bush, D.I. (1990). "Observations of photo-elastic pullout tests on geotextiles and geogrids." *4th International Conference on Geotextiles, Geomembranes and Related Products, The Hague. The Netherlands*, Vol.2, 747-751.

Mitchell, J.K. and Zornberg, J.G. (1995). "Reinforced Soil Structures with Poorly Draining Backfills. Part II: Case Histories and Applications." *Geosynthetics International*, 2(1), 265-307.

Murray, R.T. and Boden, J.B. (1979). “Reinforced Earth Wall Constructed with Cohesive Fill.” *Colloque Internation sur le Renforcement des Sols, , Paris, France,* Vol.2, 569-577.

Palmeira, E.M. (2004). “Bearing force mobilization in pull-out tests on geogrids.” *Geotextiles and Geomembrens*, 22(6), 481-509.

Palmeira, E.M. (2009). “Soil–geosynthetic interaction: Modelling and analysis.” *Geotextiles and Geomembrens*, 27(5), 368-390.

Palmeira, E.M. & Milligan, G.W.E. (1989a.). “Scale and other factors affecting the results of pull-out tests of grids buried in sand.” *Geotechnique*, 39(3), 511-524.

Sego, D.C., Scott, E.A., Richards, E.A. and Liu, Y. (1990). “Performance of a Geogrid in a Cohesive Soil Test Embankment.” *Proceedings of Fourth International Conference on Geotextiles, Geomembranes and Related Products, Balkema, 1990, The Hague, Netherlands*, Vol. 1, 67-72.

Teixeira, S., Bueno, B., and Zornberg, J. (2007). ”Pullout Resistance of Individual Longitudinal and Transverse Geogrid Ribs.” *J. Geotech. Geoenviron. Eng.*, 133(1), 37–50.

Toriihara, M., Matsumotoa, S. and Hirama K. (1992). “Construction and Measurement of Embankment Reinforced with Geogrid using In-situ Cohesive Soil.” *proceedings of Seiken Symposium No. 11, Tokyo, Japan*, 295-299.

Zornberg, J.G. and Mitchell, J.K. (1994). “Reinforced Soil Structures with Poorly Draining Backfills. Part I: Reinforcement Interactions and Functions.” *Geosynthetics International*, 1(2), 103-147.